

**TIME-OPTIMAL REORIENTATION MANEUVERS
OF AN AIRCRAFT**

by

Spiro Bocvarov


Dissertation submitted to the Faculty of the
Virginia Polytechnic Institute and State University
in partial fulfillment of the requirements for the degree of

DOCTOR OF PHILOSOPHY

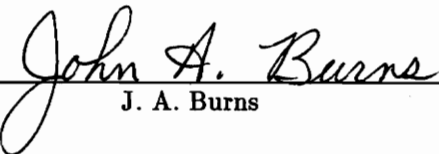
in

Aerospace Engineering

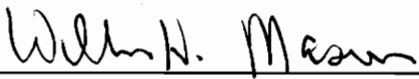
APPROVED:


F. H. Lutze, Chairman


E. M. Cliff


J. A. Burns


S. L. Hendricks


W. H. Mason

July 1991

Blacksburg, Virginia

2

LD
5655
V856
1991
B628
C.2

TIME-OPTIMAL REORIENTATION MANEUVERS
OF AN AIRCRAFT

by

Spiro Bocvarov

Committee Chairman: Frederick H. Lutze
Aerospace and Ocean Engineering

(ABSTRACT)

The problem of time-optimal fuselage-reorientation maneuvering of a combat aircraft, with and without thrust-vectoring capability, was analyzed.

An accurate mathematical model for the reorientation maneuvers of interest was developed, to ensure practical value of the analysis. In particular, an effective method for smooth fitting of the aerodynamic data was devised.

The Minimum Principle from optimal control theory was applied and the optimal-control problems of interest cast into a form of numerical multipoint boundary-value problems. These are extremely difficult to solve. To alleviate their treatment, a hybrid approach was adopted. Homotopy ideas were combined with comprehensive analyses of the structure of the dynamical equations and engineering insight into the mechanics of the reorientation motions. The approach successfully yielded a number of extremal solutions for a few typical reorientation maneuvers. The nature and essential characteristics of the extremal motions were understood, as well as their domains of existence. A few parametric studies showed how aircraft design parameters should be tailored to allow for improved maneuverability.

ACKNOWLEDGEMENTS

I wish to express my appreciation to Dr. Frederick H. Lutze and Dr. Eugene M. Cliff for their understanding, guidance and support in the course of the research and for the successful completion of this study.

I am grateful to Dr. William H. Mason for his valuable comments on my work. I feel thankful to have the opportunity to associate with Dr. John A. Burns and Dr. Scott L. Hendricks.

Special thanks and credit for the fast and successful completion of this work are also due to the ICAM group.

Finally, I would like to acknowledge the financial support that I received from DARPA under Contract No. ACMP-F49620-87-C-0016.

CONTENTS

Page

Abstract ii

Acknowledgements iii

Chapter I. INTRODUCTION

1.1 Introduction 1

1.2 Thrust-Vectoring Enhancement 2

1.3 Scope of the Study 3

1.4 Mathematical Modeling 4

1.5 Optimal Control Theory 5

1.6 Homotopy Method and Parametric Studies 6

1.7 Time-Optimal Maneuvering 7

1.8 Related Results 8

1.9 Contents 8

Chapter II. MATHEMATICAL MODEL

2.1 Simplifying Assumptions 10

2.2 Reference Frames 11

2.3 Kinematical Relations 13

2.4 Dynamical Relations 14

2.5	Center of Mass Motion	17
2.6	Scaled Mathematical Model	18
Chapter III. OPTIMAL CONTROL PROBLEM		
3.1	General Formulation of an Optimal Control Problem	20
3.2	Scaled Mathematical Model of the Aircraft	22
3.3	Boundary Conditions and Cost Function	23
3.4	Adjoint Variables Dynamics	24
3.5	Optimality Conditions	25
3.6	Interpretation of Results	27
3.7	Numerical Multipoint Boundary-Value Problems	28
3.8	Homotopy Approach	29
Chapter IV. NUMERICAL RESULTS		
4.1	Homotopy Schemes	31
4.2	Defenition of Maneuvers	33
4.3	Maneuver-1 Results	33
4.4	Maneuver-2 Results	37
4.5	Common Features	39
Chapter V. PARAMETRIC STUDIES		
5.1	Significance of Parametric Studies	41
5.2	Benefit in Maneuvering Time Due to Thrust-Vectoring	41
5.3	Amount of Thrust-Vectoring Power	43
5.4	Contribution of the Thrust-Vectoring Roll Power	43
5.5	Minimum-Time Fuselage Pointing Problem	44

Chapter VI. CONCLUDING REMARKS 50

References 51

Figures 1 to 8 54-82

Appendix A 83

Appendix B 112

Vita 122

LIST OF FIGURES

	Page
Figure 1. Maneuver-1 Details of an extremal (with TV)	54–59
Figure 2. Maneuver-1 Details of an extremal (without TV)	60–65
Figure 3. Maneuver-2 Details of an extremal (with TV)	66–71
Figure 4. Maneuver-2 Details of an extremal (without TV)	72–77
Figure 5. Example of evolution of extremal solutions	78–79
Figure 6a. Maneuver-1: time vs. initial and final angle-of-attack	80
Figure 6b. Maneuver-2: time vs. final angle-of-attack	80
Figure 7a. Maneuver-1: time vs. thrust-vectoring power	81
Figure 7b. Maneuver-1: time vs. thrust-vectoring roll power	81
Figure 8a. Maneuver-1: time vs. body-roll angle ϕ_f	82
Figure 8b. Maneuver-2: time vs. body-roll angle ϕ_f	82
Figure A-1a. Static roll coefficient (analytical model)	86
Figure A-1b. Static roll coefficient (HARV data)	87
Figure A-2a. Static pitch coefficient (analytical model)	89
Figure A-2b. Static pitch coefficient (HARV data)	90
Figure A-3a. Static yaw coefficient (analytical model)	92
Figure A-3b. Static yaw coefficient (HARV data)	93

Figure A-4a. Roll-damping coefficient (analytical model)	95
Figure A-4b. Roll-damping coefficient (HARV data)	96
Figure A-5a. Pitch-damping coefficient (analytical model)	98
Figure A-5b. Pitch-damping coefficient (HARV data)	99
Figure A-6a. Yaw-damping coefficient (analytical model)	101
Figure A-6b. Yaw-damping coefficient (HARV data)	102
Figure A-7a. Roll coefficient due to differential aileron (analytical model)	104
Figure A-7b. Roll coefficient due to differential aileron (HARV data)	105
Figure A-8a. Pitch coefficient due to horizontal tail (analytical model)	107
Figure A-8b. Pitch coefficient due to horizontal tail (HARV data)	108
Figure A-9a. Yaw coefficient due to rudder (analytical model)	110
Figure A-9b. Yaw coefficient due to rudder (HARV data)	111
Figures B1 & B2. Shape functions Q and C for w=10,20,30	117
Figures B3 & B4. Shape functions R and E for w=10,20,30	118
Figure B5. Shape function $T(\alpha)$	119
Figure B6. Shape function $S(\alpha)$	119
Figure B7. Shape function $Y(\alpha,\beta)$	120
Figure B8. Shape function $Z(\alpha,\beta)$	121

CHAPTER I

INTRODUCTION

In this chapter the objective of the thesis is presented. The problem of interest is stated and the major ideas about how it has been attacked are given. Finally, the structure and contents of the thesis are briefly outlined.

1.1 Introduction. A desire for achieving air superiority leads to a requirement for more maneuverable fighter aircraft. Two important issues, which affect the capabilities of such aircraft, are selection of design parameters (e.g. aerodynamic-control surfaces power, stability properties) and optimal guidance and control of the aircraft. Aircraft which are dynamically more stable require more control power to maneuver, and vice versa: aircraft with reduced dynamical stability require less control power to perform the same level of maneuvers. Given that sufficient control power is available, a question of interest is how to apply the controls to perform the desired maneuvers in some optimal fashion. In particular, one would like to utilize the inherent stability properties of the aircraft along with the available control power when performing specific maneuvers. It is highly desirable that new design concepts account for and take advantage of the interdependence between the design characteristics and the control properties of the aircraft. Modern computers already allow for use of very complex and accurate mathematical models and thus permit computing control laws, and simulation studies of the influence of various design parameters upon aircraft dynamic characteristics.

One particular problem related to the issue of air superiority of a fighter aircraft

is rapid (minimum-time) fuselage pointing. In the past, traditional missile attacks during aerial encounters have been made from behind the opposing aircraft. However, the new all-aspect missiles have less restrictions on location with respect to the opposing aircraft at launch. Thus, sometimes in combat situations, the pilot may need to reorient the fuselage of the aircraft in the direction of an oncoming adversary aircraft before firing a missile. Immediately after that he may need to reorient the fuselage again and shoot a missile into another adversary aircraft. This example illustrates the motivation for studying minimum-time reorientation maneuvers for fighter aircraft. We want to determine how existing aircraft can perform time-optimal reorientation maneuvers. We want to gain some insight and understanding in the nature of time-optimal maneuvering. Furthermore, we want to know how future design concepts should be tailored to allow for improved fuselage reorientation capability.

This work describes some major ideas and concepts conceived in a study which focused upon understanding time-optimal maneuvering of aircraft. It shows some of the considerations taken into account, the ingredients of the problem of interest, formulation of the problem in mathematical terms and a method for solution. No attempt was made in the study to solve the problem completely. This is a formidable task since many parameters influence the answer to the questions of interest. However, the ideas and methods presented can serve as a basis for future work on the problem of time-optimal maneuvering. An important contribution of the study is that it shows that sophisticated mathematical models of aircraft can be used in conjunction with optimization software.

1.2 Thrust-Vectoring Enhancement. Various analyses show that in future aerial combat situations (dog-fights), according to the current trends in development of missiles and radar technology, the more agile vehicle, capable of maneuvering at higher angles-of-attack (α), will have air superiority [1][2][3][4]. Designing such a vehicle

(supermaneuverable aircraft) is a very complex and challenging task. Radically new concepts may emerge in the future. However, if such an aircraft is to be built by upgrading existing design concepts, then enhancing the aircraft with thrust-vectoring (TV) capability is a very appealing idea. At high α 's, especially those beyond that required for maximum-lift, the effectiveness of the aerodynamic-control surfaces decreases rapidly with increase in α . Thus, TV-generated (propulsive) moments can be used to maintain control of the aircraft at high α . At low α the propulsive moments can supplement those generated by the aerodynamic-control surfaces and increase the agility (see [5][6][7]) of the aircraft. In addition, thrust-vectoring can be used to control the aircraft in case of mechanical failure or malfunction of the aerodynamic-control surfaces.

Several research programs, which focus upon utilizing TV-control, are currently underway. One of them is the F/A-18 based High Angle-of-Attack Research Vehicle (HARV) program. Data from the HARV program is used in this study. Accordingly, the numerical results correspond to this aircraft. However, the discussion and methodology in analyzing the results can be considered quite general.

One particular problem associated with the TV-system is the choice of optimal design parameters. We are interested in how much control should a TV-system possess in the direction of each of the body-axes in order to supplement the aerodynamic-control surfaces generated moments most effectively. An attempt was made in the course of the study to answer this question.

1.3 Scope of the Study. We restrict our interest to “small” reorientation maneuvers (less than 60° in polar coordinates, from the original direction of flight). Also, the analysis is restricted to maneuvers at lower values of Mach number ($M < 0.4$). Rapid reorientation at higher Mach numbers seems not to be desirable because the high accelerations the aircraft experiences in this case are unacceptable for the pilot.

Simulation analyses and practical experience show that when reorienting the aircraft rapidly from a steady state straight-line flight into a specified direction, during the maneuver the aircraft center-of-mass does not deviate significantly from the line of the original velocity direction (the reorientation maneuvers are fast enough so that significant linear displacements, due to the aerodynamic forces acting upon the aircraft, do not take place). Accordingly, the translational motion of the aircraft can be neglected and only the rotational motion of the aircraft analyzed. One can imagine the aircraft in a wind tunnel, free to rotate about the center-of-mass. We are interested in how the aerodynamic-control surfaces and the TV-system can be utilized most effectively, so as to reorient the aircraft from one attitude to another in minimum time.

As an initial step towards answering the above question, it is assumed that aerodynamic controls will be used only in a “conventional” way, each control affecting a single axis (i.e. differential ailerons for roll, the rudder for yaw and the horizontal tail for pitch control only). Actually, one can use the ailerons to produce a certain amount of yawing or pitching moment. The horizontal tail can be used to produce a certain amount of yawing or rolling moment (actually, for some aircraft the horizontal tail is the primary roll-control surface). “Nonconventional” use of the aerodynamic-control surfaces (i.e. taking advantage of cross coupling effects) is interesting from a theoretical standpoint and may indeed have some impact upon the results for time-optimal reorientation maneuvering and upon some design parameters of future aircraft. However, at this stage it is important that a thorough understanding should be accumulated first for time-optimal maneuvering by using the aerodynamic-control surfaces in a “conventional” manner only. More thorough description of the assumptions made is given in Chapter 2.

1.4 Mathematical Modeling. A mathematical model of the vehicle-environment

dynamical system, appropriate for the class of optimal control problems of interest, is developed. As already mentioned, for the maneuvers of interest motion of the aircraft center-of-mass can be neglected. This leads to a three degrees-of-freedom model. There are six states total, which include the angular rates and three angles which specify the attitude of the aircraft. Among them are the angle-of-attack α and the sideslip angle β . This model has singular points at $\beta = -90^\circ$ and $\beta = +90^\circ$. Though singularities in a model can potentially cause numerical difficulties, this model was adopted because of the advantages it offers. Most significantly, the aerodynamic-moment coefficients depend upon (the state variables) α and β and thus no coordinate transformation is necessary.

The mathematical model incorporates a model of the aerodynamic moments acting upon the aircraft (these include the control moments generated by the aerodynamic-control surfaces). Special care was exerted in modelling the aerodynamic moments. While essential characteristics have been preserved, certain peculiarities have been omitted. Their effect upon the results obtained is most likely negligible, and can be investigated in future studies.

In modeling the aerodynamic-moment coefficients a problem of 2-D surface fitting arises. 2-D splines do not seem to produce satisfactory fits for optimization purposes since oscillations in the surfaces commonly occur. Therefore, a convenient and effective method for fitting 2-D surfaces was developed. The method is described in Appendix B.

1.5 Optimal Control Theory. The problems of interest can be attacked, at least in principle, by using parameter-optimization techniques. In one version of this approach the state and the control variables are approximated by piecewise polynomial functions. This approach can produce accurate results for some problems. However, our interest is in understanding trends as problem parameters are varied. To reliably

capture these trends, the approach adopted throughout the study is based on the theory of optimal control.

The Minimum Principle is a theory which brings out a set of necessary conditions that the system of interest (in particular, the control signals) needs to satisfy, if it is to behave in an optimal manner according to some prescribed criterion. This set of necessary conditions can be cast into the form of a multipoint boundary-value problem (MPBVP) which can be treated numerically. A solution of the MPBVP corresponds to a so called extremal solution (briefly: extremal). The optimal solution of the problem is, according to the Minimum Principle, an extremal solution (one of the extremals). This method has the advantage of providing very precise extremal solutions to optimal control problem (unlike the parameter-optimization techniques where various variables need to be approximated). However, the method itself has two major drawbacks. First, for the problem of interest, there is no theory which can assure or rule out the existence of extremal solutions for a reorientation maneuver of interest. Also, if extremal solutions exist, their number is unknown. Second, the MPBVPs that we are interested in are extremely difficult to solve. The numerical schemes are based on Newton-type methods and the domain of attraction for any solution can be quite small. Thus, a very precise guess for the unknowns is required for the numerical procedure in the MPBVP-solvers to converge. This difficulty led to the idea of adopting some homotopy ideas (more specifically: the continuation method) in the process of solving the numerical MPBVPs.

1.6 Homotopy Method and Parametric Studies. The essence of the homotopy continuation method is that a solution to a given MPBVP can serve as an initial guess for a new MPBVP, which differs from the previous one by a small perturbation in the mathematical model parameters or the boundary conditions. Thus, one can try to solve first a MPBVP with a simplified mathematical model and/or different

boundary conditions. Then various parameters of the mathematical model and/or the boundary conditions can be gradually varied, in some fashion, until the nominal value of the mathematical model parameters or the desired boundary conditions are met. In addition, by varying a single parameter of the mathematical model or a boundary condition and keeping track of the evolution of various aspects (variables) of the obtained extremal solutions, one might be able to get some insight and eventually understand the essential features of the extremals considered.

There exist some theories about convergence of homotopy methods. Some of them state necessary conditions that need to be met to ensure convergence. No attempt was made to verify such conditions since the mathematical model is rather complex. Indeed, in most cases the evolution of various variables, in the course of the homotopy continuations, provided enough information to predict, for small variations of the mathematical model parameters or boundary conditions, the outcome of the subsequent runs. However, there were occasions when such simple continuation procedures failed.

1.7 Time-Optimal Maneuvering. When trying to understand time-optimal aircraft reorientation maneuvering, one needs to be able to answer questions like these: What is the role of the thrust-vectoring generated moments in the course of the reorientation maneuvers? What is the role of the aerodynamic-surface generated control moments? What is the significance of the aerodynamic damping? How do the gyroscopic moments affect the motion? Do the aircraft static aerodynamic moments (C_i^0 , $i=1,m,n$; see Equations 2-C1,C2,C3) have a supportive role in the course of the maneuver? These and similar questions led to the idea of tracking and analyzing information about all the variables (effects) that affect the dynamics of the rotational motion of the aircraft. Understanding the role of various effects ultimately facilitated better understanding of the nature of the motions represented by the extremal

solutions. Equally important is the fact that by keeping track of the evolution of various model variables, in the course of the homotopy procedures, it was possible to make judicious decisions how the homotopy continuation should be performed and thus successfully solve the MPBVPs encountered (which are extremely difficult for numerical treatment).

An attempt to generate extremal solutions for a very large number of reorientational maneuvers is possible, at least in principle, and ultimately should be done. However, in this study the effort was concentrated upon a few typical reorientation maneuvers. In addition to extremal solutions for an aircraft with nominal design parameters, results of a few parametric studies are presented. Such results further help understanding time-optimal reorientation maneuvering.

1.8 Related Results. A lot of work has been done in the area of optimal satellite angular-rate control, reorientation and maneuvering in vacuum [8][9]. Also a lot of work has been done in the area of optimal trajectories in atmospheric flight [10]. However, only recently has work appeared in the area of time-optimal aircraft reorientation problems [11], inspired by the quest for improved agility of combat aircraft. Most of those studies use point-mass models in studying minimum-time velocity change problems [12].

1.9 Contents. In Chapter 2 the mathematical model of the vehicle-environment system is derived. There is a discussion about which assumptions are made and what is neglected. The obtained mathematical model is then scaled appropriately.

In Chapter 3 a class of optimal control problems of interest is formulated mathematically and a set of necessary conditions for optimality is derived. Also discussed is how the set of necessary conditions for optimality is cast into a multipoint boundary-value problem and how the results obtained should be interpreted. In addition, the

numerical techniques used in solving the multipoint boundary-value problems are described.

In Chapter 4 the homotopy approach for obtaining the desired results by starting from solutions to simpler problems and solving a hierarchy of more complex problems is briefly explained. Then, four particular extremal solutions are described for two representative maneuvers, both with and without thrust-vectoring. The emphasis is upon establishing terminology and methodology for analysis and interpretation of the results. Detailed plots accompany the discussion to illustrate the individual contribution and role of various effects in the course of the maneuvers.

Finally, Chapter 5 contains results of a few parametric studies. The gain in maneuvering time, due to the thrust-vectoring enhancement of an aircraft, is discussed and supplemented by some numerical results. The influence of some thrust-vectoring system design parameters upon maneuvering time is shown. Also, an effect of the final orientation on maneuvering time is discussed.

Some suggestions for future research is given in the Concluding Section. Figures 1 to 7 contain a number of plots that supplement the discussion in Chapters 4 and 5. Appendices A and B contain detailed information about modelling the aerodynamic-moment coefficients.

CHAPTER II

MATHEMATICAL MODEL

A mathematical model of the vehicle-environment dynamical system is derived in this chapter. The system of interest is highly complex, therefore certain assumptions and simplifications are made in the derivation of the mathematical model, in coherence with the optimal control problem of interest. The mathematical model is scaled appropriately.

2.1 Simplifying Assumptions. The aircraft itself and the interacting environment represent a very complex dynamical system. Some analyses combined with prior knowledge and experience about the problem of interest suggest that simplifications can be made without significantly affecting the accuracy of the mathematical model.

The interest in time-optimal reorientation maneuvers is limited to lower values of the Mach number ($M < 0.4$). Rapid reorientation at higher Mach numbers seems not to be desirable since the high accelerations the aircraft experiences in this case are unacceptable for the human pilot. Of course, one may study these motions subject to bounds on the induced acceleration levels. This work remains to be done.

Analyses by simulation show that while reorienting the aircraft rapidly from a steady state straight-line flight to certain specified directions, the aircraft center-of-mass does not deviate significantly from the line in the original velocity direction (the deviation is in the order of a fraction of a degree). In fact, the reorientation maneuvers are fast enough so that significant linear deviations, due to the aerodynamic forces acting upon the aircraft, do not take place. This important fact leads

to a major simplification in the mathematical model used to represent the aircraft and the interacting environment, without any considerable effect upon the accuracy of the model (the error is in the order of 1%). Accordingly, for the rapid reorientation maneuvers of interest, the translational motion of the aircraft can be neglected and only the rotational motion of the aircraft analyzed. One can imagine the aircraft in a wind tunnel, free to rotate about the center-of-mass. We are interested in how the aerodynamic-control surfaces and the TV-system can be utilized most effectively, so as to reorient the aircraft from one attitude to another in minimum time.

To obtain initial results for such a complex problem, it is assumed that aerodynamic controls are used in a “conventional” way, each control affecting a single axis. Thus, the ailerons are used in a differential manner for roll control, the rudder for yaw control, and the horizontal tail for pitch control only. “Nonconventional” use of the aerodynamic-control surfaces (i.e. taking advantage of cross coupling effects) is interesting from a theoretical standpoint and may indeed have some impact upon the results for time-optimal reorientation maneuvering and upon some design parameters of future aircraft. However, the author believes that thorough understanding should be accumulated for time-optimal maneuvering by using the aerodynamic-control surfaces in a conventional manner only, before nonconventional control is considered.

2.2 Reference Frames. Three reference frames will be considered in the derivation of the kinematical and dynamical equations of motion. These are the inertial horizontal reference frame; the wind reference frame; and, a body-fixed reference frame. Each is represented by a set of unit vectors, respectively:

$$(\hat{i}^h, \hat{j}^h, \hat{k}^h), \quad (\hat{i}^w, \hat{j}^w, \hat{k}^w) \quad \text{and} \quad (\hat{i}^b, \hat{j}^b, \hat{k}^b)$$

The orientation (attitude) of the aircraft can be described in different ways, for example by using various sets of Euler angles (ψ, θ, φ) , or Euler parameters $(\beta_0, \beta_1, \beta_2, \beta_3)$

[8][13]. A mathematical model using Euler parameters is appealing since the kinematical equations are free of singularities, unlike a model with Euler angles. However, the aerodynamic forces and moments acting on the aircraft depend upon the aerodynamic angles α (angle-of-attack) and β (sideslip angle). Thus, a mathematical model directly involving α and β as state variables would require no conversion in the calculation of the aerodynamic forces and moments, or their derivatives with respect to the state variables of the model (which appear in the dynamics of the adjoint variables).

Based upon the assumption of a model with “fixed” center-of-mass, it is possible to devise a set of angles (α, β, μ) that can describe the attitude of the aircraft uniquely almost everywhere. Exceptions are the orientations that correspond to sideslip angles $\beta = +90^\circ$ and $\beta = -90^\circ$, which appear as singular points in the kinematical equations. The singularities of the model at $\beta = +90^\circ$ and $\beta = -90^\circ$ do not cause serious difficulties in the numerical procedures.

The angle μ is defined and can be visualized most easily in the following manner. We consider a horizontal, earth fixed reference frame (x_h, y_h, z_h) in the wind tunnel, having the x_h axis parallel to the air-stream velocity-vector and in the opposite direction. Due to the assumption that the motion of the center-of-mass of the aircraft does not deviate from a straight line (which effectively means that the air stream has a constant direction in the wind tunnel), the x_w axis of the wind reference frame (x_w, y_w, z_w) remains parallel to the x_h axis of the horizontal reference frame. This means that the wind reference frame is constrained to roll around the x_h axis only. In other words $\bar{\omega}^w$, the angular velocity of the wind reference frame with respect to the inertial frame, has a non-zero component only along its x_w axis.

At initial time, prior to the beginning of a maneuver, the wind reference frame coincides with the horizontal reference frame. This situation may correspond, for example, to a steady-state level flight in the vertical plane. As the aircraft starts

maneuvering and $\bar{\omega}^w \neq 0$, the relative position of the wind reference frame with respect to the earth fixed (local horizontal) reference frame can be uniquely specified with a roll angle, denoted by μ , the angular rate being $p_w = d\mu/dt$. The aerodynamic angles α and β specify uniquely the orientation of the aircraft body-fixed reference frame with respect to the wind reference frame.

2.3 Kinematical Relations. According to the definition of the aerodynamic angles α and β , the transformation matrix from body-fixed reference frame coordinates to wind reference frame coordinates is given by $L_{wb}(\alpha, \beta) = L_z(\beta) L_y(-\alpha)$, where L_y and L_z are the elementary transformation matrices (single rotation around the y and z axis, respectively). Thus:

$$L_{wb}(\alpha, \beta) = \begin{bmatrix} +\cos \alpha \cos \beta & \sin \beta & +\sin \alpha \cos \beta \\ -\cos \alpha \sin \beta & \cos \beta & -\sin \alpha \sin \beta \\ -\sin \alpha & 0 & \cos \alpha \end{bmatrix}$$

The relative angular velocity of the body-fixed reference frame with respect to the wind reference frame is [14]:

$$\bar{\omega}^{rel} = \bar{\omega}^b - \bar{\omega}^w = -\hat{k}_w \frac{d\beta}{dt} + \hat{j}_b \frac{d\alpha}{dt}$$

It follows that:

$$L_{wb} \begin{bmatrix} p \\ q \\ r \end{bmatrix} - \begin{bmatrix} p_w \\ q_w \\ r_w \end{bmatrix} = - \begin{bmatrix} 0 \\ 0 \\ 1 \end{bmatrix} \frac{d\beta}{dt} + L_{wb} \begin{bmatrix} 0 \\ 1 \\ 0 \end{bmatrix} \frac{d\alpha}{dt}$$

This yields the following set of equations:

$$\begin{aligned} p_w &= +p \cos \alpha \cos \beta + \left(q - \frac{d\alpha}{dt} \right) \sin \beta + r \sin \alpha \cos \beta \\ q_w &= -p \cos \alpha \sin \beta + \left(q - \frac{d\alpha}{dt} \right) \cos \beta - r \sin \alpha \sin \beta \\ r_w &= -p \sin \alpha + r \cos \alpha + \frac{d\beta}{dt} \end{aligned}$$

Based upon the assumption made, $q_w = 0$ and $r_w = 0$, we get the following set of differential equations which govern the dynamics of the angles specifying the attitude

of the aircraft (kinematical equations):

$$\begin{aligned}\frac{d\alpha}{dt} &= q - (p \cos \alpha + r \sin \alpha) \tan \beta \\ \frac{d\beta}{dt} &= p \sin \alpha - r \cos \alpha \\ \frac{d\mu}{dt} &= p_w = (p \cos \alpha + r \sin \alpha) \frac{1}{\cos \beta}\end{aligned}$$

Obviously, this system is ill-defined when $\cos \beta = 0$.

2.4 Dynamical Relations. The Euler rigid-body rotational equations are given by the following set of differential equations [13][14]:

$$\begin{aligned}I_x \frac{dp}{dt} &= (I_y - I_z) qr + u_x(\delta_x) + \frac{\rho(h)V^2(M, h)}{2} S b C_l(\alpha, \beta, \delta_a^r, \delta_a^l, p, M, \dots) \\ I_y \frac{dq}{dt} &= (I_z - I_x) rp + u_y(\delta_y) + \frac{\rho(h)V^2(M, h)}{2} S \bar{c} C_m(\alpha, \beta, \delta_e^r, \delta_e^l, q, M, \dots) \\ I_z \frac{dr}{dt} &= (I_x - I_y) pq + u_z(\delta_z) + \frac{\rho(h)V^2(M, h)}{2} S b C_n(\alpha, \beta, \delta_r^r, \delta_r^l, r, M, \dots)\end{aligned}$$

In the above expressions, δ_x , δ_y and δ_z denote the TV-controls. The body-fixed reference frame axes coincide with the principal axes of inertia of the aircraft.

The Euler equations as shown are valid under the assumption that the aircraft is a rigid body. Actually, in the course of the maneuver there is mass change in amount and distribution (e.g. the aerodynamic-control surfaces and the TV-system deflect, the mass of the aircraft varies due to the fuel exhaust, there are aeroelastic effects, etc.). However, analyses show that the above effects can be neglected, with no significant loss in the accuracy of the mathematical model. For example, the mass of the moving aerodynamic-control surfaces is negligible compared to the mass of the aircraft, so their movement does not vary the mass distribution of the aircraft significantly. In the mathematical model the dynamics of the aerodynamic-control surfaces is neglected since their response to pilot controls is very fast compared to the time of the reorientation maneuvers.

The current implementations of the TV-system can be plausibly modelled in the following way:

$$\left. \begin{aligned} u_x(\delta_x) &= u_x^{max} \delta_x \\ u_y(\delta_y) &= u_y^{max} \delta_y \\ u_z(\delta_z) &= u_z^{max} \delta_z \end{aligned} \right\} \quad \text{where} \quad |\delta_x|^n + |\delta_y|^n + |\delta_z|^n \leq 1.0$$

u_x^{max} , u_y^{max} and u_z^{max} denote the maximum roll, pitch and yaw power the TV-system can provide, and δ_x , δ_y and δ_z are the (scaled) TV-controls. It was found that $n = 2$ models the TV-system quite accurately and this value is used in the mathematical model of the HARV. It is also a nice choice for analytical reasons (see Section 3.5, the optimality conditions).

The aerodynamic forces and moments acting upon the aircraft are very complex functions, each depending upon the angles α and β as well as the Mach number, altitude and deflections of all of the aerodynamic-control surfaces. However, analyses of the aerodynamic data for the HARV shows that many of these dependencies can be neglected for the problem considered.

For example, the center-of-mass of the aircraft moves, due to fuel sloshing and exhaustion, relative to the aerodynamic-reference center (not to be confused with the aerodynamic center; it is just an arbitrary point with respect to which the aerodynamic data is given). However, the displacement is small and stays within a few inches from the aerodynamic-reference center. Therefore, it can be assumed that the aircraft center-of-mass coincides with the aerodynamic-reference center. Thus the aerodynamic forces (lift, drag and sideslip force) have no effect upon the total aerodynamic moments acting upon the aircraft. Furthermore, the Mach number and the dynamic pressure can be assumed to be constant throughout the maneuvers.

The assumption that the aerodynamic-control surfaces will be used for conventional moment control allows for additional simplifications. It is assumed that there are three

primary controls (Δ_a , δ_e and δ_r) such that:

$$\delta_a^r = -\delta_a^l = \Delta_a$$

$$\delta_e^r = +\delta_e^l = \delta_e$$

$$\delta_r^r = +\delta_r^l = \delta_r$$

The subscripts a , e and r refer to the aileron, elevator and the rudder, and the superscripts r and l stand for the right and the left control-surface, respectively. Δ_a stands for differential aileron. All these controls are scaled to the interval $[-1, +1]$, and (for the extreme values of $+1$ and -1) their sign equals the sign of the aerodynamic moment generated by the corresponding control-surface. The usual sign conventions for aerodynamic-control surfaces are not followed here. The signs of the controls are selected so that a positive control provides positive aerodynamic moment.

Under these circumstances and assumptions an accurate representation of the aerodynamic moments and control-surface effectiveness is obtained if the following functional dependencies are assumed for the aerodynamic-moment coefficients:

$$C_l = C_l(\alpha, \beta, p, \Delta_a) = C_l^0(\alpha, \beta) + C_l^\zeta(\alpha, p) + C_l^c(\alpha, \Delta_a) \quad (2-C1)$$

$$C_m = C_m(\alpha, \beta, q, \delta_e) = C_m^0(\alpha, \beta) + C_m^\zeta(\alpha, q) + C_m^c(\alpha, \delta_e) \quad (2-C2)$$

$$C_n = C_n(\alpha, \beta, r, \delta_r) = C_n^0(\alpha, \beta) + C_n^\zeta(\alpha, r) + C_n^c(\alpha, \delta_r) \quad (2-C3)$$

Here C_i^0 , C_i^ζ and C_i^c ($i \in \{l, m, n\}$) denote the rigid-body static (all control-surfaces in neutral position, or more precisely in their trimmed position prior to the beginning of the reorientation maneuver), rate damping, and aerodynamic control-surface contributions to the aerodynamic-moment coefficients, respectively.

The error due to the simplifications made seems not to exceed the measurement error (in the data available for the HARV) for α less than 75° . Data for the aerodynamic-moment coefficients for the HARV is available at a certain set of grid-points within

the intervals $\beta \in [-20^\circ, +20^\circ]$ and $\alpha \in [-10^\circ, +90^\circ]$. In addition, a program is available for linear interpolation of the data between the grid-points [15]. For use with optimization numerical code, analytical *model functions* for the aerodynamic-moment coefficients (C_l, C_m, C_n) were developed. The model functions are parametrically dependent combinations (sums and products) of elementary (rational and transcendental) functions. They are smooth and indeed have an infinite number of derivatives. These model functions fit the data available within less than 5% error (see Appendix A).

2.5 Center-of-Mass Motion. A good estimate of the actual motion of the center-of-mass of the HARV in the course of a maneuver (the deviation from a straight line trajectory) can be obtained by simulation, using the aerodynamic data available for the HARV. Since the horizontal reference frame is inertial, the equations of motion follow from the Newtons law:

$$\frac{d^2}{dt^2} \begin{bmatrix} x_h \\ y_h \\ z_h \end{bmatrix} = \frac{1}{M} \begin{bmatrix} X_h \\ Y_h \\ Z_h \end{bmatrix} + \begin{bmatrix} 0 \\ 0 \\ g \end{bmatrix}$$

where M is the mass of the vehicle, g is the gravity acceleration and X_h, Y_h and Z_h the components of the aerodynamic (D, S and L) and propulsive forces (P_x, P_y and P_z) in the directions of the horizontal reference frame axes. These components can be obtained from the following relation:

$$\begin{bmatrix} X_h \\ Y_h \\ Z_h \end{bmatrix} = L_{hb}(\alpha, \beta, \mu) \begin{bmatrix} -D \\ S \\ -L \end{bmatrix} + \begin{bmatrix} P_x \\ P_y \\ P_z \end{bmatrix}$$

where:

$$L_{hb}(\alpha, \beta, \mu) = L_{hw}(\mu) L_{wb}(\alpha, \beta)$$

$$= L_x(-\mu) L_{wb}(\alpha, \beta)$$

$$= \begin{bmatrix} 1 & 0 & 0 \\ 0 & \cos \mu & -\sin \mu \\ 0 & \sin \mu & \cos \mu \end{bmatrix} \begin{bmatrix} +\cos \alpha \cos \beta & \sin \beta & +\sin \alpha \cos \beta \\ -\cos \alpha \sin \beta & \cos \beta & -\sin \alpha \sin \beta \\ -\sin \alpha & 0 & \cos \alpha \end{bmatrix}$$

$$= \begin{bmatrix} \cos \alpha \cos \beta & \sin \beta & \sin \alpha \cos \beta \\ -\cos \alpha \sin \beta \cos \mu + \sin \alpha \sin \mu & \cos \beta \cos \mu & -\sin \alpha \sin \beta \cos \mu - \cos \alpha \sin \mu \\ -\cos \alpha \sin \beta \sin \mu - \sin \alpha \cos \mu & \cos \beta \sin \mu & -\sin \alpha \sin \beta \sin \mu + \cos \alpha \cos \mu \end{bmatrix}$$

The initial conditions are:

$$\begin{bmatrix} x_h(0) \\ y_h(0) \\ z_h(0) \end{bmatrix} = \begin{bmatrix} 0 \\ 0 \\ 0 \end{bmatrix} \quad \text{and} \quad \begin{bmatrix} \dot{x}_h(0) \\ \dot{y}_h(0) \\ \dot{z}_h(0) \end{bmatrix} = \begin{bmatrix} V(M, h) \\ 0 \\ 0 \end{bmatrix}$$

2.6 Scaled Mathematical Model. The mathematical model of the aircraft is scaled so that it is well-posed for the numerical procedures in the optimization software. This scaling is done in the following manner. Let

$$\tau = kt \quad \frac{p}{k} = P \quad \frac{q}{k} = Q \quad \frac{r}{k} = R$$

where k is a scaling constant. It follows that:

$$\dot{\alpha} \equiv \frac{d\alpha}{d\tau} = \frac{d\alpha}{kdt} = Q - (P \cos \alpha + R \sin \alpha) \tan \beta \quad (2-S1)$$

$$\dot{\beta} \equiv \frac{d\beta}{d\tau} = \frac{d\beta}{kdt} = P \sin \alpha - R \cos \alpha \quad (2-S2)$$

$$\dot{\mu} \equiv \frac{d\mu}{d\tau} = \frac{d\mu}{kdt} = (P \cos \alpha + R \sin \alpha) \frac{1}{\cos \beta} \quad (2-S3)$$

The Euler rotational equations are transformed accordingly:

$$\dot{P} \equiv \frac{dP}{d\tau} = \frac{dp}{k^2 dt} = J_x \frac{q}{k} \frac{r}{k} + \frac{1}{I_x} \frac{u_x^{max}}{k^2} \delta_x + \frac{1}{I_x} \frac{B}{k^2} C_l(\dots)$$

$$\dot{Q} \equiv \frac{dQ}{d\tau} = \frac{dq}{k^2 dt} = J_y \frac{r}{k} \frac{p}{k} + \frac{1}{I_y} \frac{u_y^{max}}{k^2} \delta_y + \frac{1}{I_y} \frac{C}{k^2} C_m(\dots)$$

$$\dot{R} \equiv \frac{dR}{d\tau} = \frac{dr}{k^2 dt} = J_z \frac{p}{k} \frac{q}{k} + \frac{1}{I_z} \frac{u_z^{max}}{k^2} \delta_z + \frac{1}{I_z} \frac{B}{k^2} C_n(\dots)$$

where

$$J_x = \frac{I_y - I_z}{I_x} \quad J_y = \frac{I_z - I_x}{I_y} \quad J_z = \frac{I_x - I_y}{I_z}$$

$$B = \frac{1}{2} \rho V^2 S b \quad C = \frac{1}{2} \rho V^2 S \bar{c}$$

We can set the scaling constant to have the following form:

$$k = \sqrt{\frac{u_s^{max}}{I_s}}$$

where u_s^{max} and I_s are *scaling parameters* that can be chosen arbitrarily (the values $u_s^{max} = u_y^{max}$ and $I_s = I_y$ are used). Finally, we get:

$$\dot{P} = J_x QR + J_{sx} a_x \delta_x + J_{sx} B_s C_l(\alpha, \beta, p, \Delta_a) \quad (2-S4)$$

$$\dot{Q} = J_y RP + J_{sy} a_y \delta_y + J_{sy} C_s C_m(\alpha, \beta, q, \delta_e) \quad (2-S5)$$

$$\dot{R} = J_z PQ + J_{sz} a_z \delta_z + J_{sz} B_s C_n(\alpha, \beta, r, \delta_r) \quad (2-S6)$$

where the constants introduced to abbreviate the notation are given by:

$$\begin{aligned} J_{sx} &= \frac{I_s}{I_x} & J_{sy} &= \frac{I_s}{I_y} & J_{sz} &= \frac{I_s}{I_z} \\ a_x &= \frac{u_x^{max}}{u_s^{max}} & a_y &= \frac{u_y^{max}}{u_s^{max}} & a_z &= \frac{u_z^{max}}{u_s^{max}} \\ B_s &= \frac{B}{u_s^{max}} & C_s &= \frac{C}{u_s^{max}} \end{aligned}$$

All the above constants are dimensionless. The time unit is τ and the angles are given in radian measure.

The scaled mathematical model was used in the study for defining the optimal control problems of interest and in the actual numerical computations of the extremal trajectories. The *state vector* is $\mathbf{x} = (\alpha, \beta, \mu, P, Q, R)^T$. As can be seen, μ is an ignorable state variable (i.e. does not appear in the right-hand side of the differential equations 2-S1 to 2-S6). However, if the translational motion of the aircraft is included, μ is not ignorable.

CHAPTER III

OPTIMAL CONTROL PROBLEM

In this chapter a mathematical formulation of a class of optimal control problems of interest is given. First, a mathematical formulation of a general optimal control problem and a theorem concerning some necessary conditions for optimality (*The Minimum Principle*) are presented. Then the scaled mathematical model of the aircraft is shown along with the restrictions upon the controls, the desired state boundary conditions and the cost function. These define the optimal control problem completely. Next, the necessary conditions for optimality are derived. They include the dynamics of the adjoint variables and the minimization of the Hamiltonian. The convexity of the control domain and its implications are mentioned briefly. Also it is discussed briefly how the results, obtained by using the necessary conditions for optimality, can be interpreted.

3.1 General Formulation of an Optimal-Control Problem. We consider a dynamical system (*control process*) whose behavior can be modelled by a system of differential equations of the following form:

$$\frac{dx^i}{dt} = f^i(x^1, \dots, x^n, u^1, \dots, u^m), \quad i = 1, 2, \dots, n; \quad (3-1)$$

where x^i are *state variables* which characterize the system and u^i are *control variables* which influence the course of the process. For brevity, we define a *state vector* \mathbf{x} and a *control vector* \mathbf{u} :

$$\mathbf{x} = (x^1, x^2, \dots, x^n)^T \in R^n$$

$$\mathbf{u} = (u^1, u^2, \dots, u^m)^T \in U \subset R^m$$

Also, we write the system dynamics (3-1) in a vector form as:

$$\frac{d\mathbf{x}}{dt} = \mathbf{f}(\mathbf{x}, \mathbf{u}) \quad (3-2)$$

We assume that the *control domain* U is compact and convex and consider only bounded measurable functions $\mathbf{u}(\cdot)$ for control. We want to guide (control) the system from a given *initial state* $\mathbf{x}_0 = (x_0^1, \dots, x_0^n)^T$ to a given *final state* $\mathbf{x}_f = (x_f^1, \dots, x_f^n)^T$. No restrictions on the state vector $\mathbf{x}(\cdot)$ are imposed. A control vector $\mathbf{u}(\cdot) = (u^1(\cdot), \dots, u^m(\cdot))^T \in U$ which can accomplish that is called an *admissible* control vector. The *objective* (the optimal control problem) is to find, among all admissible control vectors, the one which renders minimum value of a given *cost functional* J of the following form:

$$J = \int_{t_0}^{t_f} f^0(\mathbf{x}(t), \mathbf{u}(t)) dt$$

The initial and final time (t_0 and t_f) are not specified and, since the system is autonomous, we see that it is only $T = t_f - t_0$ that is unknown and t_0 can be chosen arbitrarily. We also assume that $f^i(\mathbf{x}, \mathbf{u})$ and $\frac{\partial f^i(\mathbf{x}, \mathbf{u})}{\partial x^j}$ are continuous on $R^n \times U$ ($i=0,1,2, \dots, n; j=1,2, \dots, n$).

Under the assumptions made, the following theorem [16][17][18][19] gives some necessary conditions that a solution of the optimal control problem stated above needs to satisfy:

MINIMUM PRINCIPLE. *Let $\mathbf{u}(t)$, $t_0 \leq t \leq t_f$ be an admissible control such that the corresponding trajectory $\mathbf{x}(t)$, which begins at the point \mathbf{x}_0 at some time t_0 passes, at some time t_f through the point \mathbf{x}_f . In order that $\mathbf{u}(t)$ and $\mathbf{x}(t)$ be optimal it is necessary that there exists a nonzero vector function $\boldsymbol{\lambda}(t) = (\lambda^0(t), \lambda^1(t), \dots, \lambda^n(t))^T$ corresponding to $\mathbf{u}(t)$ and $\mathbf{x}(t)$ such that:*

1)

$$\frac{dx^i}{dt} = \frac{\partial H}{\partial \lambda^i}, \quad \frac{d\lambda^j}{dt} = -\frac{\partial H}{\partial x^j}, \quad i, j = 1, 2, \dots, n$$

where

$$H = H(\boldsymbol{\lambda}, \mathbf{x}, \mathbf{u}) = \sum_{k=0}^n \lambda^k f^k(\mathbf{x}, \mathbf{u})$$

is a function further referred to as the *variational Hamiltonian* of the system.

2) for every t , $t_0 \leq t \leq t_f$, the Hamiltonian attains its minimum at $\mathbf{u}(t)$

$$H(\boldsymbol{\lambda}(t), \mathbf{x}(t), \mathbf{u}(t)) = \min_{\mathbf{u} \in U} H(\boldsymbol{\lambda}(t), \mathbf{x}(t), \mathbf{u}) \quad (3-3)$$

That is how the optimal control vector $\mathbf{u}^*(\cdot)$ is determined. We refer to Equation 3-3 as the *optimality condition*.

3) $\lambda^0 = \text{const.} \geq 0$ and $H(\boldsymbol{\lambda}(t), \mathbf{x}(t), \mathbf{u}(t)) = 0$ for $t_0 \leq t \leq t_f$.

3.2 Scaled Mathematical Model of the Aircraft. The scaled mathematical model of the aircraft is given by the following set of differential equations:

$$\dot{\alpha} = Q - (P \cos \alpha + R \sin \alpha) \tan \beta \quad (3-S1)$$

$$\dot{\beta} = P \sin \alpha - R \cos \alpha \quad (3-S2)$$

$$\dot{\mu} = (P \cos \alpha + R \sin \alpha) \frac{1}{\cos \beta} \quad (3-S3)$$

$$\dot{P} = \underbrace{\epsilon_t J_{sx} a_x \delta_x}_{L_{tv}} + \underbrace{\epsilon_{\bar{q}} J_{sx} B_s C_l(\alpha, \beta, p, \Delta_a)}_{L_{aero}} + \underbrace{J_x Q R}_{L_{rp}} \quad (3-S4)$$

$$\dot{Q} = \underbrace{\epsilon_t J_{sy} a_y \delta_y}_{M_{tv}} + \underbrace{\epsilon_{\bar{q}} J_{sy} C_s C_m(\alpha, \beta, q, \delta_e)}_{M_{aero}} + \underbrace{J_y R P}_{M_{rp}} \quad (3-S5)$$

$$\dot{R} = \underbrace{\epsilon_t J_{sz} a_z \delta_z}_{N_{tv}} + \underbrace{\epsilon_{\bar{q}} J_{sz} B_s C_n(\alpha, \beta, r, \delta_r)}_{N_{aero}} + \underbrace{J_z P Q}_{N_{pq}} \quad (3-S6)$$

where

$$C_l(\alpha, \beta, p, \Delta_a) = \underbrace{C_l^0(\alpha, \beta)}_{L_0} + \underbrace{\epsilon_\zeta C_l^\zeta(\alpha, p)}_{L_\zeta} + \underbrace{\epsilon_c A_l^c(\alpha) \Delta_a}_{L_{ac}} \quad (3-C1)$$

$$C_m(\alpha, \beta, q, \delta_e) = \underbrace{C_m^0(\alpha, \beta)}_{M_0} + \underbrace{\epsilon_\zeta C_m^\zeta(\alpha, q)}_{M_\zeta} + \underbrace{\epsilon_c E_m^c(\alpha) \delta_e + \epsilon_c F_m^c(\alpha)}_{M_{ac}} \quad (3-C2)$$

$$C_n(\alpha, \beta, r, \delta_r) = \underbrace{C_n^0(\alpha, \beta)}_{N_0} + \underbrace{\epsilon_\zeta C_n^\zeta(\alpha, r)}_{N_\zeta} + \underbrace{\epsilon_c R_n^c(\alpha) \delta_r}_{N_{ac}} \quad (3-C3)$$

The analytical representations of the aerodynamic-moment coefficients (C_l, C_m, C_n) are shown in Appendix A. Here $\epsilon_t, \epsilon_{\bar{q}}, \epsilon_\zeta$ and ϵ_c are *homotopy variables*. Their role is explained in Chapter 4. The mathematical model represents the physical system of interest when each homotopy variable has unit value. Individual terms in the dynamical equations and the aerodynamic-moment coefficients are underbraced and denoted by different symbols. Understanding the contribution and role of each of these terms in the dynamical behavior of the mathematical model is crucial for understanding the nature of extremal reorientation motions of the aircraft.

3.3 Boundary Conditions and a Cost Function. We want to guide the system from a given initial state \mathbf{x}_0 to a given terminal state \mathbf{x}_f in minimum time. We will consider a class of maneuvers which can be characterized by:

$$\begin{aligned} \mathbf{x}_0 &= (\alpha(t_0), \beta(t_0), \mu(t_0), P(t_0), Q(t_0), R(t_0))^T \\ &= (\alpha_0, \beta_0, \mu_0, 0, 0, 0)^T \\ \mathbf{x}_f &= (\alpha(t_f), \beta(t_f), \mu(t_f), P(t_f), Q(t_f), R(t_f))^T \\ &= (\alpha_f, \beta_f, \mu_f, 0, 0, 0)^T \end{aligned}$$

The cost function here is:

$$J = \int_{t_0}^{t_f} f^0(\mathbf{x}(t), \mathbf{u}(t)) dt = \int_{t_0}^{t_f} 1 dt = t_f - t_0 = T$$

These define the class of minimum-time rest-to-rest reorientation maneuvers.

3.4 Adjoint Variables Dynamics. The dynamics of the adjoint variables λ_α , λ_β , λ_μ , λ_P , λ_Q and λ_R is given by the following set of differential equations:

$$\frac{d\lambda_v}{dt} = -\frac{\partial H}{\partial v}, \quad v \in \{\alpha, \beta, \mu, P, Q, R\}$$

where

$$H = H(\boldsymbol{\lambda}, \mathbf{x}, \mathbf{u})$$

is the *variational Hamiltonian* of the system (normality is assumed; $\lambda^0 = +1 > 0$), given by:

$$\begin{aligned} H = & +1 + \lambda_\alpha [Q - (P \cos \alpha + R \sin \alpha) \tan \beta] & (3-4) \\ & + \lambda_\beta [P \sin \alpha - R \cos \alpha] \\ & + \lambda_\mu [(P \cos \alpha + R \sin \alpha) \frac{1}{\cos \beta}] \\ & + \lambda_P [\epsilon_t J_{sx} a_x \delta_x + \epsilon_{\bar{q}} J_{sx} B_s C_l(\alpha, \beta, p, \Delta_a) + J_x QR] \\ & + \lambda_Q [\epsilon_t J_{sy} a_y \delta_y + \epsilon_{\bar{q}} J_{sy} C_s C_m(\alpha, \beta, q, \delta_e) + J_y RP] \\ & + \lambda_R [\epsilon_t J_{sz} a_z \delta_z + \epsilon_{\bar{q}} J_{sz} B_s C_n(\alpha, \beta, r, \delta_r) + J_z PQ] \end{aligned}$$

Thus, the dynamics of the adjoint variables is represented by the following set of differential equations:

$$\dot{\lambda}_\alpha = -\frac{\partial H}{\partial \alpha} = -\lambda_\alpha(+P \sin \alpha - R \cos \alpha) \tan \beta \quad (3-L1)$$

$$\begin{aligned} & -\lambda_\beta(+P \cos \alpha + R \sin \alpha) \\ & -\lambda_\mu(-P \sin \alpha + R \cos \alpha) \frac{1}{\cos \beta} \\ & -\lambda_P \epsilon_{\bar{q}} J_{sx} B_s \frac{\partial C_l}{\partial \alpha} - \lambda_Q \epsilon_{\bar{q}} J_{sy} C_s \frac{\partial C_m}{\partial \alpha} - \lambda_R \epsilon_{\bar{q}} J_{sz} B_s \frac{\partial C_n}{\partial \alpha} \end{aligned}$$

$$\dot{\lambda}_\beta = -\frac{\partial H}{\partial \beta} = +\lambda_\alpha(+P \cos \alpha + R \sin \alpha) \frac{1}{\cos^2 \beta} \quad (3-L2)$$

$$\begin{aligned} & -\lambda_\mu(+P \cos \alpha + R \sin \alpha) \frac{\sin \beta}{\cos^2 \beta} \\ & -\lambda_P \epsilon_{\bar{q}} J_{sx} B_s \frac{\partial C_l}{\partial \beta} - \lambda_Q \epsilon_{\bar{q}} J_{sy} C_s \frac{\partial C_m}{\partial \beta} - \lambda_R \epsilon_{\bar{q}} J_{sz} B_s \frac{\partial C_n}{\partial \beta} \end{aligned}$$

$$\dot{\lambda}_\mu = -\frac{\partial H}{\partial \mu} = 0 \quad (3-L3)$$

$$\dot{\lambda}_P = -\frac{\partial H}{\partial P} = -\lambda_Q J_y R - \lambda_R J_z Q - \lambda_P \epsilon_{\bar{q}} J_{sx} B_s \frac{\partial C_l}{\partial P} \quad (3-L4)$$

$$+ \lambda_\alpha \cos \alpha \tan \beta - \lambda_\beta \sin \alpha - \lambda_\mu \frac{\cos \alpha}{\cos \beta}$$

$$\dot{\lambda}_Q = -\frac{\partial H}{\partial Q} = -\lambda_R J_z P - \lambda_P J_x R - \lambda_Q \epsilon_{\bar{q}} J_{sy} C_s \frac{\partial C_m}{\partial Q} - \lambda_\alpha \quad (3-L5)$$

$$\dot{\lambda}_R = -\frac{\partial H}{\partial R} = -\lambda_P J_x Q - \lambda_Q J_y P - \lambda_R \epsilon_{\bar{q}} J_{sz} B_s \frac{\partial C_n}{\partial R} \quad (3-L6)$$

$$+ \lambda_\alpha \sin \alpha \tan \beta + \lambda_\beta \cos \alpha - \lambda_\mu \frac{\sin \alpha}{\cos \beta}$$

3.5 Optimality Conditions. Only the following part of the Hamiltonian:

$$\begin{aligned} H^c = & +\lambda_P [\epsilon_t J_{sx} a_x \delta_x + \epsilon_{\bar{q}} J_{sx} B_s A_l^c(\alpha) \Delta_a] \quad (3-5) \\ & +\lambda_Q [\epsilon_t J_{sy} a_y \delta_y + \epsilon_{\bar{q}} J_{sy} C_s E_m^c(\alpha) \delta_e] \\ & +\lambda_R [\epsilon_t J_{sz} a_z \delta_z + \epsilon_{\bar{q}} J_{sz} B_s R_n^c(\alpha) \delta_r] \end{aligned}$$

depends upon the control vector $(\delta_x, \delta_y, \delta_z, \Delta_a, \delta_e, \delta_r)^T$.

As stated in Section 2.4, the thrust-vectoring controls δ_x , δ_y and δ_z obey the following constraint:

$$|\delta_x|^2 + |\delta_y|^2 + |\delta_z|^2 \leq 1$$

Therefore, the optimal controls (which minimize the Hamiltonian) are computed as:

$$\begin{aligned}\delta_x &= -\frac{\lambda_P J_{sx} a_x}{\sqrt{(\lambda_P J_{sx} a_x)^2 + (\lambda_P J_{sy} a_y)^2 + (\lambda_R J_{sz} a_z)^2}} \\ \delta_y &= -\frac{\lambda_Q J_{sy} a_y}{\sqrt{(\lambda_P J_{sx} a_x)^2 + (\lambda_P J_{sy} a_y)^2 + (\lambda_R J_{sz} a_z)^2}} \\ \delta_z &= -\frac{\lambda_R J_{sz} a_z}{\sqrt{(\lambda_P J_{sx} a_x)^2 + (\lambda_P J_{sy} a_y)^2 + (\lambda_R J_{sz} a_z)^2}}\end{aligned}\tag{3-6}$$

The aerodynamic controls appear linearly in the system dynamics and are independent: $\Delta_a, \delta_e, \delta_r \in [0, 1]$. Therefore, the control domain $(\Delta_a, \delta_e, \delta_r)$ is a cube. When λ_P , λ_Q and λ_R are not equal to zero, the optimality condition yields:

$$\begin{aligned}\Delta_a &= -\text{sgn}(\lambda_P \epsilon_{\bar{q}} J_{sx} B_s A_i^c(\alpha)) \equiv +\text{sgn}(\lambda_P) \\ \delta_e &= -\text{sgn}(\lambda_Q \epsilon_{\bar{q}} J_{sy} C_s E_m^c(\alpha)) \equiv +\text{sgn}(\lambda_Q) \\ \delta_r &= -\text{sgn}(\lambda_R \epsilon_{\bar{q}} J_{sz} B_s R_i^c(\alpha)) \equiv +\text{sgn}(\lambda_R)\end{aligned}\tag{3-7}$$

The points where the adjoint variables λ_P , λ_Q or λ_R cross (transversally) through zero are called *switching points*. At these points the corresponding control Δ_a , δ_e or δ_r switches from +1 to -1 or vice versa and can conventionally be assumed zero. There might exist trajectories such that some of λ_P , λ_Q or λ_R stay zero along a time interval of finite length. The existence of such trajectories (*singular trajectories*) is not examined in the present study.

The software used for numerical search of extremal trajectories requires a fairly good estimate of the points where λ_P , λ_Q and λ_R cross through zero. A good way to get an estimate is to assume that the aerodynamic controls Δ_a , δ_e and δ_r are not

independent, but related as:

$$|\Delta_a|^n + |\delta_e|^n + |\delta_r|^n \leq 1$$

For this case, the optimal controls can be calculated by using the Kuhn-Tucker necessary conditions (or the Lagrange-multiplier rule). They yield Equations 3-6 and 3-8:

$$\begin{aligned}\Delta_a &= -\text{sgn}(\lambda_P) \cdot \frac{|\lambda_P J_{sx} B_s A(\alpha)|^{\frac{1}{n-1}}}{\Sigma_n} \\ \delta_e &= -\text{sgn}(\lambda_Q) \cdot \frac{|\lambda_Q J_{sy} C_s E(\alpha)|^{\frac{1}{n-1}}}{\Sigma_n} \\ \delta_r &= -\text{sgn}(\lambda_R) \cdot \frac{|\lambda_R J_{sz} B_s R(\alpha)|^{\frac{1}{n-1}}}{\Sigma_n}\end{aligned}\tag{3-8}$$

where

$$\Sigma_n = \left\{ |\lambda_P J_{sx} B_s A(\alpha)|^{\frac{n}{n-1}} + |\lambda_Q J_{sy} C_s E(\alpha)|^{\frac{n}{n-1}} + |\lambda_R J_{sz} B_s R(\alpha)|^{\frac{n}{n-1}} \right\}^{\frac{1}{n}}$$

As $n \geq 2$ increases, the control domain $(\Delta_a, \delta_e, \delta_r)$ deforms from a sphere into a cube-like shape. Satisfactory estimates are obtained for $n = 6$.

The control hodograph is the set of points $(\dot{P}, \dot{Q}, \dot{R}) \subset R^3$ as the controls $\delta_x, \delta_y, \delta_z, \Delta_a, \delta_e$ and δ_r take all the possible values. One can easily visualize its shape. It is convex, but not strictly convex. This means that the occurrence of chattering extremals can not be ruled out.

3.6 Interpretation of Results. A trajectory that satisfies the necessary conditions for optimality and the given boundary conditions is called an *extremal trajectory*, or briefly an extremal. The sequence of switching points for a given extremal (i.e. their order and total number) will be further referred to as a *switching structure* of the extremal.

The extremal which yields a minimum value of the cost function is the actual optimal trajectory. There is no theory which can assure existence of extremals for a

given optimal control problem; furthermore, if extremal solutions exist, their number is unknown. In general, one should attempt to find more extremals. The extremal which renders minimum value to the cost function can be considered to be *the best* extremal. Engineering judgement and analyses can further help explain the nature of the extremals. In many cases one can explain the characteristics which make one of them better than the others (for a given reorientation maneuver).

3.7 Numerical Multipoint Boundary-Value Problems. Additional scaling needs to be done upon the state and the adjoint dynamical equations (Equations 3-S1 to 3-S6 and 3-L1 to 3-L6) in order to cast the set of necessary conditions into a form of a system of nonlinear equations, appropriate for numerical processing. Another independent variable is introduced:

$$z = \frac{\tau}{T}$$

where T is the unknown scaled extremum time. Thus, we get the following system of differential equations:

$$\frac{dT}{dz} = 0, \quad \frac{dx^i}{dz} = T \frac{\partial H}{\partial \lambda^i}, \quad \frac{d\lambda^j}{dz} = -T \frac{\partial H}{\partial x^j}, \quad i, j = 1, \dots, 6$$

Initial and terminal points (boundary conditions) are:

$$\mathbf{x}_0 = (\alpha_0, \beta_0, \mu_0, P_0, Q_0, R_0)^T$$

$$\mathbf{x}_f = (\alpha_f, \beta_f, \mu_f, P_f, Q_f, R_f)^T$$

An additional requirement is the Hamiltonian (Equation 3-4) to be zero at time T (this is a consequence of the optimality condition; see Section 3-1). The above system of differential equations and boundary conditions represents a well defined system of seven nonlinear equations with seven unknowns. The unknowns are the initial values of the adjoint variables: $\lambda_\alpha(t_0)$, $\lambda_\beta(t_0)$, $\lambda_\mu(t_0)$, $\lambda_P(t_0)$, $\lambda_Q(t_0)$, $\lambda_R(t_0)$ and the time T .

By choosing an initial guess for these unknowns, the system of differential equations can be integrated from $z = 0$ to $z = 1$, using the optimality conditions to determine the controls along the trajectory. The trajectory will end at a certain point $\mathbf{x}(T)$:

$$\mathbf{x}(T) = (\alpha(T), \beta(T), \mu(T), P(T), Q(T), R(T))^T$$

We can also compute $H(T)$. The output of the so formed system of seven nonlinear equations is:

$$(\alpha(T) - \alpha_f, \beta(T) - \beta_f, \mu(T) - \mu_f, P(T) - P_f, Q(T) - Q_f, R(T) - R_f, H(T) - 0)^T$$

We want this output (vector) to be zero. For the case of a model with no aerodynamic bang-bang controls, that explains in principle how we cast the set of necessary conditions for optimality into a system of nonlinear equations.

If aerodynamic bang-bang controls are used, additional unknowns need to be introduced. These are the switching points s_i ($i = 1, 2, \dots, s$ and $0 < s_i < 1$). Associated with each switching point s_i is a switching condition $\lambda_v = 0$ where $v \in \{P, Q, R\}$. Thus, the number of unknowns and the number of conditions that need to be satisfied are equal again. Extremal solutions were found with 3,4,5,6 and 7 switching points.

Initially, IMSL subroutines [20] were used for solving the system of nonlinear equations (for rigid-body reorientation problems in vacuum; $\epsilon_{\bar{\gamma}} = 0$, Equations 3-S4,S5,S6) and a certain number of extremal solutions obtained. For the subsequent work a special software package designed for solving multipoint boundary-value problems with switching points and jumping conditions, that appear in optimal control, was used [21][22].

3.8 Homotopy Approach. The relevant numerical multipoint boundary-value problems are extremely difficult to solve. They require a very good estimate of the unknowns ($\lambda(0)$, $T = t_f - t_0$ and the location of the switching points). A homotopy

approach was adopted throughout the study so that solutions to simpler problems were utilized to obtain solutions to more complex problems.

The essence of the homotopy method is that a solution to a particular problem can serve as a fairly good initial guess for a new MPBVP, which differs from the previous one by a small perturbation in the model parameters or the boundary conditions [23]. Thus, starting from a known extremal, by varying a model parameter (or the boundary conditions) one can get a series of extremals, solutions to a number of MPBVPs. Such a series of extremals will further be referred to as *a family of extremals*.

CHAPTER IV

NUMERICAL RESULTS

In this chapter the problem of choice of homotopy schemes is briefly addressed and results (extremal solutions) for two reorientational maneuvers are presented, both for an aircraft with and without thrust-vectoring capability. The discussion is supplemented by a number of plots in Figures 1 to 4. All results belong to one family of extremal solutions and have some interesting characteristics in common.

4.1 Homotopy Schemes. In the mathematical model of the aircraft four homotopy variables are introduced. They are $\epsilon_{\bar{q}}$, ϵ_t , ϵ_ζ and ϵ_c (Equations 3-S1 to 3-S6 and 3-C1 to 3-C3). They can control independently some physical quantities of the mathematical model (the dynamic pressure, the thrust-vectoring (moment) power, the amount of damping and the aerodynamic-control surfaces (moment) power, respectively). The mathematical model represents the physical system of interest when each of these homotopy variables has a unit value. Actually, in the study a number of other parameters (constants that appear in the mathematical model) were varied (used as homotopy variables) in order to facilitate some understanding about the nature of the extremal solutions, their domain of existence, and evolution. A brief explanation about the choice of homotopy schemes follows.

First a dozen different extremal solutions were found for a few reorientation maneuvers in vacuum, or equivalently for a model with $\epsilon_t = 1$ and $\epsilon_{\bar{q}} = 0$. This was a difficult problem in itself and some understanding about spatial and time symmetries of extremal rest-to-rest reorientation maneuvers was needed. Such considerations yielded

a few analytical results, among which are certain group properties of the adjoint variables and necessary conditions that they need to satisfy for certain reorientation maneuvers. In the next step the vacuum results (note: these were results for a vehicle with thrust-vector control only) were used as starting points for obtaining extremal solutions for the nominal mathematical model. This was done in two phases. In the first phase, solutions were found for a model without aerodynamic-control surfaces (by first increasing $\epsilon_{\bar{q}}$ from 0 to 1 with $\epsilon_c = 0$, after which ϵ_{zeta} was increased from 0 to 1). In the second phase, the aerodynamic-control surfaces were introduced (ϵ_c was increased from 0 to 1). After that, the TV-power was decreased to zero (ϵ_t decreased from 1 to 0) and thus extremal solutions obtained for an aircraft with aerodynamic-control surfaces only (without TV-control). This global scheme was partially directed by the numerical difficulties experienced in the course of the work.

The transition from a vacuum model to a model without aerodynamic-control surfaces (the first phase) deserves special attention. First a set of *linear* model functions for the static moment-coefficients were developed. Let them be denoted by: $C_i^{lin}(\alpha, \beta)$, $C_m^{lin}(\alpha, \beta)$ and $C_n^{lin}(\alpha, \beta)$. These functions are linear in both α and β direction and roughly approximate the real aerodynamic data (see Appendices A and B). Starting from the extremals for motion in vacuum, intermediate results were obtained by gradually increasing a dummy homotopy parameter (say $\epsilon_{\bar{q}}^{lin}$) from 0 to 1. Next, the homotopy was continued by using the scheme:

$$\epsilon_{\bar{q}}^{lin} \cdot C_i^{lin}(\alpha, \beta) \cdot (1 - \epsilon_{\bar{q}}) + \epsilon_{\bar{q}} \cdot C_i^0(\alpha, \beta) \quad i \in \{l, m, n\}$$

As $\epsilon_{\bar{q}}$ was increased from 0 to 1 a transition from the linear model functions to the desired model functions was done. When $\epsilon_{\bar{q}} = 1$ the contribution of the linear model functions vanishes. They can be discarded from the mathematical model, after which $\epsilon_{\bar{q}}$ takes the role of a scaling factor for the dynamic pressure (not all of the extremals

from the vacuum case could be extended by the described homotopy scheme; only several remained). Following this, the aerodynamic-damping terms were included by increasing ϵ_ζ from 0 to 1.

4.2 Definition of Maneuvers. Results about extremal solutions for two types of reorientation maneuvers are presented in this and the next chapter. The first type of maneuver (*Maneuver-1*) is customarily called a *roll-around-the-velocity-vector maneuver* (RVV maneuver) and is characterized by the following initial and final states: $\mathbf{x}_0 = (\alpha_0, 0^0, 0^0, 0, 0, 0)^T$ and $\mathbf{x}_f = (\alpha_f, 0^0, \mu_f, 0, 0, 0)^T$, with $\alpha_0 = \alpha_f$. Only the case $\mu_f = 90^0$ is considered further. Therefore, maneuvers of this type will sometimes be referred to as 90^0 -RVV maneuvers. A maneuver of this type can be fully characterized by a single constant $\alpha_{0f} = \alpha_0 = \alpha_f$.

The second type of maneuver (*Maneuver-2*) is characterized by the following initial and final states: $\mathbf{x}_0 = (10^0, 0^0, 0^0, 0, 0, 0)^T$ and $\mathbf{x}_f = (\alpha_f, 0^0, 90^0, 0, 0, 0)^T$. This maneuver will be sometimes referred to as 90^0 -Roll maneuver. It can be fully characterized by a single constant α_f . This maneuver can be viewed as reorientation of an aircraft from an initial steady-state, straight and level flight to a certain direction in the horizontal plane, with no sideslip angle.

These two maneuvers are of interest for themselves, but also may be considered to be part of a more complex, composite maneuver in a combat situation. Imagine the aircraft performing Maneuver-2 first, firing a missile, then changing its attitude by performing Maneuver-1 and firing another missile in the new direction.

By varying the angles α_{0f} or α_f , and thus the initial and final orientation (or the final orientation only) of the aircraft, we can get a series of solutions, all belonging to one family of extremals.

4.3 Maneuver-1 Results. Details about one particular extremal solution are pre-

sented in Figures 1a to 1l. The extremal corresponds to Maneuver-1 for $\alpha_{of} = 30^\circ$. In principle, it is possible to perform a roll-around-the-velocity-vector maneuver in which the angle-of-attack α is kept constant and the sideslip angle β zero. For smaller values of α , this can be done by rolling while adjusting the elevator (to keep α constant) and the rudder (to keep $\beta = 0$). An extremal was found which resembles to this motion. Several studies on various amounts of control power for roll, pitch and yaw suggest that such an extremal exists if the aircraft does not possess much roll power. However, the aircraft considered possesses a lot of roll power from the aileron, especially at lower α . The extremal solution described next is quite different in nature.

As can be seen from Figures 1a and 1c, the aircraft pitches down during the first part of the trajectory, then pitches up during the rest of the maneuver. It rolls and yaws in the positive direction all the time, as one would expect. Figure 1b shows the orientation of the aircraft in time, in terms of the standard set of Euler angles ψ , θ and ϕ (one can visualize the attitude of the aircraft easier in these terms). The adjoint variables λ_P , λ_Q and λ_R , which are responsible for the determination of the extremal controls, are shown in Figure 1d. The aerodynamic and the TV-controls are shown in Figures 1e and 1f. The essential feature of this maneuver is that the aircraft pitches down and up because it has a lot of pitch power from the elevator and from the TV-system and because at lower α the aileron is more powerful. The relative magnitude (proportion) of the power the aircraft has for roll, pitch and yaw can be seen from Figures 1g, 1i and 1k. Also the individual contribution of the TV-system, the aerodynamic moments and the gyroscopic moments (Equations 3-S4 to 3-S6) can be seen. A remarkable feature of this extremal is that most of the time throughout the maneuver the gyroscopic moments tend to support the thrust-vectoring and aerodynamic-control-surfaces generated moments (Figures 1i and 1k;

the gyroscopic terms in the yaw and the pitch channels are more powerful than the control terms and act quite supportively).

The individual contributions of the aerodynamic terms can be seen in Figures 1h, 1j and 1l (see also Equations 3-C1,C2,C3). The maneuver does not take a lot of advantage of the dihedral effect: the sideslip angle tends to stay below 5° , which is a desirable feature since higher β means considerable side accelerations that may not be acceptable for the human pilot. The dehidral effect seems to have a supportive role in the (normalized) time interval from $\tau \approx 0.4$ to $\tau \approx 0.6$ (Figure 1h) and slightly opposing effect during the rest of the maneuver. In fact, when analyzing extremal problems of the type considered, one must always keep in mind that there might be some trade-offs on local level which help the extremal globally. This might be a plausible explanation why the extremal motion considered does not take advantage of the dehidral effect: the generated static moments are much lower than the gyroscopic or the control moments; exerting control power to keep the aircraft in orientation which produces supporting dehidral moments is not effective.

The extremal described is the only extremal found for the nominal value of the aircraft parameters. Another extremal is found to exist for an aircraft possessing less roll power. The Minimum Principle *requires* the controls to be utilized in a certain way (to minimize the variational Hamiltonian, eg. bang-bang for the aerodynamic-control surfaces). This explains why, given an initial and a final state, a particular extremal might not exist as the aircraft design parameters are varied. The relative amount of control power the aircraft possesses for roll, pitch and yaw are important design parameters which can affect the existence of extremals, for rotation maneuvers, or their characteristics. This can be seen from Figure 2, where an extremal solution is shown for the same maneuver for the case where the aircraft has no TV-power. It was obtained by using the previous solution and decreasing the homotopy parameter ϵ_t

from 1 to 0. In Figure 1g it can be seen that the TV-power in the roll channel is very small when compared to the aileron power. However, in the pitch and yaw channel (Figures 1i and 1k) the TV-power is comparable to the control-surfaces power. So, in the case of no thrust-vectoring, the aircraft possesses (relatively) more roll power than an aircraft with thrust-vectoring. Perhaps the most distinctive characteristic of the solution in Figure 2 is that the aileron has negative sign at the beginning of the trajectory (where one would expect positive angular acceleration) and positive sign at the very end of the trajectory (where one would expect angular deceleration). A plausible explanation for this phenomena is that if the Minimum Principle requires the aerodynamic controls to be used in full power (bang-bang), and the aileron possesses a lot of roll power, then it is necessary that that power is neutralized for a certain amount, so that the pitch and yaw power can accomplish their task by the time the aileron has rolled the aircraft as much as it is necessary (though the roll, pitch and yaw amount of angular motion are not independent and are related through the nature of the trajectory, one can still imagine that certain reorientation maneuvers need more roll, pitch and/or yaw motion than others).

The above claim is supported by the following result. Starting from the extremal solution described by Figure 2, a series of extremal solutions were generated by decreasing the maximal thrust-vectoring roll power (this was done by gradually decreasing the maximum absolute value of Δ_a , from 1.0 to 0.6). This scaling does not change the shape of $C_i^e(\alpha, \beta)$ qualitatively, just decreases the maximal aileron roll power at a given α . It was clearly noted that the last switching point (Figure 2e) was moving towards $\tau = 1.0$ and ceased to exist beyond a certain value of Δ_a . As Δ_a was further decreased, the first switching point moved rapidly towards $\tau = 0.0$. The described evolution is illustrated in Figure 2e and Figures 5a–5d. These results clearly show that as the maximal roll power is decreased, (for this particular maneuver and extremal

solution) the balance of control power in the roll, pitch and yaw channel becomes more appropriate; so it is less necessary for the aileron to act the “wrong way” at the beginning and at the end of the trajectory (in order to counteract its own excess of power). The aileron power was decreased 40%. However, the total maneuvering time increased from $t_{\Delta_a=1.0} = 2.698374s$ to $t_{\Delta_a=0.6} = 2.781385s$, or only about 3.08%.

4.4 Maneuver-2 Results. Details about another pair of extremal solutions are presented in Figures 3 and 4. These correspond to Maneuver-2 for $\alpha_f = 45^\circ$, for an aircraft with and without TV-power, respectively. The extremal with TV-power is derived from the extremal presented in Figure 1, by gradually decreasing α_0 from 30° to 10° and increasing α_f gradually from 30° to 45° . Consequently, they can be considered to be members of the same family of extremals.

By examining the plots in Figure 3, one can easily see that the basic nature of the motion, represented by this extremal trajectory, is similar to the motion of the extremals shown in Figures 1 and 2. The aircraft pitches down a little, then pitches up, while rolling and yawing (Figures 3a to 3c). From Figures 3g to 3l it can be seen that various effects support each other most of the time. A notable exception is the gyroscopic moment in the yaw channel (Figure 3k), which seems to severely oppose the controls in the interval from $\tau \approx 0.4$ to $\tau \approx 0.6$. Questions naturally arise, such as: why this happens and is it desirable or not?

To answer these questions, one needs to notice that the maneuver considered inherently requires a large amount of pitching motion, considerable amount of roll motion and relatively low amount of yaw motion. One can easily see that when the aircraft pitches up and rolls positive, the gyroscopic term N_{pq} is negative. This explains why the gyroscopic term opposes the controls in the time-interval mentioned.

To answer the second question, one needs to recall that the Minimum Principle requires the aerodynamic controls to be bang-bang (singular arcs may exist; then

other conditions need to be satisfied). Since little yaw motion is needed for this maneuver (much less than the rudder can provide when used bang-bang, with full power), there are a few possible solutions. One is that less yaw power can be inserted by the TV-system; this is controlled by the (relative) magnitude of the adjoint variable λ_R . However, this might not be enough by itself. Another solution is the rudder to counteract itself by acting in the opposite way of the actual motion, as it was the case with the aileron in Figure 2l. Third, the rudder may take intermediate values (singular arc in the middle of the trajectory). Figure 4d shows an example of such a phenomenon: in this case the adjoint variable λ_P tends to stay close to zero during a certain time interval. And finally, as it is the case in Figure 3, the opposing gyroscopic term, which has significant value, can take the responsibility of neutralizing the undesired positive yaw power in the first part of the trajectory, where the rudder is positive and has more power due to the lower α . In the second part of the trajectory the aircraft is at higher α . Here it needs to have the yaw rate decreased. The yaw power is decreased due to increased α (Figure A9). Thus, the powerful gyroscopic term helps the decrease of the yaw rate in the second part of the trajectory. This discussion suggests that the non-supportive role of the gyroscopic term in the yaw channel (with respect to the controls) during a period of time is indeed quite beneficial.

Figure 4 shows details of an extremal of the same family as above, for the same maneuver as in Figure 3, for an aircraft without thrust-vectoring. As was explained in Section 4.3, without thrust-vectoring the aircraft has relatively more roll power. By comparing to the case with thrust-vectoring, one can easily conclude that most of the effects support each other and that similar trade-offs are made. However, an exception appears with the aileron, which takes the “wrong” sign at the end of the trajectory. An explanation again would be that it simply counteracts itself. Though

it lasts about 20% of the time, it does not produce much roll moment since α is high and its power is significantly decreased. An interesting question here is why the aileron does not provide the “wrong” roll at the beginning, but does that at the end? Does this feature help the maneuvering time for this extremal motion, and how? A simple explanation might be that by doing so, the roll angular-rate better helps the M_{rp} term in the pitch channel (Figure 4i) where it is needed most (to pitch up) and simultaneously counteracts the rudder in the last part of the trajectory, from $\tau \approx 0.7$ to $\tau = 1.0$ (where it might be more powerful than it is needed).

4.5 Common Features. The extremal solutions for the maneuvers discussed in this chapter show some common features. The aircraft first pitches down, then it pitches up, while rolling and yawing in the positive sense (most of the time), and thus it takes advantage of the gyroscopic moments. Furthermore, most of the effects seem to have supportive role, with some exceptions where trade-offs occur that apparently improve the extremal globally. For a particular maneuver and a particular extremal solution, the relative magnitude of control power in the roll, pitch and the yaw channel is an important feature. If not ideally proportioned, the controls may need to neutralize their own power that appears to be in excess. They can be neutralized through the cross-coupling (gyroscopic) effects. This phenomenon appears because the Minimum Principle requires that the controls be used in a certain way (with full power, e.g. bang-bang for the aero-controls). Some results suggest that singular extremal solutions may exist, and the appearance of the singular arcs seems to be another way to balance the excess of control power in a certain channel (for a particular maneuver). Obviously, the control power can not be proportioned well for all maneuvers; the purpose of this discussion is to present some factors that affect and issues related to time-optimal maneuvering; many other factors may influence the choice of the control-system design parameters.

Finally, an interesting question arises about the sideslip angle magnitude. For the maneuvers presented and most others examined, it stays quite small (less than 10° , and often less than 5°). Big sideslip angles are not desirable since pilots can not tolerate high side-accelerations. Thus, if solutions with (unacceptably) large β were obtained, it would have been necessary to impose a constraint on β and solve optimization problems with the state-constraint. The same holds true for the accelerations \dot{p} , \dot{q} and \dot{r} . In order to understand why β remains small in the extremal solutions presented, one needs to review carefully the role of the aerodynamic static moment coefficient components in the course of the maneuvers. While $C_m^0(\alpha)$ appears to play an important supportive role in the pitch channel (C_m^0 does not effectively depend on β for $|\beta| < 20^\circ$), $C_l^0(\alpha, \beta)$ and $C_n^0(\alpha, \beta)$ seem to have less important roles (their magnitudes are of much lower intensity than the control power and the damping power). In some cases they act supportively, in some cases not (their sign depends upon the sign of β). In order to develop more significant values of C_l^0 and C_n^0 , the aircraft needs to increase the sideslip angle considerably (say 15° to 20°), with a proper sign, and eventually maintain it (furthermore, for some α there does not exist a sideslip angle such that both the roll and yaw channel benefit; compare Figures A1 and A3 and consider the need for roll and yaw power in the course of the maneuvers in Figures 1 to 4). Thus, instead of deliberately exerting control power to increase β , the aircraft performs the maneuver in such a way that it takes a lot of advantage of the gyroscopic effects, and if β evolves such that the developed static moments are not supportive, it does not affect the overall performance significantly (this is one of the trade-offs that in general an extremal inherently contains).

Here it needs to be stressed that the whole discussion pertains to one particular family of extremal solutions and specific types of reorientation maneuvers and for the aircraft mathematical model under consideration.

CHAPTER V

PARAMETRIC STUDIES

Results related to a few parametric studies are presented in this chapter. The gain in maneuvering time, due to the thrust-vectoring enhancement of the aircraft, is shown for a number of maneuvers belonging to one particular family of extremal solutions. The influence of two thrust-vectoring system design parameters upon maneuvering time is discussed. Those parameters are the (maximal) available thrust-vectoring power and the amount of thrust-vectoring roll power. Finally, a set of results is presented to support the answer to the question whether zero sideslip angle at the terminal point yields the best maneuvering time.

5.1 Significance of Parametric Studies. The term *Parametric Studies* is used here to denote a set of related results, obtained by varying a parameter of the aircraft model or a boundary condition of the maneuvers considered. In the context of the problems of interest, parametric studies provide a useful means for investigating the performance of a particular control system design under various circumstances (for example: different reorientation maneuvers) and how various control system designs (e.g. different thrust-vectoring systems) perform for some reorientation maneuvers of interest. Coupled with other design objectives and requirements, parametric studies can help the designer make judicious decisions in the course of the design process.

5.2 Benefit in Maneuvering Time Due to Thrust-Vectoring. Results for two sets of extremals are shown in Figure 6a. They show the aircraft maneuvering

time for two sets of 90° -RVV maneuvers (Maneuver-1). Independent variable is the angle-of-attack α_{0f} (the horizontal axis). The maneuvering time is represented on the vertical axis in (real) seconds. The lower set (lower curve) corresponds to an aircraft with nominal design parameters, while the upper set corresponds to an aircraft without thrust-vector control ($\epsilon_t = 0$). All these results belong to one family of extremals. The upper set of extremals is derived from the lower by decreasing the thrust-vectoring homotopy parameter ϵ_t from 1 to 0. The solid dots merely show some of the members of the family of extremals that is evaluated by varying α_{0f} . The open circles show the points where the switching structure changes along the upper or lower curve. A nominal switching structure is shown in Figure 1e. In the other switching structures some of the switching points swap (change their order) or new switching points emerge (at the beginning or at the end of the trajectory); compare Figures 1e, 2e, 3e and 4e. The dotted segments of the curves represent regions where the switching structure changes very rapidly (for example, about half a dozen different switching structures on an interval of less than five degrees). This rapid change of the switching structures in those regions indicates higher sensitivity of the solution (upon α_{0f}). From this plot one can easily estimate the gain in maneuvering time, due to the thrust-vectoring enhancement, for the reorientation maneuvers considered.

In Figure 6b the maneuvering time is shown for two sets of extremals for Maneuver-2 type of reorientation problems. As before, the lower line corresponds to an aircraft with thrust-vectoring capability, and the upper one to an aircraft without thrust-vectoring capability. Furthermore, both sets of extremals belong to the same family of extremals as those shown in Figure 6a. Below 35° , the family ceases to exist for an aircraft without thrust-vectoring capability. This feature is not thoroughly examined yet. Actually, it appears that the aircraft has unproperly balanced roll, pitch and yaw power for these reorientation maneuvers. The evolution of the adjoint

variables suggests that singular extremals might emerge and exist for smaller α_f . More specifically, the aileron is so powerful at the lower α , where most of the rolling takes place, that the elevator and the rudder can not “cope” successfully with it. Thus, the aileron can not be used with full power (bang-bang). It will need to stay at some intermediate values along a time arc of finite length, starting somewhere at the middle of the trajectory and extending till the end. (Chattering solutions may exist, as well). That is how the family of extremals evolves as α_f is being decreased along the upper curve. As a final remark here, one must note that the evolution of a family of extremals is related to and dependent upon the homotopy path selected. Bifurcation phenomena can be observed in the course of the homotopy procedures. Thus, different homotopy paths can yield different families of extremals.

5.3 Amount of Thrust-Vectoring Power. Figure 7a shows results for two families of extremals obtained by varying the homotopy parameter ϵ_t above and below its nominal value. One can give a physical interpretation of the mathematical model as corresponding to an aircraft with a more or less powerful thrust-vectoring system (e.g. by varying the size of the paddles which deflect the jet-stream). The two lines correspond to 90° -RVV maneuvers for $\alpha_{0f} = 30^\circ$ and $\alpha_{0f} = 50^\circ$, respectively. The stars denote the maneuvering time for the nominal value of the thrust-vectoring power (compare to Figure 6a, lower curve). One can see that by decreasing the thrust-vectoring power, the maneuvering time increases significantly. However, by increasing the thrust-vectoring power, the maneuvering time decreases negligibly. One can conclude that for the two particular reorientation maneuvers corresponding to the extremal considered, the nominal value of the thrust-vectoring power is a good choice. By examining plots like this one, for a variety of reorientation maneuvers and different extremals, one can make a good engineering decision (usually associated with other engineering trade-offs) about an actual implementation of a thrust-vectoring system.

5.4 Contribution of the Thrust-Vectoring Roll Power. In Figure 7b the thrust-vectoring roll power is varied, while keeping the pitch and yaw power at their nominal value. This is done by varying the a_x parameter in the mathematical model (Equations 3-S4 to 3-S6). The families of extremals correspond to the same maneuvers as in Figure 7a. Below certain values of a_x the families could not be extended. The evolution of the adjoint variables λ_P , λ_Q and λ_R suggests that singular extremals may emerge as a_x is decreased further. As can be seen, for these maneuvers and the extremal considered, maneuvering time does not change significantly as the thrust-vectoring roll power varies over a broad range of values. This fact is due to the already described particular nature of the extremal. The aircraft pitches down to lower α since in that region the aileron has a lot of roll power, which is much greater than a thrust-vectoring system can practically produce (for the HARV design). By examining plots like this one for a variety of maneuvers and extremals, a designer can make a decision about how much thrust-vectoring roll power the aircraft should possess. The designer must also include in the analysis the fact that thrust-vectoring roll power is needed at high α (where the aileron is much less effective). In actual flight, the aircraft is subjected to disturbances. If an automatic control-system is implemented for control of the aircraft in the course of the reorientation maneuvers, it should be composed of an open-loop controller and a closed-loop control subsystem (which will cope with the disturbances and the measurement error). The latter will certainly require thrust-vectoring roll power. Another criterion for the designer might be a desire for fault-tolerance: in the case of mechanical failure of the aileron, the thrust-vectoring roll power can be used to safely land the aircraft.

5.5 Minimum-Time Fuselage Pointing Problems. So far only minimum-time rest-to-rest reorientation maneuvers with zero sideslip angle at the initial and the terminal point were considered. As mentioned in Chapter 1, the desire for understanding

the minimum-time reorientation maneuvers arises from the need for the aircraft fuselage to be reoriented rapidly, in a combat situation, in order to fire a missile. In this context, other minimum-time reorientation problems can be posed. Thus, a pilot might want just to reorient the x_b -axis in a certain direction and fire. This is a less constrained problem and thus the corresponding optimal trajectory is faster (at least no slower) than an optimal trajectory where besides the orientation of the x_b -axis at the terminal point a zero sideslip angle is required.

Both problems above belong to the class of minimum-time rest-to-rest reorientation maneuvers. Another interesting class of reorientation maneuvers is the one where the angular velocity at the terminal point is restrained within a certain interval, for example:

$$p \in [-p_{max}, +p_{max}]$$

$$q \in [-q_{max}, +q_{max}]$$

$$r \in [-r_{max}, +r_{max}]$$

From Figures 1 to 4 one can see that some 10 to 20 percent of the terminal part of the trajectory the aircraft already points close to the desired final direction. The angular velocity $\bar{\omega} = (p, q, r)$ is low in the terminal portion of the trajectory (and ultimately decreases to zero), thus it takes a significant portion of the total maneuvering time for relatively small angular displacement. Furthermore, the pilot may not necessarily need a zero angular velocity to lock onto a target and fire. A problem like this can be dealt with from the standpoint of optimal control theory.

The problem of minimum-time x_b -axis pointing can be analyzed independently, as unrelated to the problem of reorientation with zero sideslip angle at the terminal point. One needs to set up an appropriate set of necessary conditions, start from the vacuum case and perform the whole homotopy procedure as it is already done for the zero

final sideslip-angle problem. However, from a practical standpoint one considers that an extremal solution is not acceptable if the angle-of-attack is negative or the sideslip angle large at the terminal point. Also, practice with the homotopy procedures shows that, for the problems considered, for small variations of the terminal conditions there is a high likelihood that an extremal will continue to exist. These observations suggest that the problem of minimum-time x_b -axis pointing can be approached by using results from the zero final sideslip-angle problem. One needs to relate the set of angles already used to specify the aircraft orientation, (α, β, μ) , to the 3-2-1 set of Euler angles (ψ, θ, ϕ) . Here ψ is the azimuth angle, θ is the elevation angle and ϕ is the so called body-roll angle. The orientation of the aircraft x_b -axis is uniquely specified by ψ and θ . If we keep these angles constant and vary ϕ , we get various orientations of the aircraft, all of which have the property that the x_b -axis points in one constant direction.

Figure 8a is related to Maneuver-1 with $\alpha_{0f} = 30^\circ$ and the extremal solution shown in Figure 1. For that maneuver at the terminal point the orientation of the aircraft can be described by $(\alpha_f = 30^\circ, \beta_f = 0^\circ, \mu_f = 90^\circ)$ or $(\psi_f = 30^\circ, \theta_f = 0^\circ, \phi_f = 90^\circ)$. Let us call this orientation the nominal one. Two series of extremals are derived from the nominal. One is derived by increasing ϕ_f from 90° to 110° by small increments of 1° to 2° . The other series is similarly derived by decreasing ϕ_f from 90° to 70° . Thus, a family of extremals is obtained. The time to perform the maneuvers of this family is shown on the vertical axis. The actual minimum of this curve is at $\phi_f^* \approx 91^\circ$. In this case the zero endpoint sideslip-angle maneuver seems to be close to the best that this extremal can offer for the x_b -axis pointing problem. As one can conclude from Figure 1 and the discussion in Section 4.3, the control power in the roll, pitch and yaw channel seems to be well balanced for this particular maneuver and extremal trajectory. The fact that the minimum time is at $\phi_f^* \approx 91^\circ$ and not at $\phi_f = 90^\circ$ can

be simply explained by noting that if the aircraft rolls a little bit more, the additional gyroscopic power supports the pitch and the yaw channel moment power and slightly helps the maneuver globally. But rolling much more increases the maneuvering time. Rolling less than $\phi_f = 90^\circ$ increases the time, too. Careful studies of the extremal solutions, in particular regarding the role of the TV-system throughout the solutions in the family considered, clearly explain this phenomena.

For $\phi_f > \phi_f^*$, the case where the aircraft needs to perform more roll motion, the TV-system exerts its power predominantly in the roll channel. However, for $\phi_f < \phi_f^*$ the aircraft needs to perform less roll motion and thus the TV-system exerts very little of its power in the roll channel (thus more TV-power goes into the pitch and yaw channels). Along the curve, at $\phi_f \approx 81^\circ$ a new switching point emerges, related to λ_P , and for lower body-roll angles ϕ_f the aileron begins with a negative sign (the “wrong” way). As ϕ_f further decreases, this initial period of aileron counter-action becomes longer. Less roll means lower roll angular-rates, which in turn decreases the gyroscopic power in the pitch and yaw channel (the gyroscopic moments are predominant in the nominal extremal, Figures 2g, 2i and 2k). Thus, although more TV-power goes into these channels, maneuvering time decreases.

For $\phi_f > \phi_f^*$, as the aircraft rolls more and thus higher roll rates are achieved, the gyroscopic term in the pitch channel becomes more powerful. The period the elevator is positive decreases (for $\phi_f < \phi_f^*$ it is increased). The bottleneck in this case becomes the elevator negative power, necessary to slow the pitch rate at the final part of the maneuver, and the rudder negative power for the same reason (the terminal point here is at higher α where the control-surface effectiveness is significantly decreased; the TV-system needs to exert more power in the roll channel to support the predominant motion). So, the pitch and yaw channel have more gyroscopic power. However, they get less TV-power and along with requirement for more roll motion,

maneuvering time increases.

Figure 8b shows results related to Maneuver-2 with $\alpha_f = 45^\circ$ and the extremal described in Section 4.4 and Figure 3. Maneuvering time decreases with ϕ_f in a broad interval. The actual minimum time occurs at $\phi_f^* = 109^\circ$. There is a relatively simple explanation for this phenomenon. One needs to notice that, for $\phi_f = 70^\circ$ and $\phi_f = 110^\circ$, α_f is (still) close to 45° and $\beta_f \approx \pm 10^\circ$. From Figures A1 and A3 one can see that $C_l^0(45^\circ, \pm 10^\circ)$ and $C_n^0(45^\circ, \pm 10^\circ)$ are significant in value. The result in Figure 8b is a good illustration of how an aircraft can take advantage of the aerodynamic static moments (which are due to nonzero sideslip angle) to perform a maneuver faster. For small ϕ_f the sideslip angle at the terminal point is negative. This causes (significant) positive roll and yaw aerodynamic static moments to develop. Thus a considerable amount of (negative) thrust-vectoring and aerodynamic-control surfaces power is needed to fight these moments. For large ϕ_f the terminal sideslip angle is positive, which yields negative roll and yaw static moments (of significant magnitude), which act quite supportively to the controls at the last part of the trajectory (help decelerate the angular rate to zero). In this case for a relatively larger portion of the first part of the trajectory the roll and yaw controls accelerate the aircraft (compared to the case of smaller ϕ_f). Thus, the developed higher gyroscopic term supports the pitch channel better. All this explains why maneuvering time decreases with increasing ϕ_f .

However, beyond $\phi_f > \phi_f^*$ time starts increasing again (not shown in the plot), and the extremal eventually may cease to exist. Namely, the yaw channel becomes a bottleneck. At $\phi_f = 110^\circ$ the controls δ_z and δ_r are positive all the time. The aircraft decelerates in the yaw direction by using the gyroscopic term and the aerodynamic static term C_n^0 . Due to the high roll and pitch rates the gyroscopic term, which is significant in value and negative all the time, starts opposing the positive action of

the yaw controls in the first part of the trajectory (Figure 3k and Section 4.4). For large ϕ_f the TV-system exerts very little power in the roll channel (the aileron is quite powerful and is supported by the aerodynamic static roll moment C_l^0), and a lot of power in the pitch and (especially) in the yaw channel, but eventually (for $\phi_f > \phi_f^*$) this can not help enough and maneuvering time increases.

One can note that for Maneuver-2 with $\alpha_f = 45^\circ$ the aircraft needs to pitch up and roll positive most of the time, which means a negative gyroscopic term in the yaw channel needs to be developed. In this particular extremal (Figure 3) the aircraft pitches down first primarily to fight against development of negative gyroscopic term in the yaw channel too early.

An extremal where the aircraft starts or ends by rolling in the “wrong” direction can not be ruled out a priori (indeed, such exist for the case of an aircraft without thrust-vectoring, Figures 2e and 4e). Actually, rolling in the “wrong” direction has no purpose of decreasing maneuvering time, but fighting against excess of power (not well balanced proportion of power in the roll, pitch and yaw channel). Thus, one can see that various trade-offs need to be made between different effects in the course of the maneuver. The trade-offs are made in portions of the trajectory (on a local level). The purpose is, obviously, to improve the extremal maneuver globally.

Also, while one extremal can yield very good results for some reorientation maneuvers, another extremal may be better for other reorientation maneuvers or different values of the aircraft design parameters.

CHAPTER VI

CONCLUDING REMARKS

The work presented demonstrates that very complex and accurate mathematical models can be used in conjunction with optimal control theory in analysing the problem of time-optimal reorientation maneuvering of aircraft. A methodology for such analyses is established, and the major ingredients of the problem identified.

This work can serve as a solid basis for future research. One should study more extremal solutions for a larger set of reorientation maneuvers. The extremal solutions should be analyzed as aircraft design parameters are varied. This can yield understanding about the domain of existence of the extremal solutions, and provide some useful design rules for the aircraft, as well.

Ultimately, it will become possible to develop an on-board automatic control system that will provide guidance of the aircraft in the course of the reorientation maneuvers.

REFERENCES

- [1] W. B. Herbst, *Future Fighter Technologies*, Journal of Aircraft 17 (August 1980), pp. 561–566.
- [2] W. B. Herbst *Dynamics of Air Combat*, Journal of Aircraft 20 (July 1983), pp. 594–598.
- [3] K. H. Well, B. Farber and E. Berger, *Optimization of Tactical Aircraft Maneuvers Utilizing High Angles of Attack*, Journal of Guidance and Control 5 (March-April 1982), pp. 131–137.
- [4] D. S. Hague, *Multiple-Tactical Aircraft Combat Performance Evaluation System*, Journal of Aircraft 18 (July 1981), pp. 513–520.
- [5] J. Kalviste, *Measure of Merit for Aircraft Dynamic Maneuvering*, SAE Technical Paper 901005, SAE Aerospace Atlantic Meeting, Dayton, OH (23–26 April 1990).
- [6] E. M. Cliff, F. H. Lutze, B. G. Thompson and K. H. Well, *Toward a Theory of Aircraft Agility*, Proceedings, AIAA Atmospheric Flight Mechanics Conference, Portland, OR (August 1990), pp. 85–93.
- [7] D. R. Riley and M. H. Drajeske, *Relationship Between Agility Metric and Flying Qualities*, SAE Technical Paper 901003, SAE Aerospace Atlantic Meeting, Dayton, OH (23–26 April 1990).

- [8] J. L. Junkins and J. D. Turner, "Optimal Spacecraft Rotational Maneuvers", Elsevier Science Publishing Company Inc., New York 1986.
- [9] J.P. Marec, "Optimal Space Trajectories", Elsevier Science Publishing Company Inc., New York 1979.
- [10] N. X. Vinh, "Optimal Trajectories in Atmospheric Flight", Elsevier Science Publishing Company Inc., New York 1981.
- [11] R. S. Chowdhry and E. M. Cliff, *Optimal Rigid-Body Reorientation Problem*, Proceedings, AIAA Atmospheric Flight Mechanics Conference, Portland, OR (August 1990), pp. 1550-1560.
- [12] K. H. Well and E. Berger, *Minimum-Time 180° Turns of Aircraft*, Journal of Optimization Theory and Applications, Vol. 38, No. 1 (September 1982), pp. 83-96.
- [13] H. Goldstein, *Classical Mechanics* (2nd edition), Addison-Wesley, Reading, Mass. 1980.
- [14] B. Etkin, "Dynamics of Atmospheric Flight", John Wiley & Sons Inc., New York 1972, pp. 104-128.
- [15] M. L. Roy and C. Buttrill, *F18NEW FORTRAN* code and *T5AERO* data for the HARV, NASA Langley Research Center (1987).
- [16] L. S. Pontriagin, V. G. Boltyanskii, R. V. Gamkrelidze and E. F. Mishchenko, "The Mathematical Theory of Optimal Processes", Interscience, New York and London 1962.
- [17] V. M. Alekseev, V. M. Tikhomirov and S. V. Fomin, "Optimal Control", Consultants Bureau, New York and London 1987.

- [18] A. E. Bryson, Jr. and Yu-Chi Ho, "Applied Optimal Control", Hemisphere Publishing Corporation, New York 1975.
- [19] R. Gabasov and F. Kirillova, "The Qualitative Theory of Optimal Processes", Control and Systems Theory, Volume 3, Marcel Dekker Inc., New York and Basel 1976.
- [20] "IMSL MATH/LIBRARY Fortran Subroutines for Mathematical Applications", IMSL, Houston, Texas.
- [21] J. Stoer and R. Bulirsch, "Introduction to Numerical Analysis", Springer-Verlag, New York 1980.
- [22] H. J. Oberle and W. Grimm, "BNDSCO - A Program for the Numerical Solution of Optimal Control Problems", English Translation of DFVLR-Mitt. 85-05, ICAM - Virginia Tech.
- [23] E. A. Coddington and N. Levinson, "Theory of Ordinary Differential Equations", McGraw-Hill, New York 1979.
- [24] S. Bocvarov, F. H. Lutze, E. M. Cliff and K. H. Well, *Time-Optimal Reorientation Maneuvers for an Aircraft With Thrust-Vector Control*, AIAA Guidance, Navigation and Control Conference, New Orleans, LA (August 1991).
- [25] S. Bocvarov, E. M. Cliff and F. H. Lutze, "Mathematical Model of the HARV for Time-Optimal Reorientation Maneuvers", ICAM - Virginia Tech.

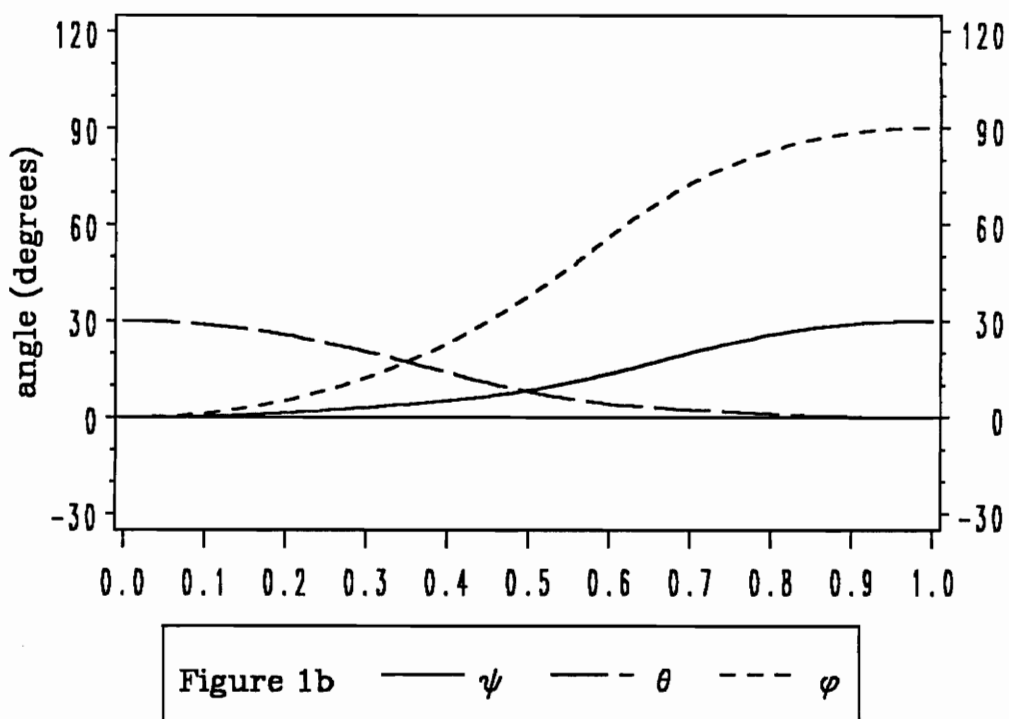
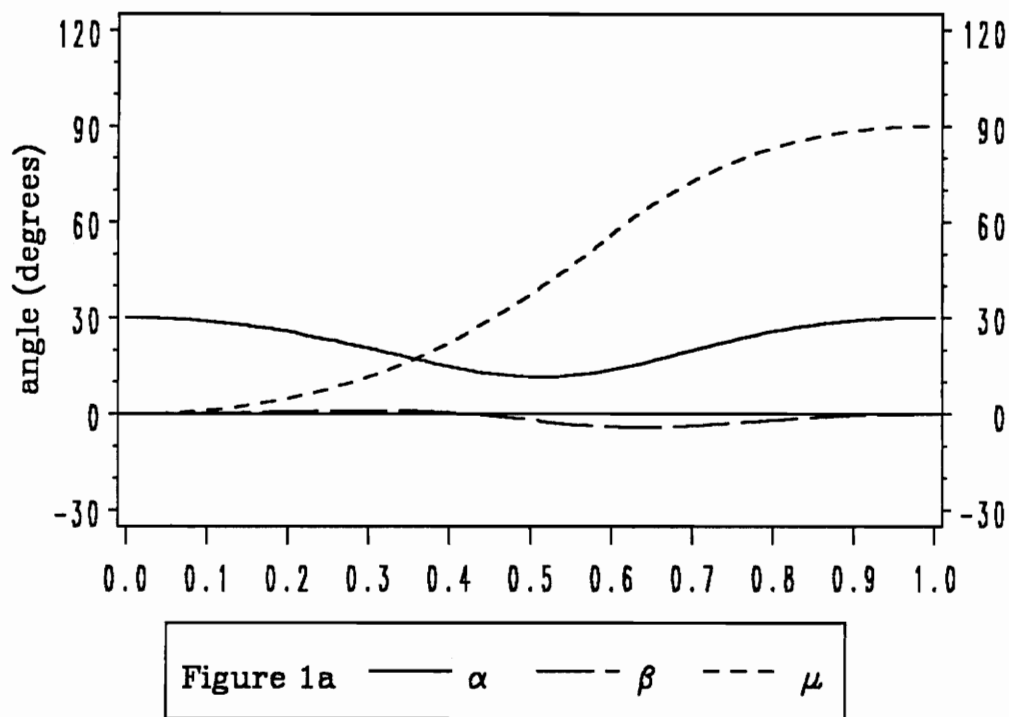


Figure 1. Maneuver-1: details of an extremal (with TV)

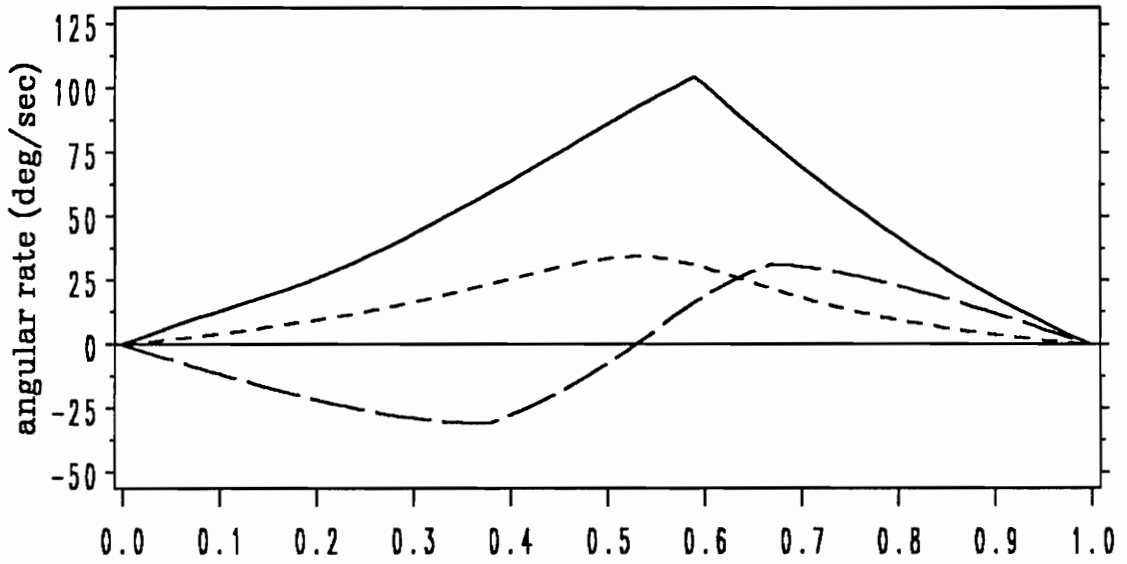


Figure 1c — p — q — r

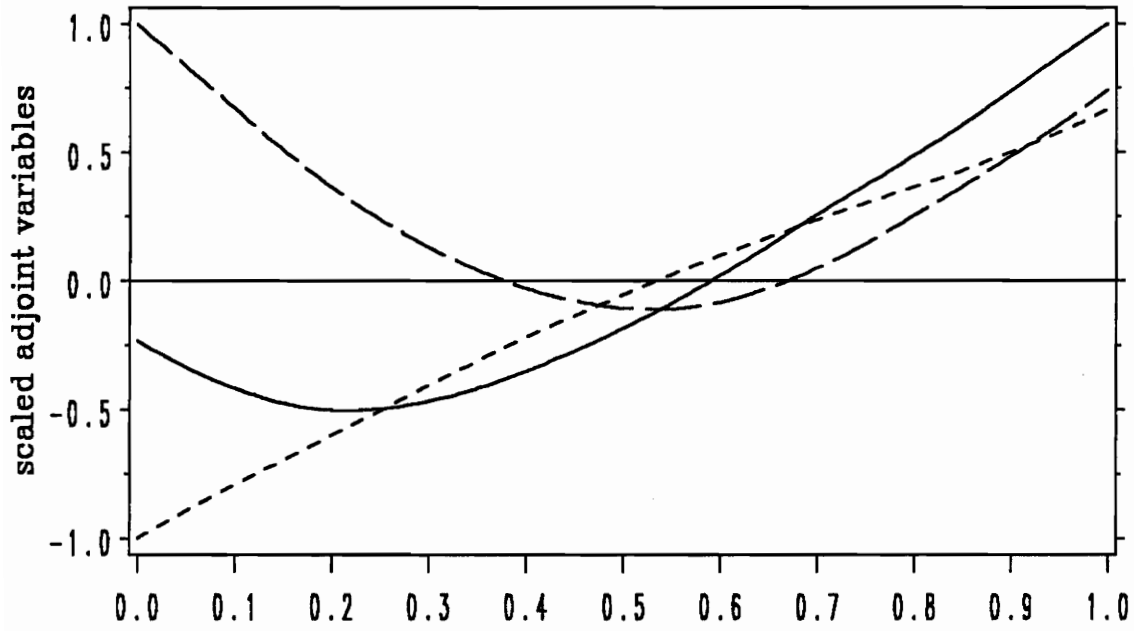


Figure 1d — λ_p — λ_q — λ_r

Figure 1. (continued)

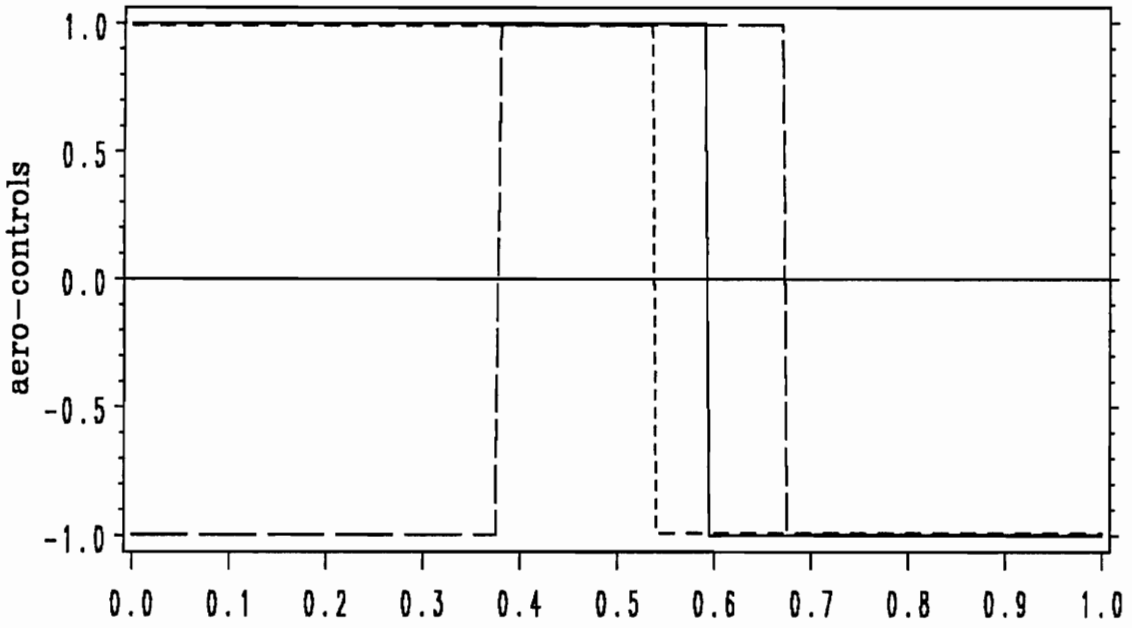


Figure 1e — $\Delta\alpha$ — δe — $\delta\tau$

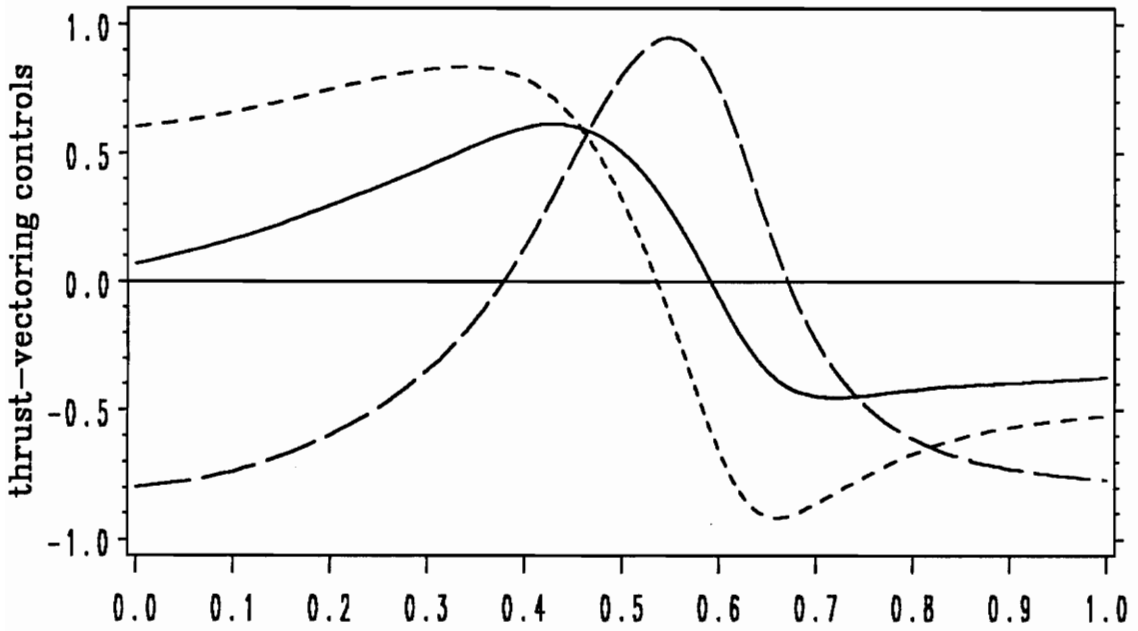


Figure 1f — δx — δy — δz

Figure 1. (continued)

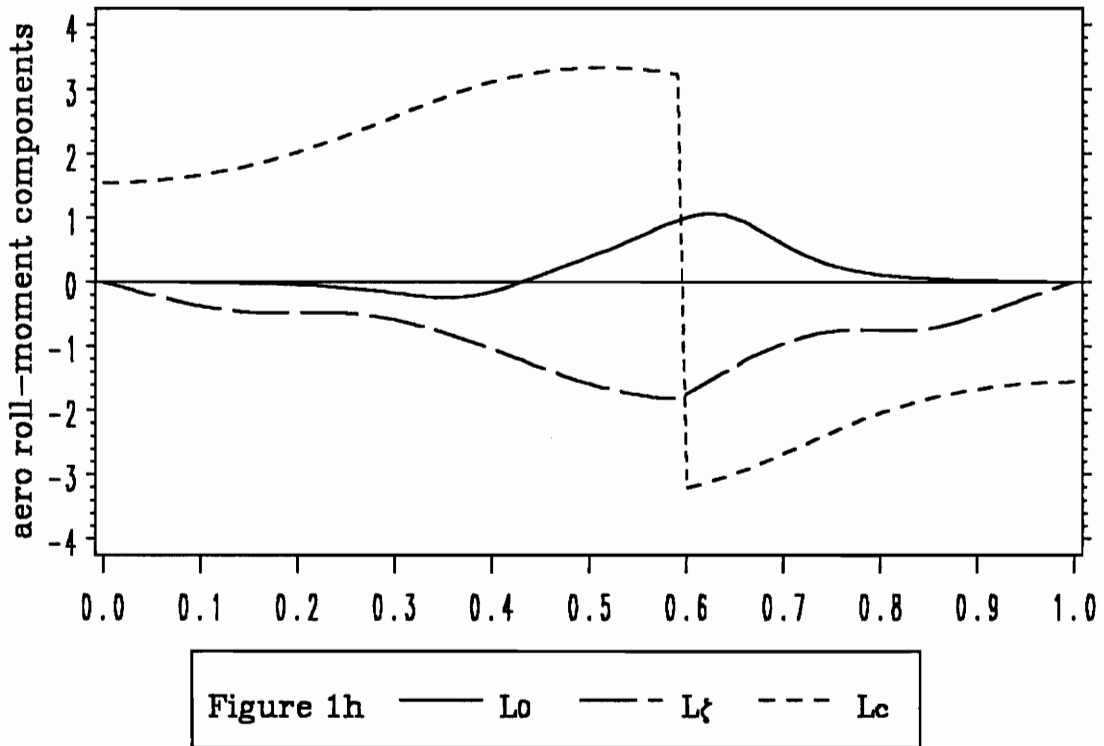
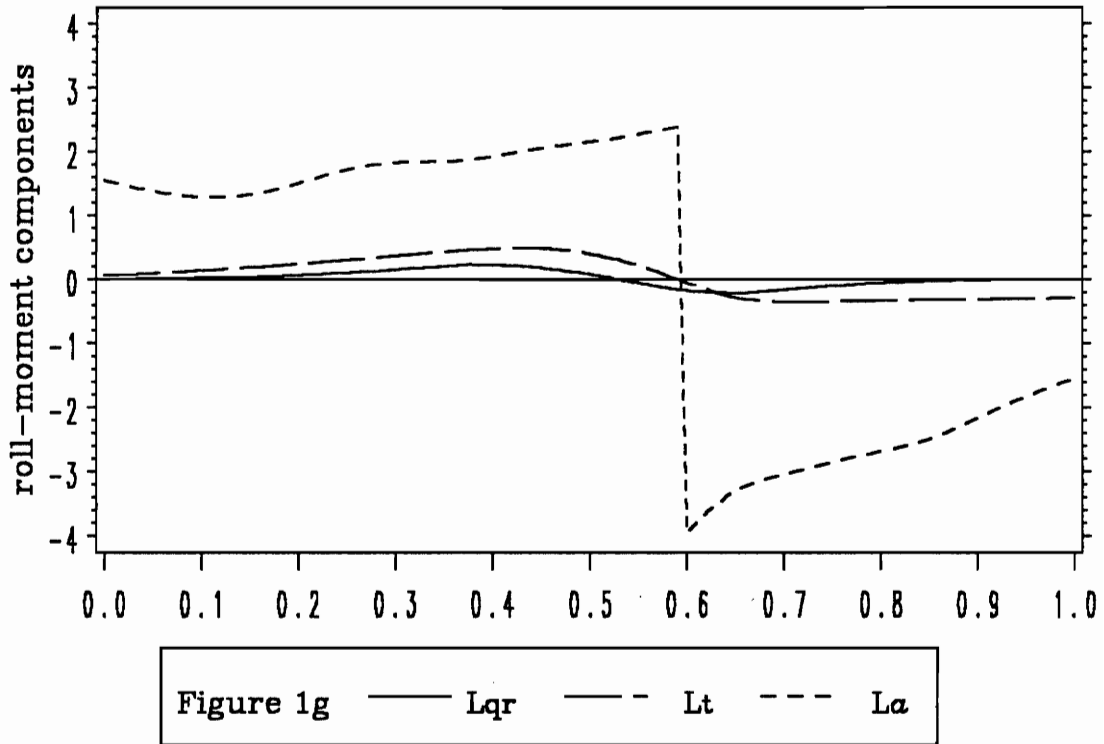


Figure 1. (continued)

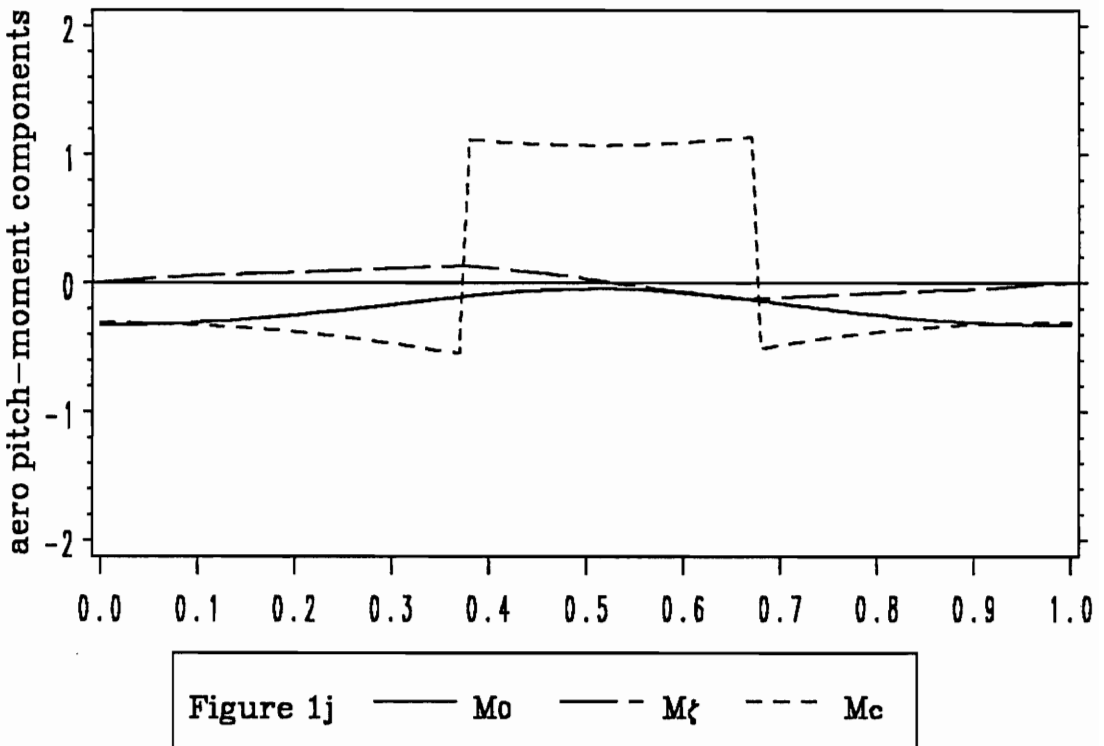
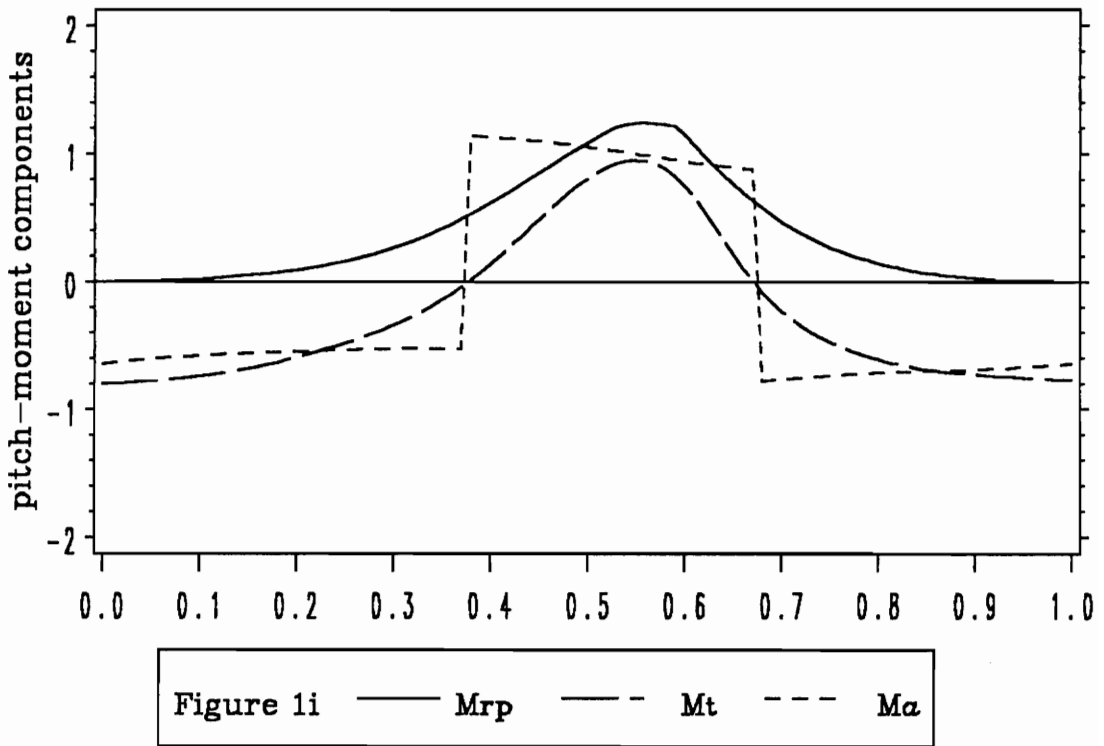


Figure 1. (continued)

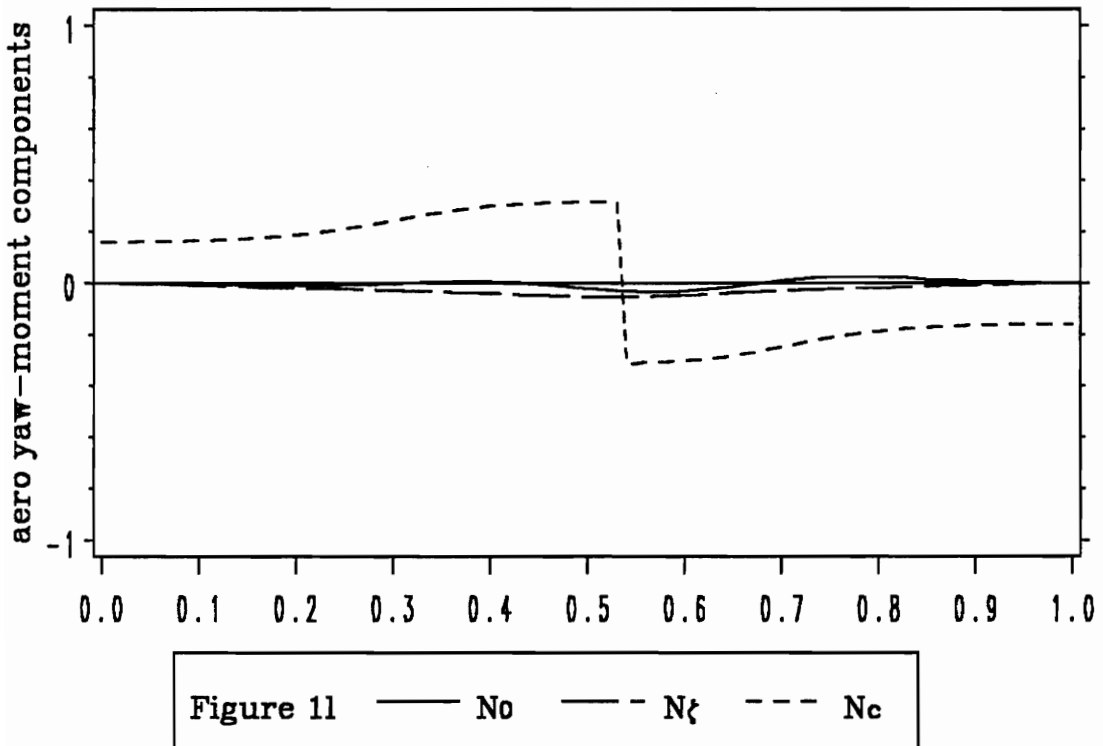
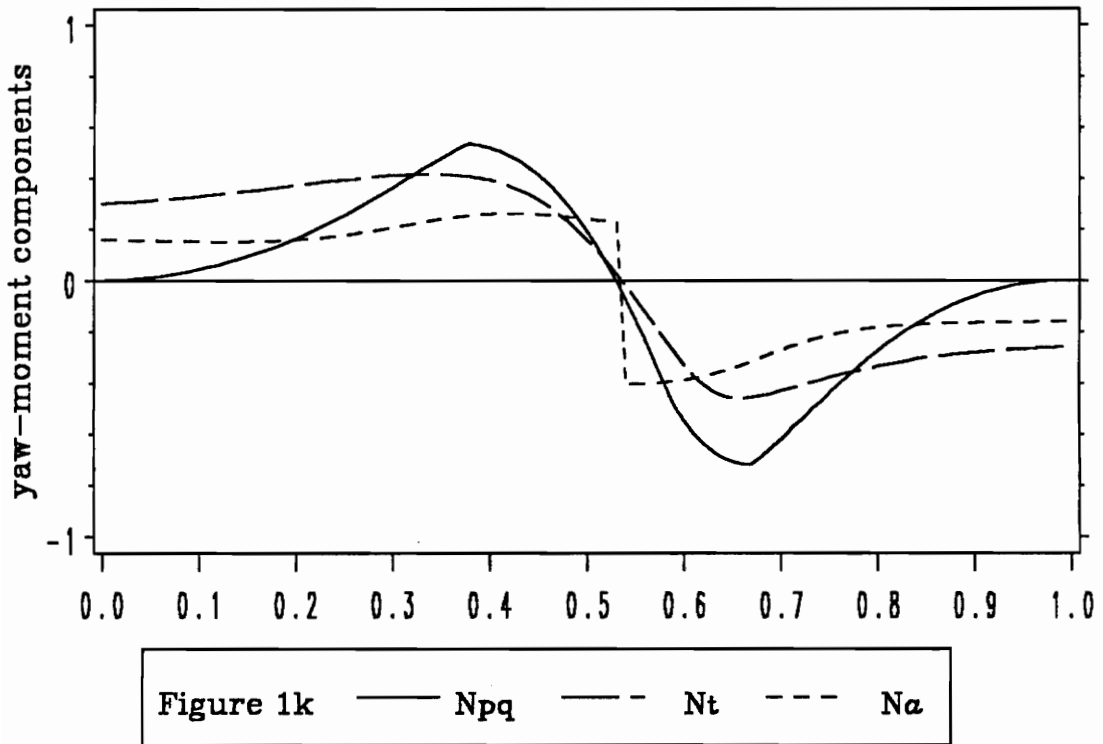


Figure 1. (continued)

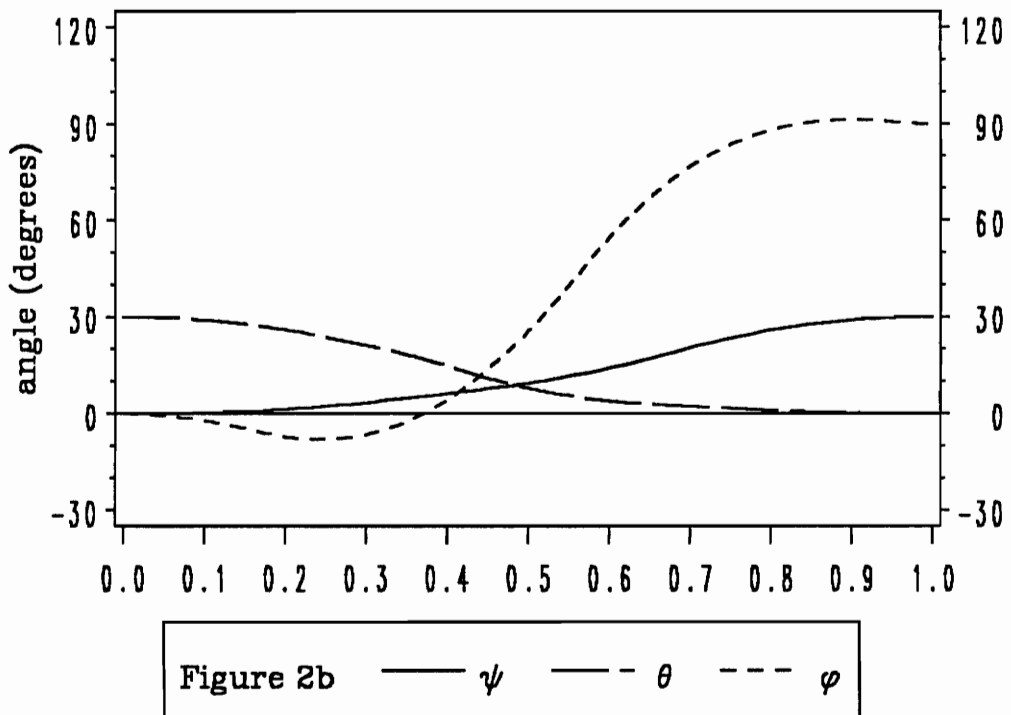
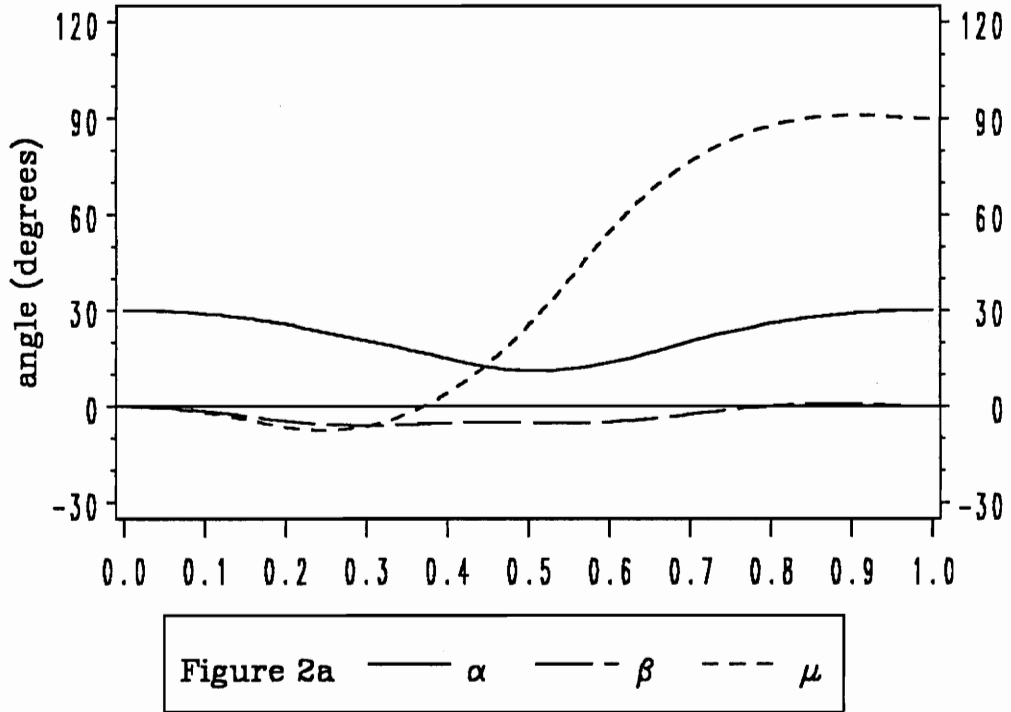


Figure 2. Maneuver-1: details of an extremal (without TV)

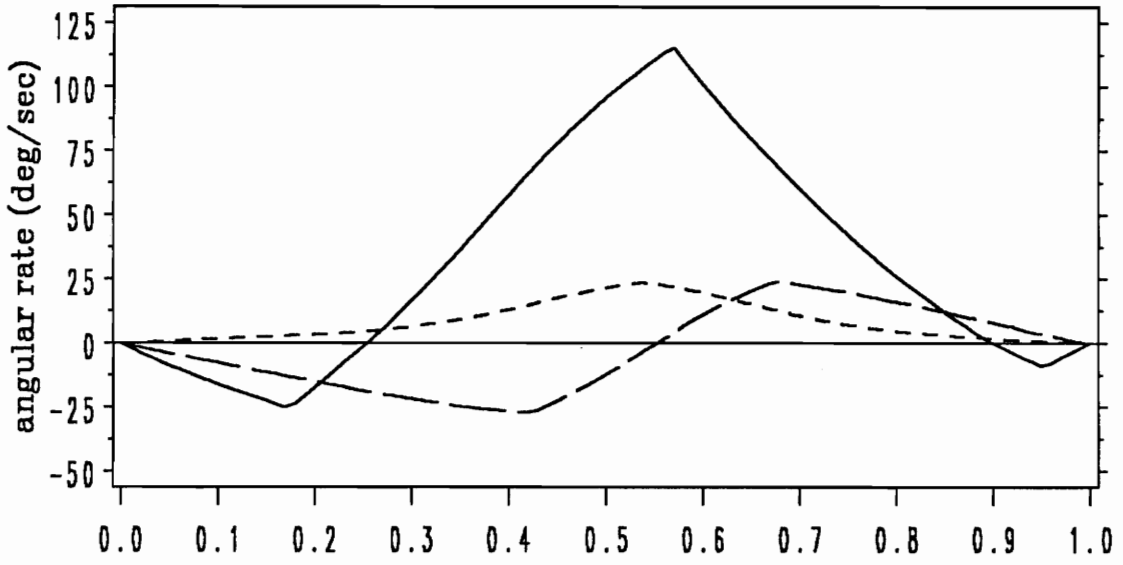


Figure 2c — p — q — r

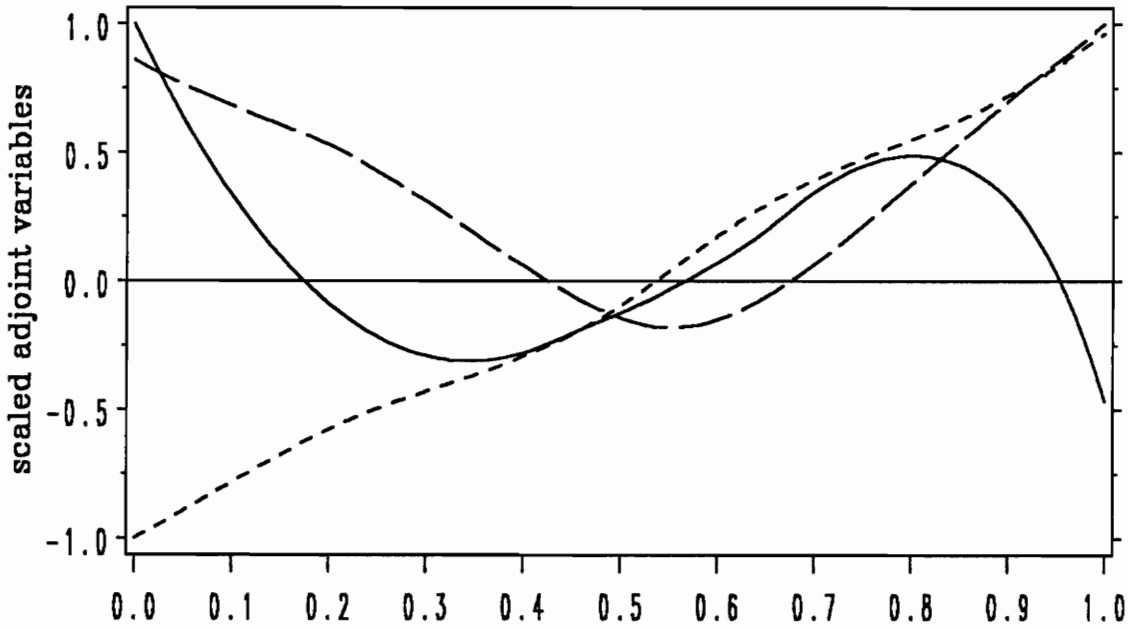


Figure 2d — λ_p — λ_q — λ_r

Figure 2. (continued)

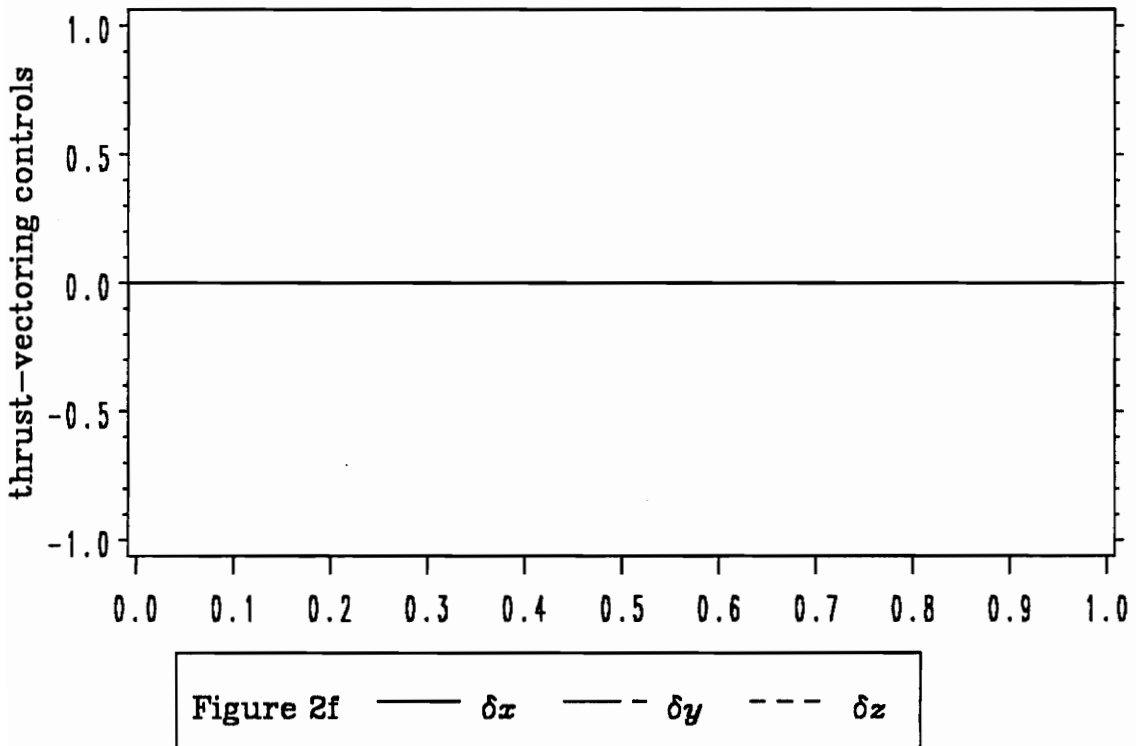
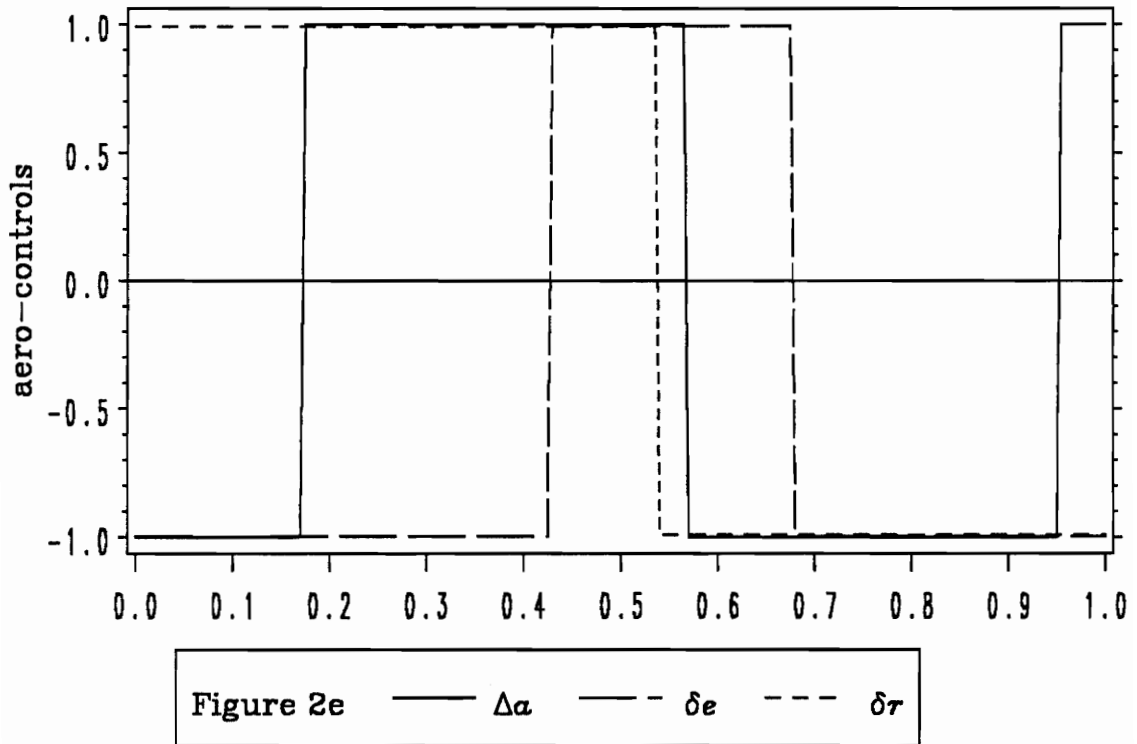


Figure 2. (continued)

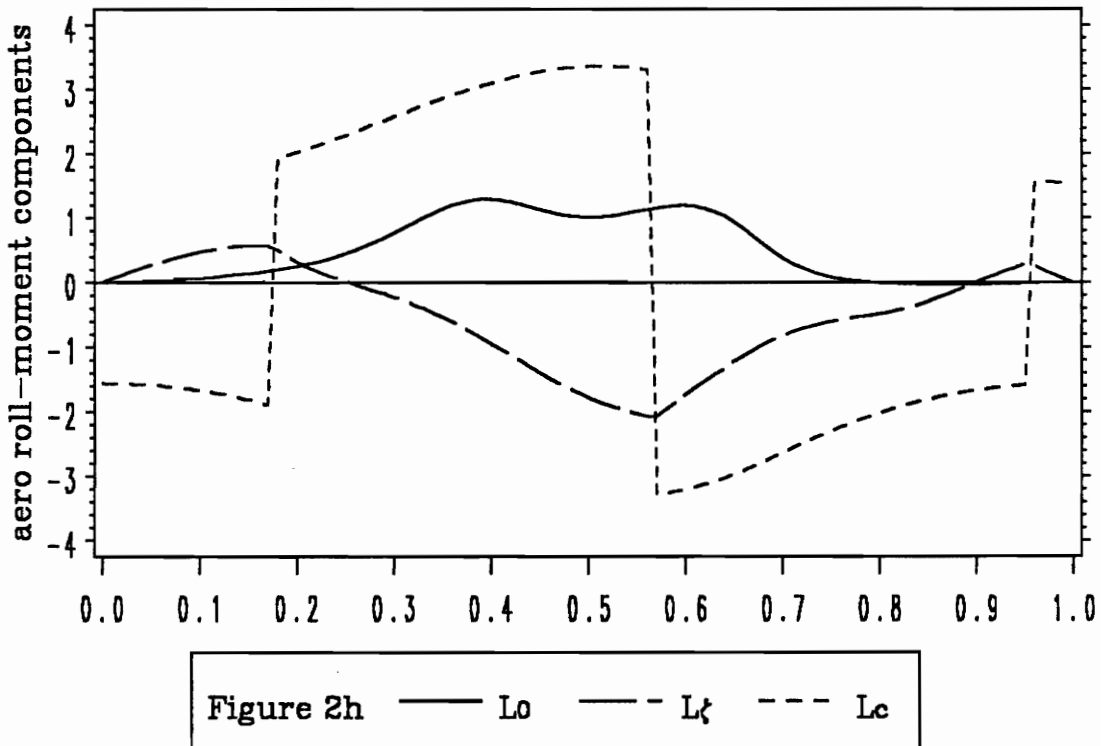
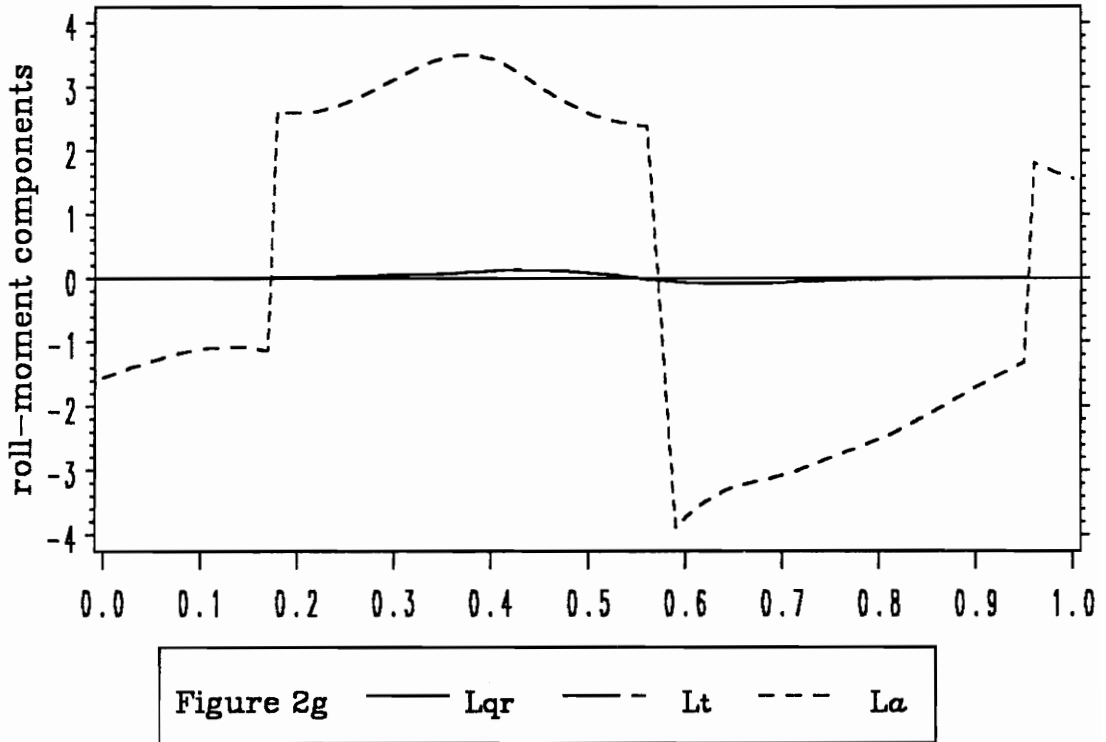


Figure 2. (continued)

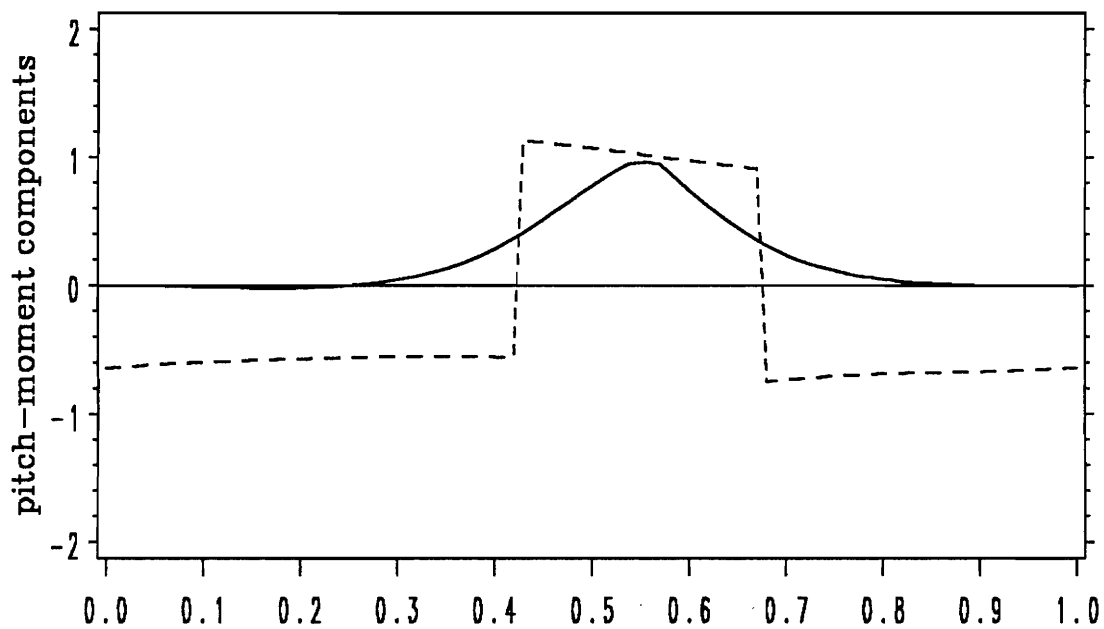


Figure 2i — M_{rp} — M_t — M_a

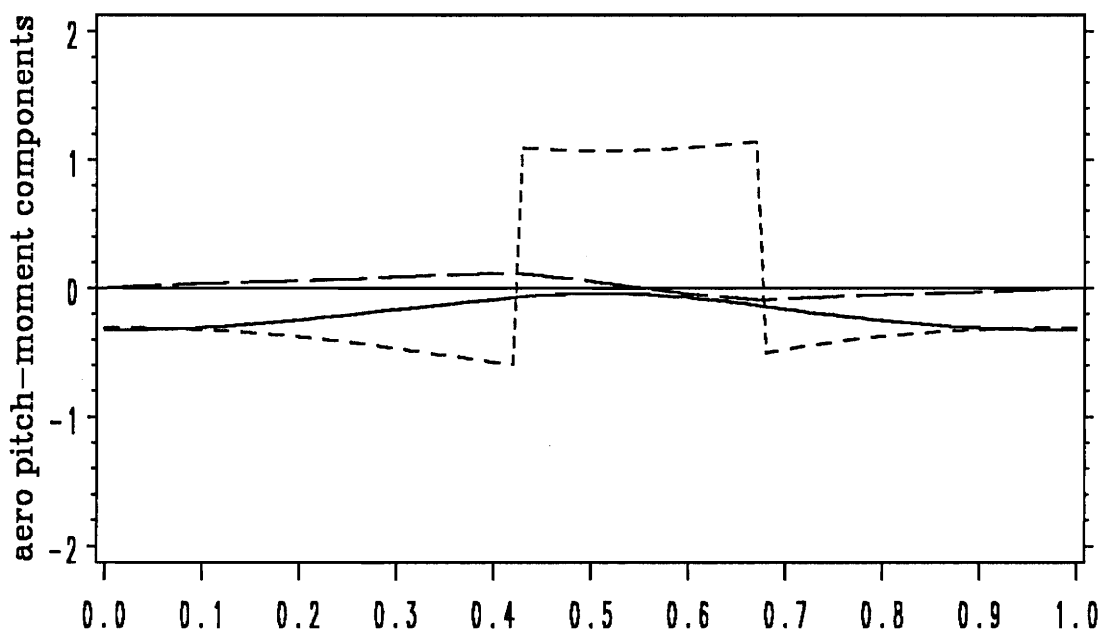


Figure 2j — M_o — M_ξ — M_c

Figure 2. (continued)

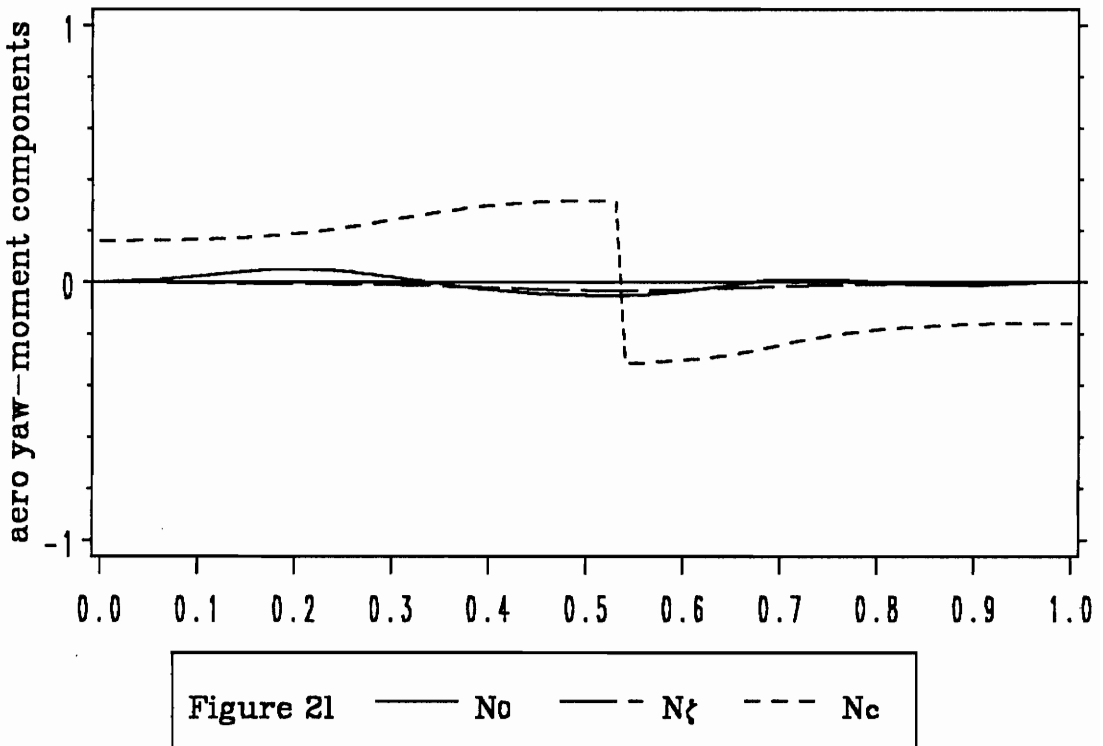
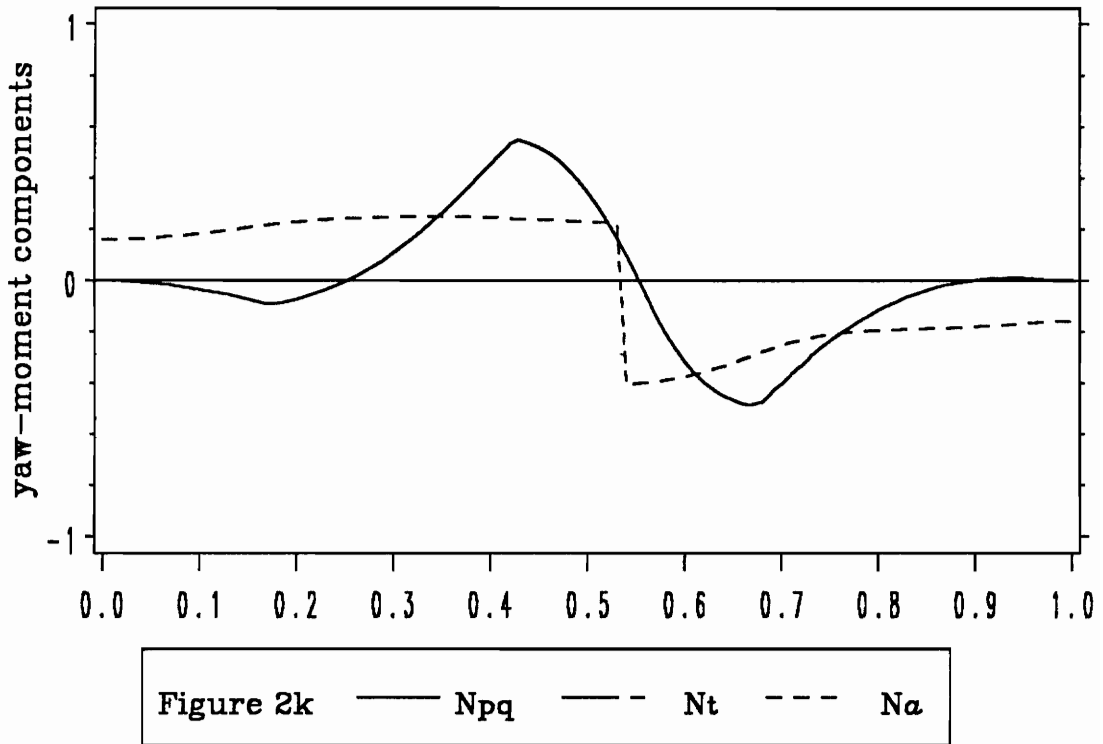


Figure 2. (continued)

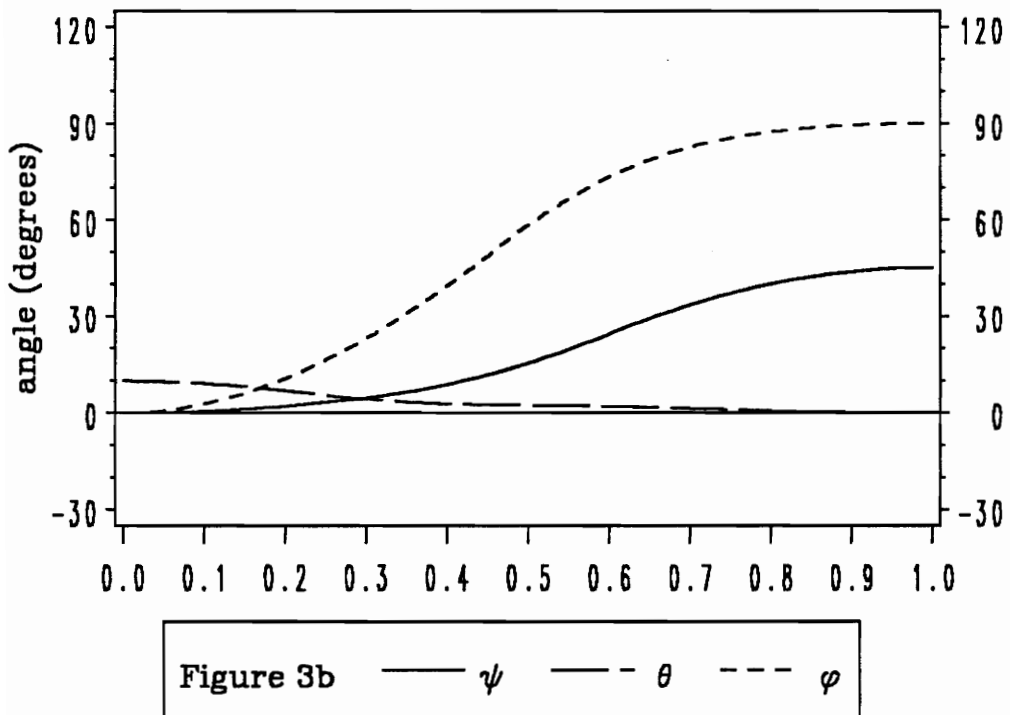
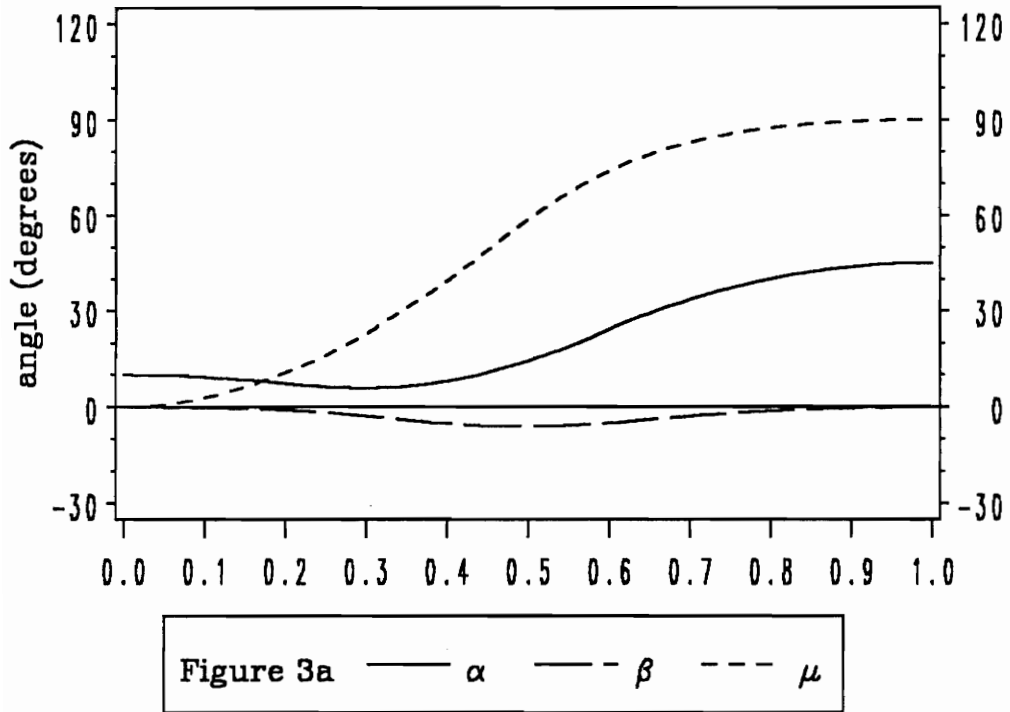


Figure 3. Maneuver-2: details of an extremal (with TV)

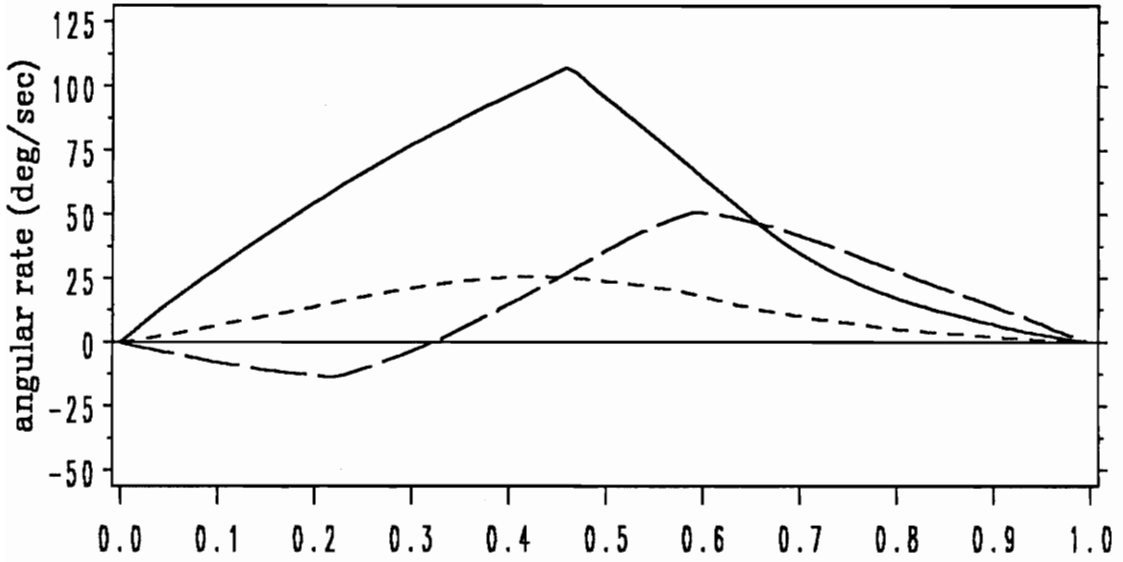


Figure 3c — p — q — r

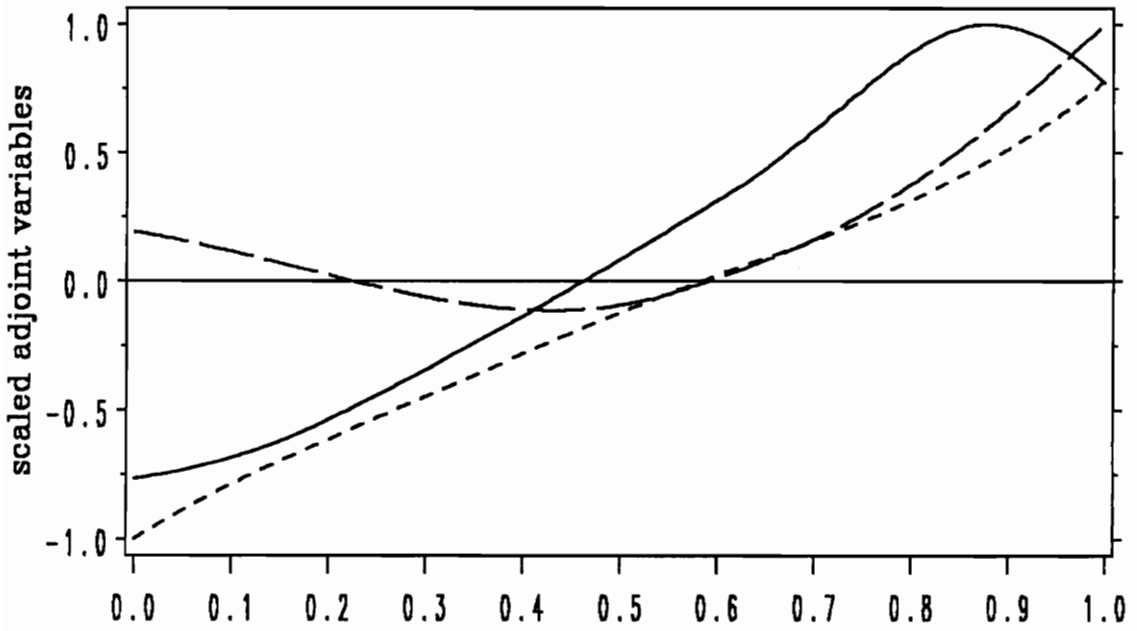


Figure 3d — λ_p — λ_q — λ_r

Figure 3. (continued)

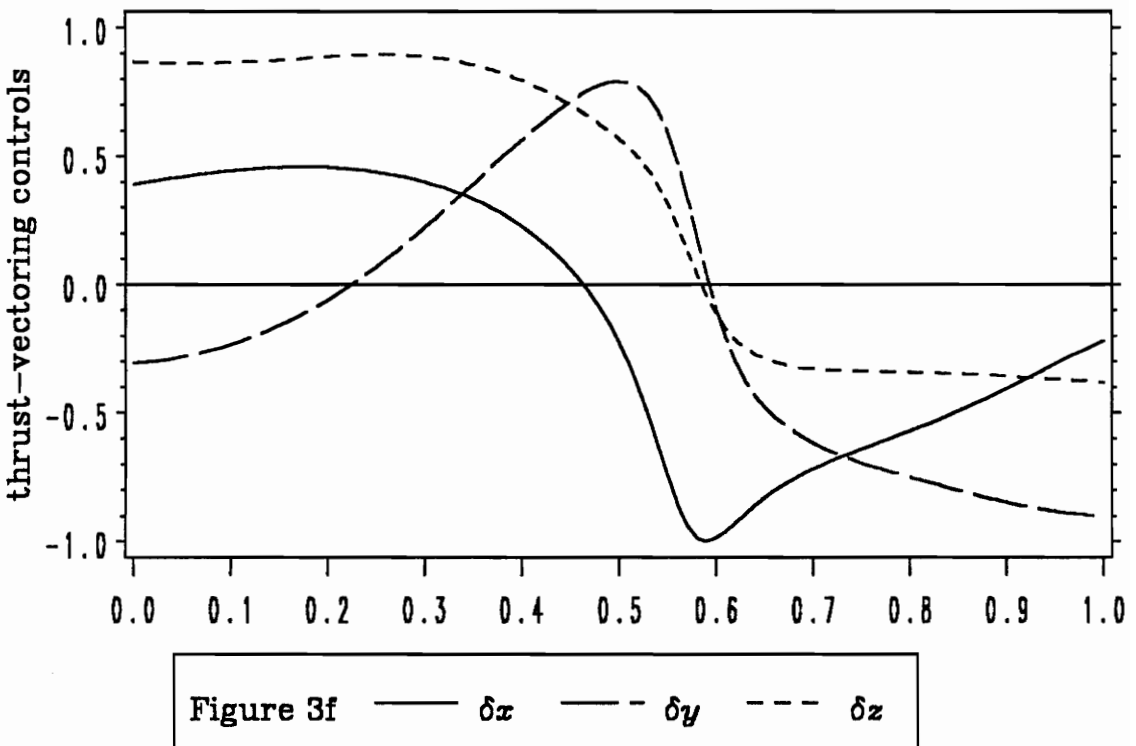
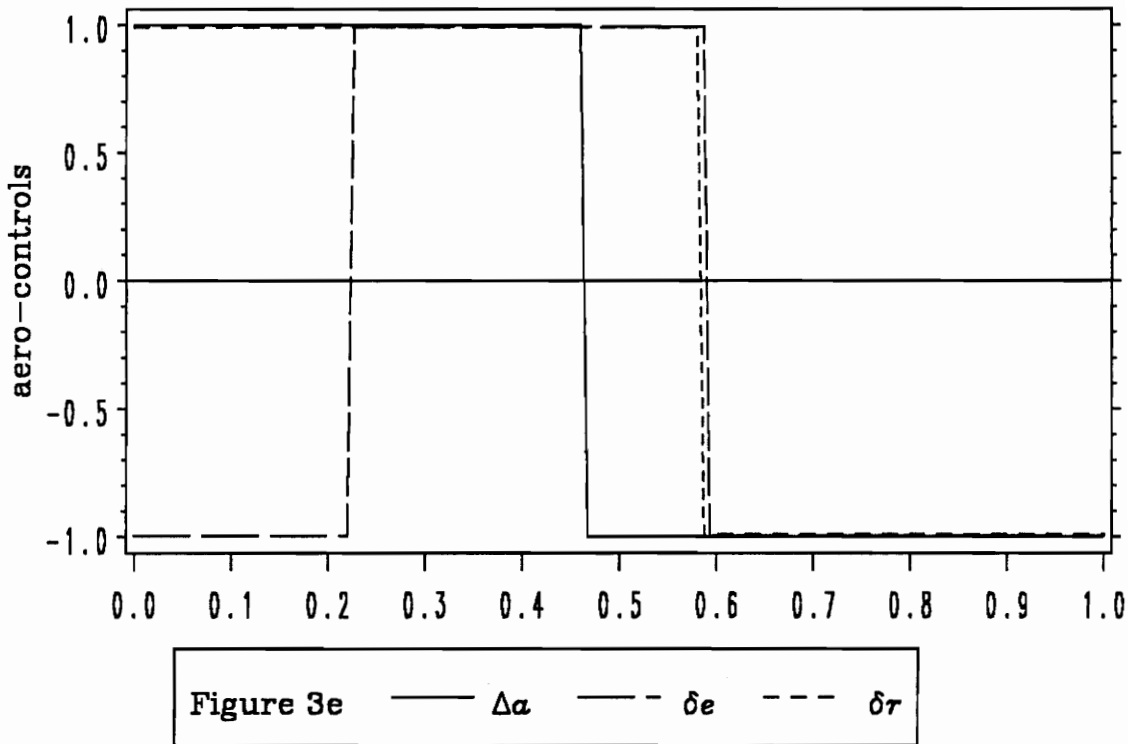


Figure 3. (continued)

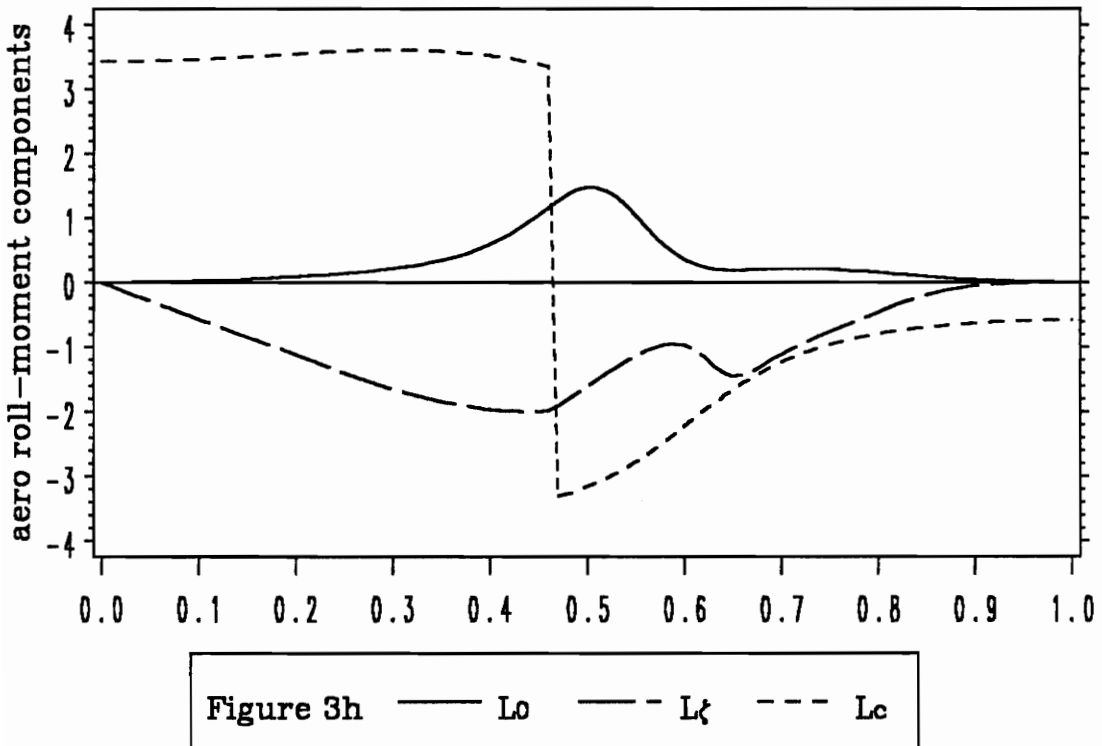
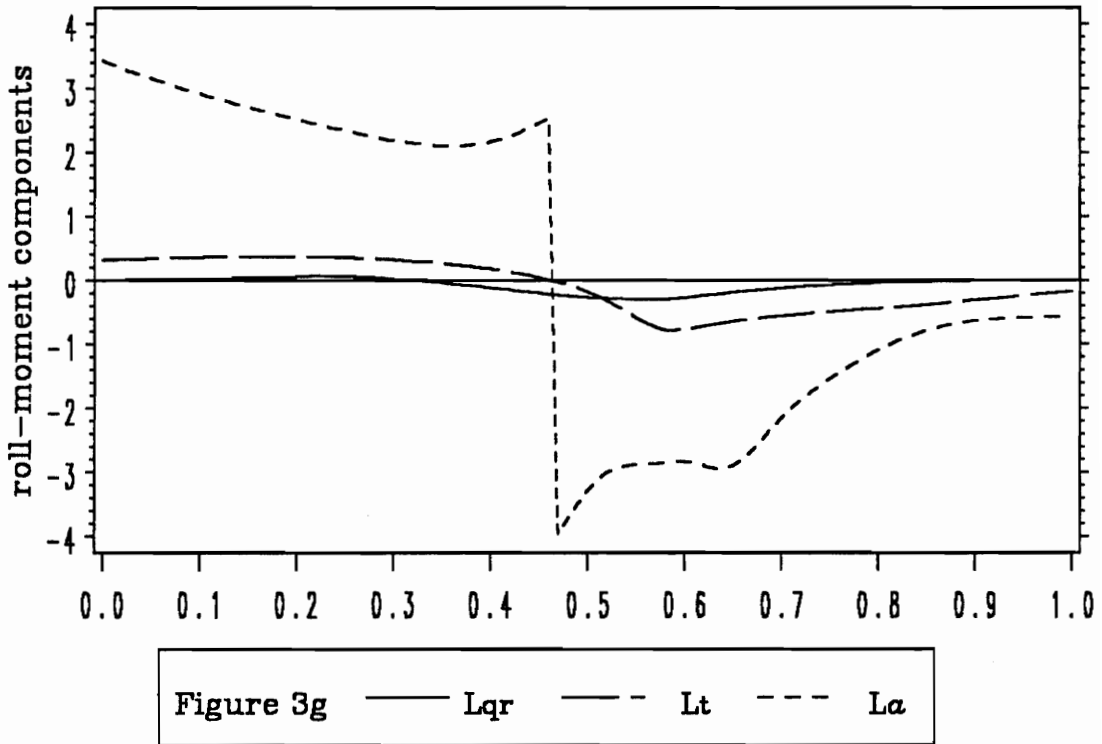


Figure 3. (continued)

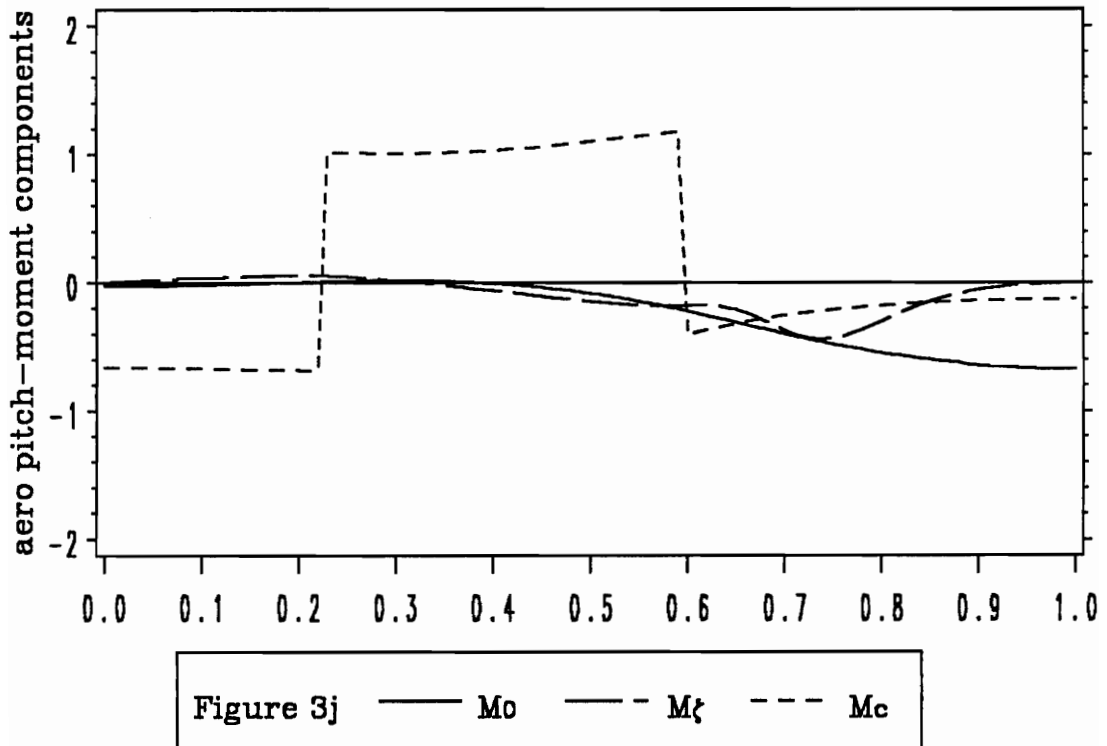
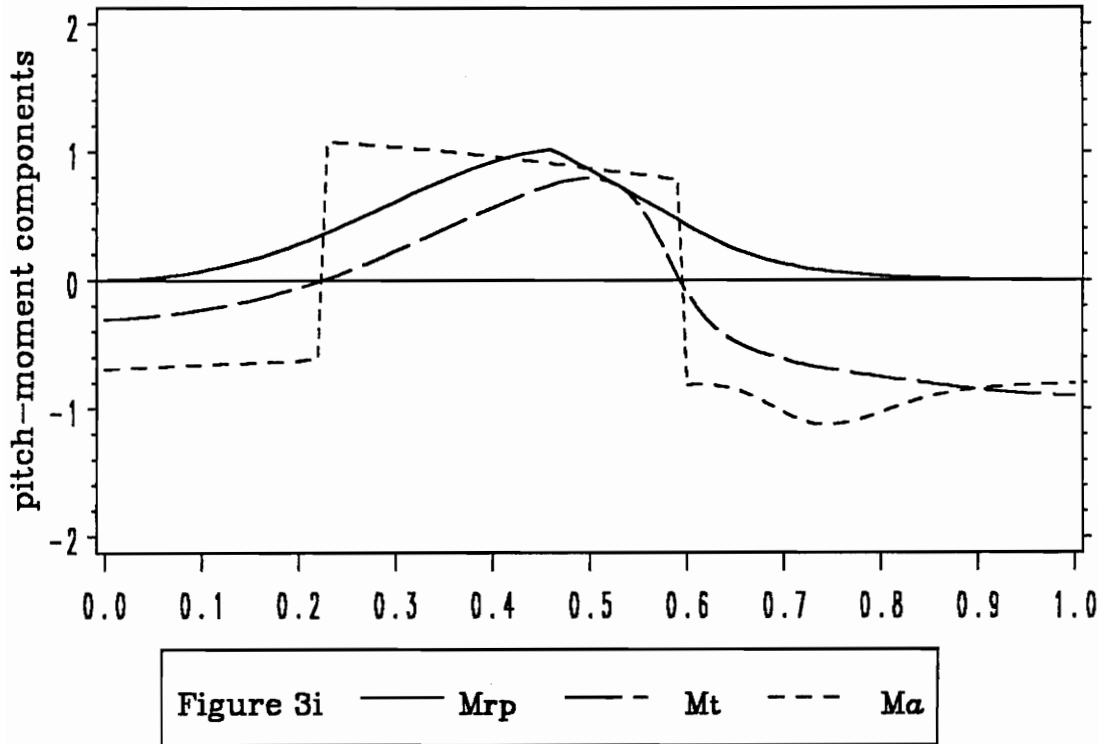


Figure 3. (continued)

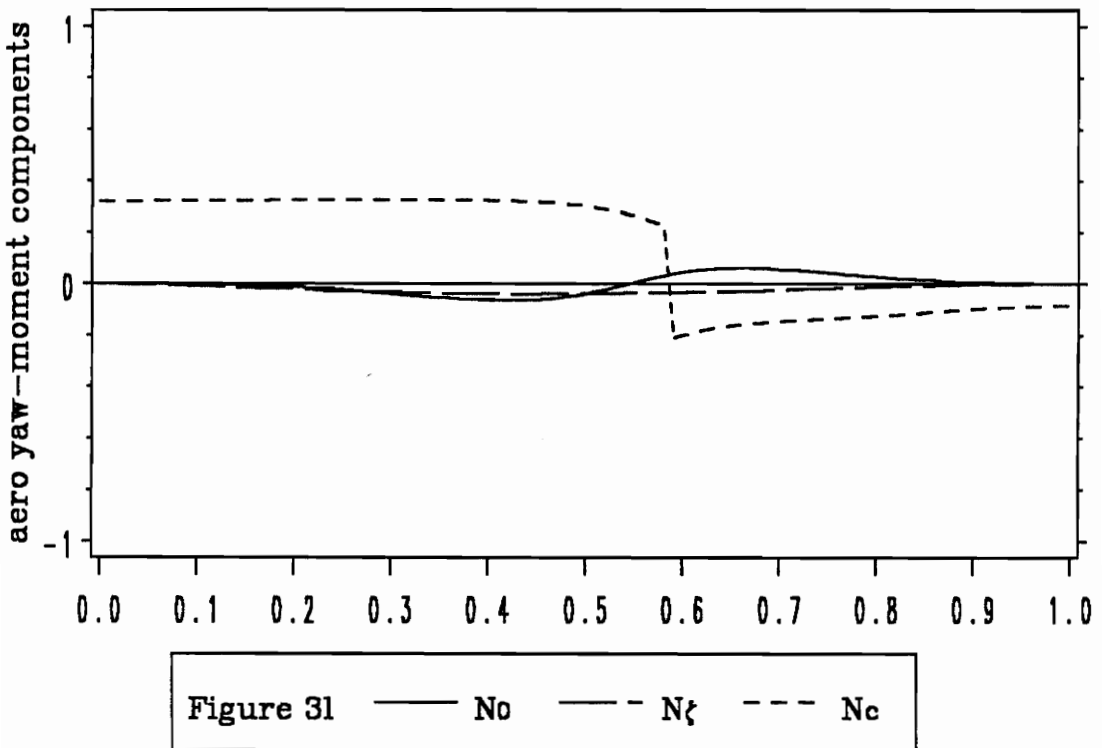
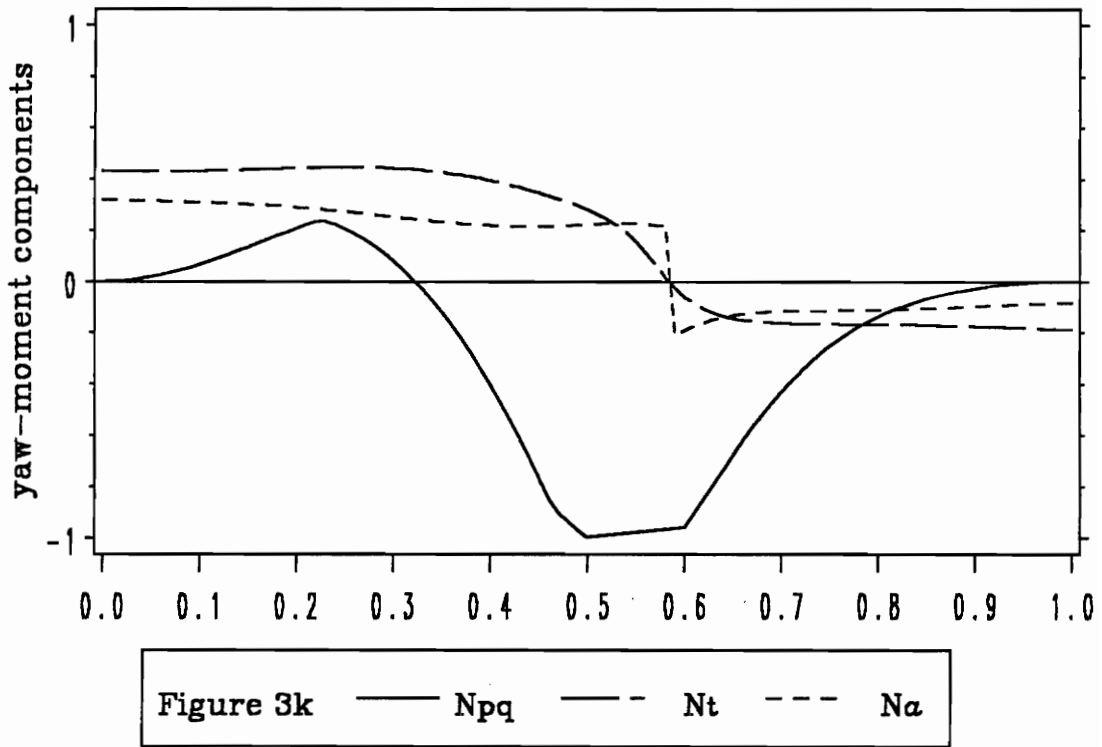


Figure 3. (continued)

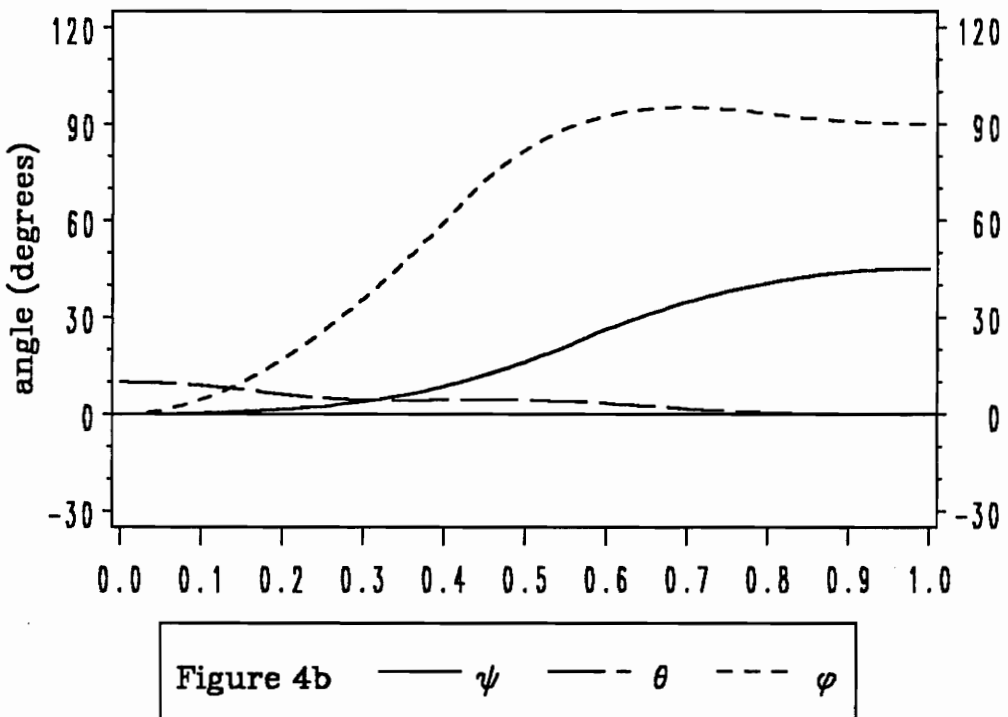
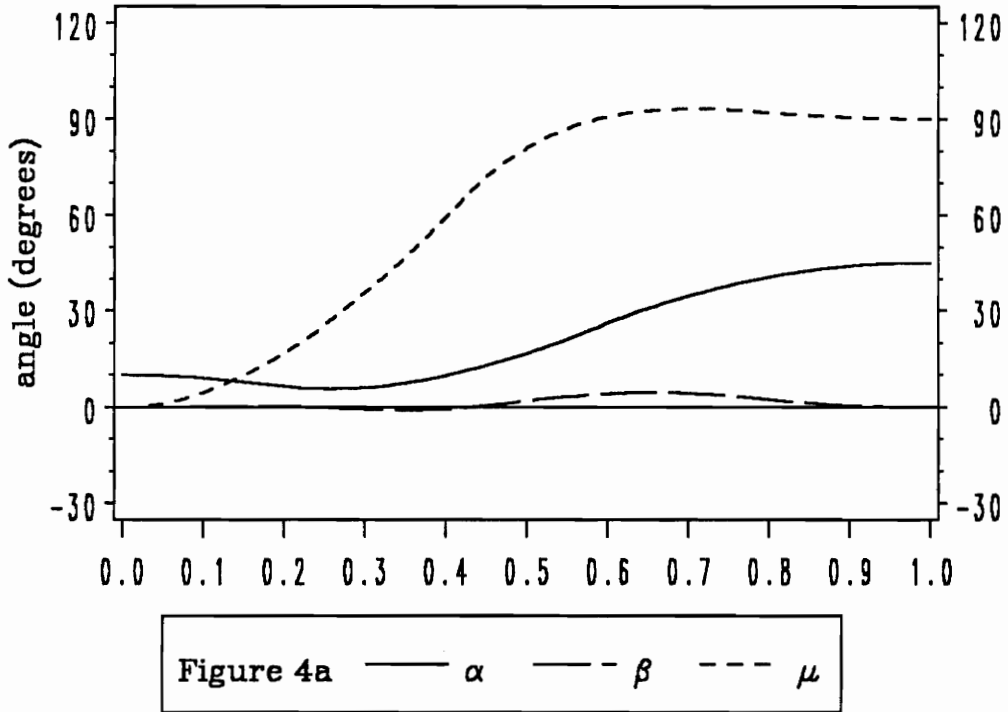


Figure 4. Maneuver-2: details of an extremal (without TV)

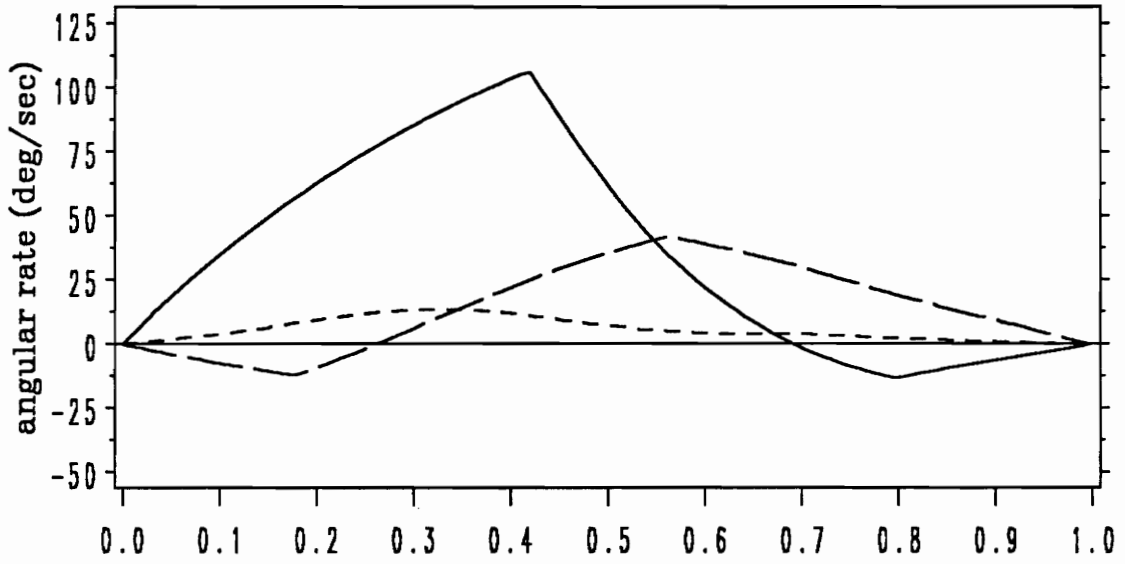


Figure 4c — p — q — r

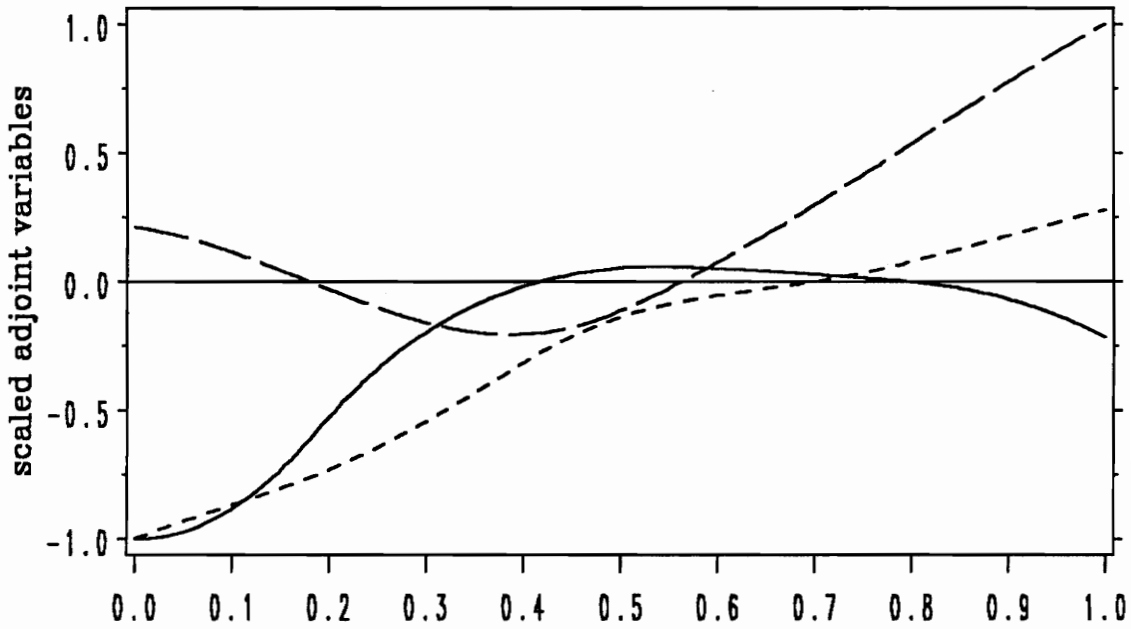


Figure 4d — λ_P — λ_Q — λ_R

Figure 4. (continued)

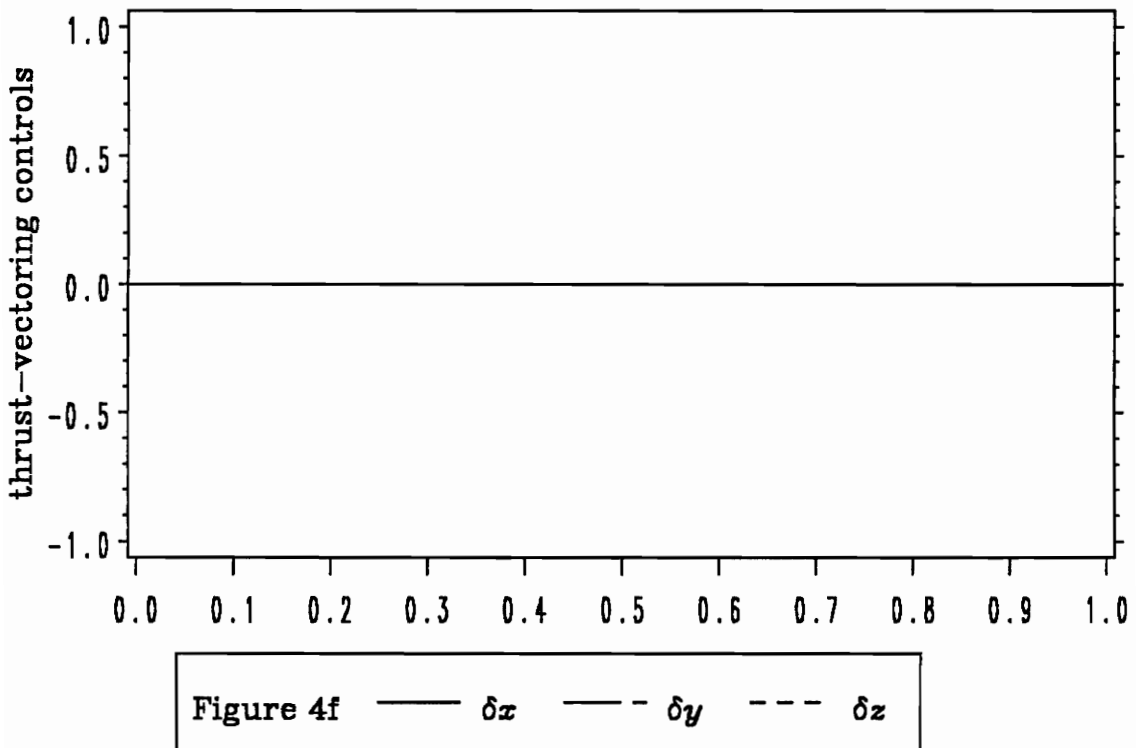
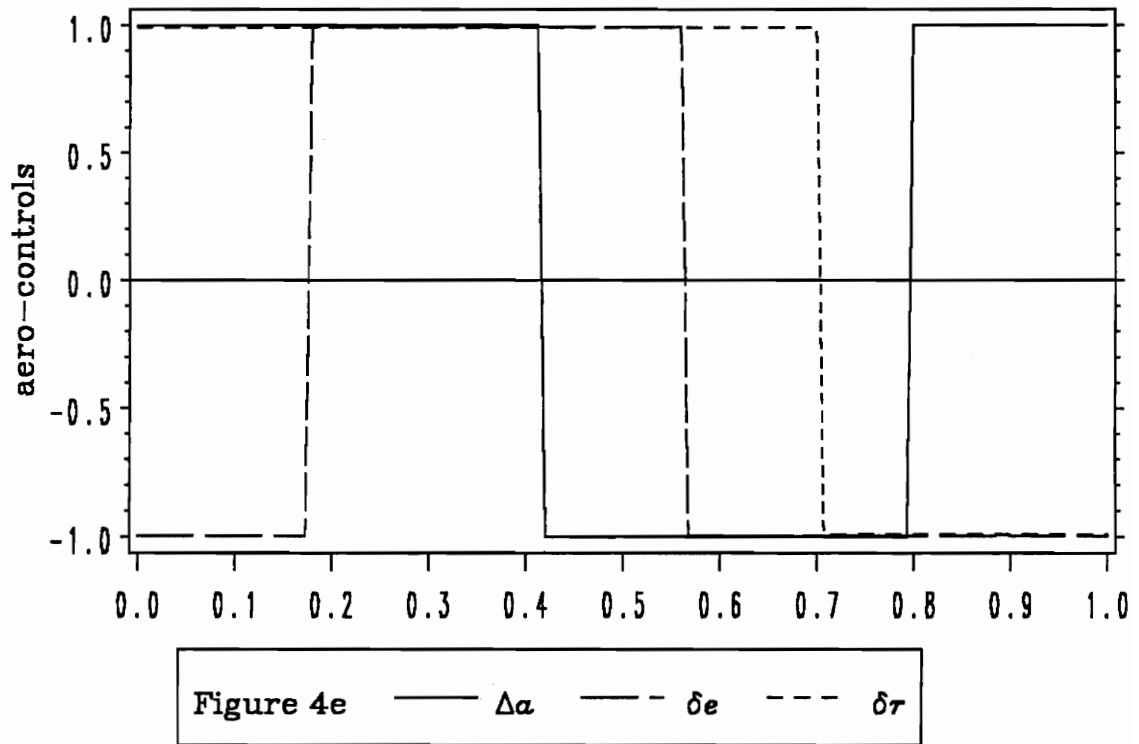


Figure 4. (continued)

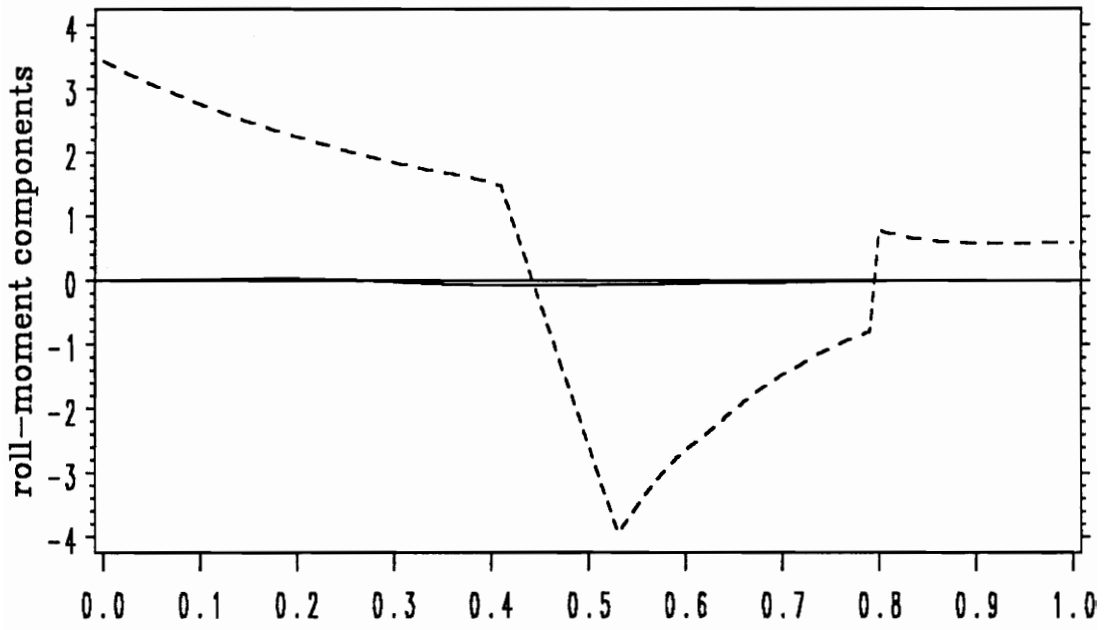


Figure 4g — L_{qr} — L_t — L_a

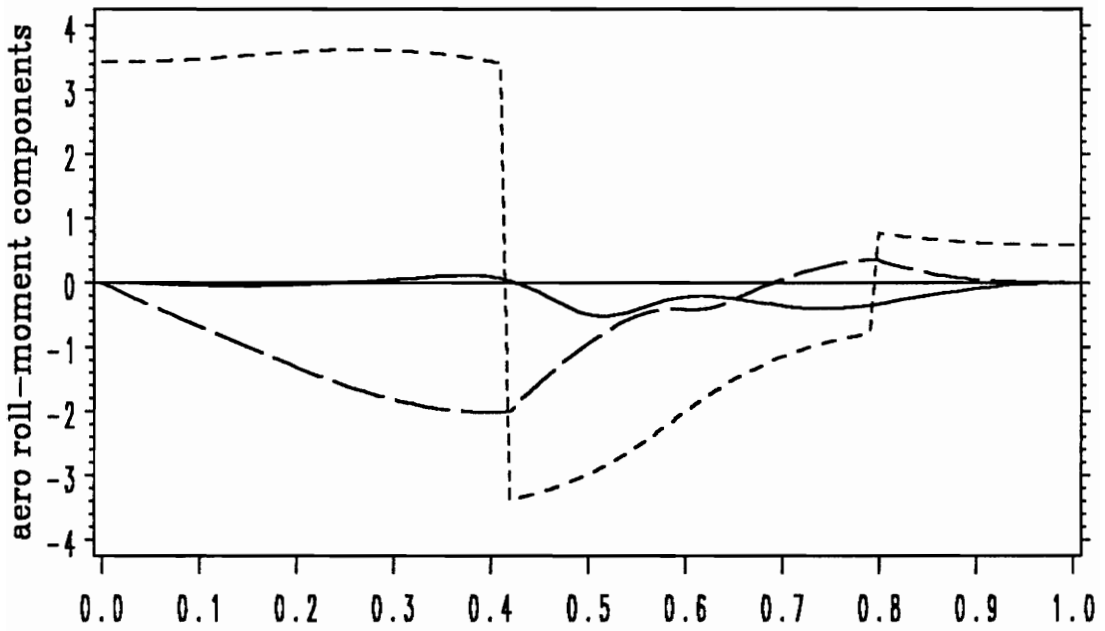


Figure 4h — L_0 — L_t — L_c

Figure 4. (continued)

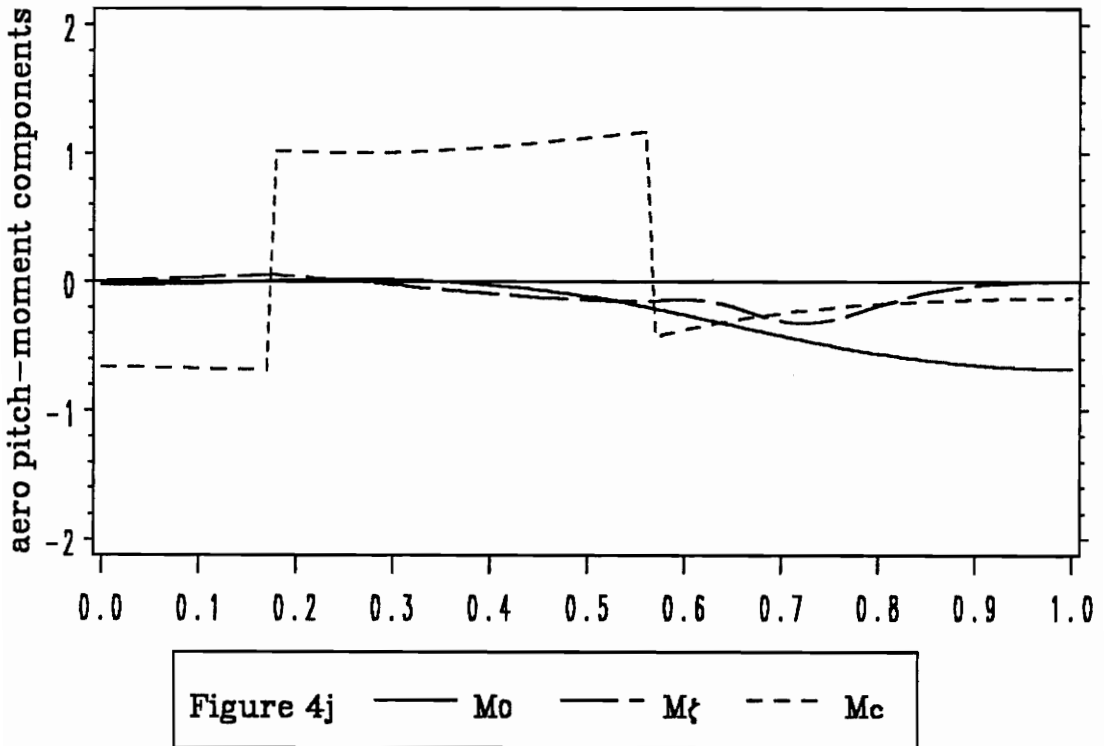
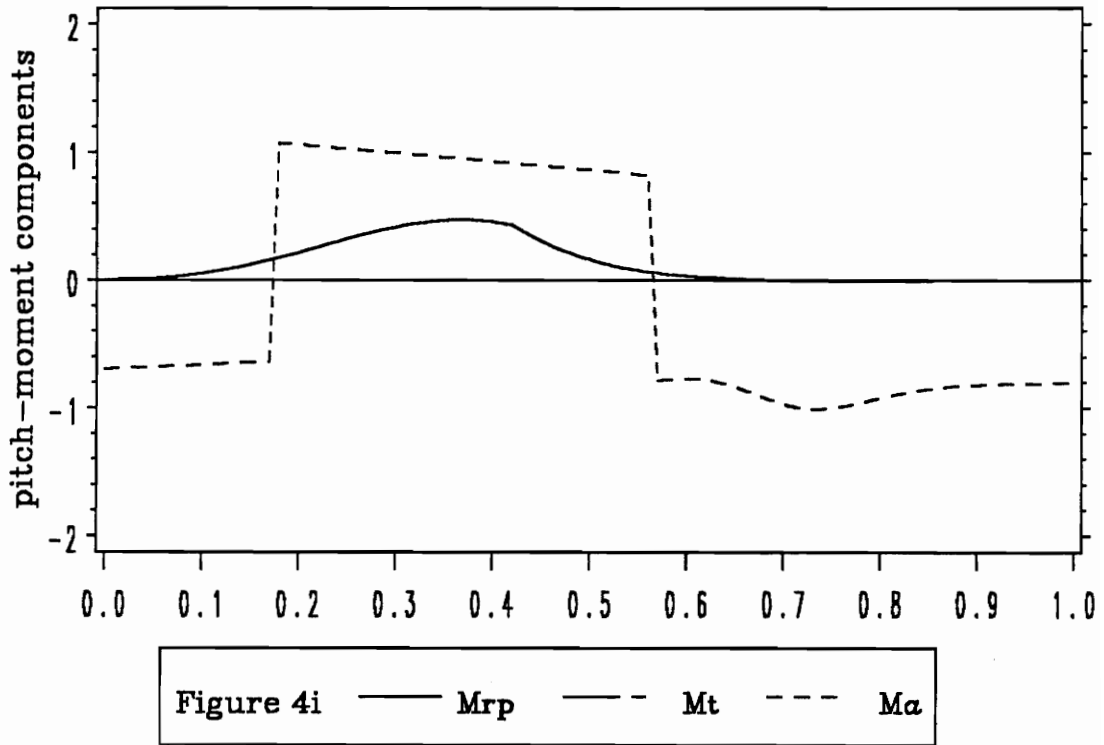


Figure 4. (continued)

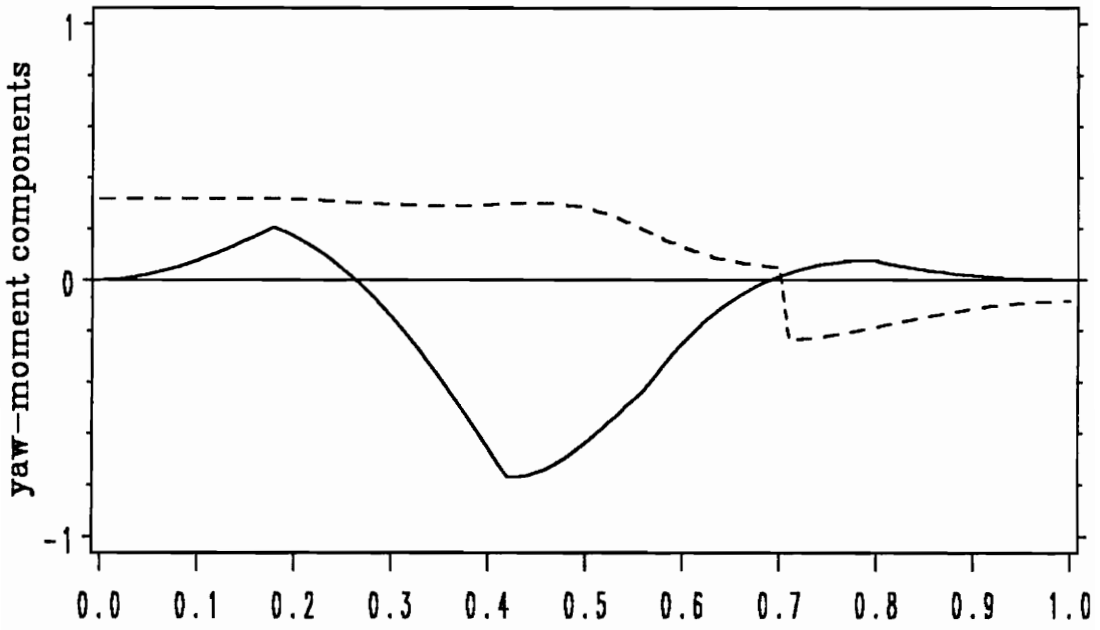


Figure 4k — N_{pq} — N_t — N_a

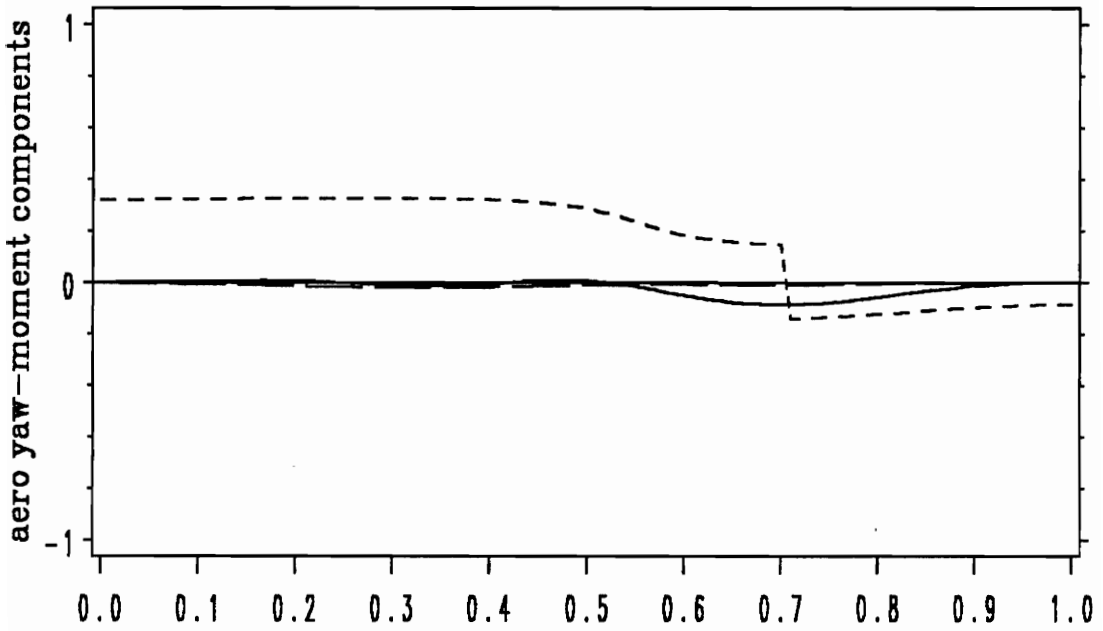


Figure 4l — N_o — N_ξ — N_c

Figure 4. (continued)

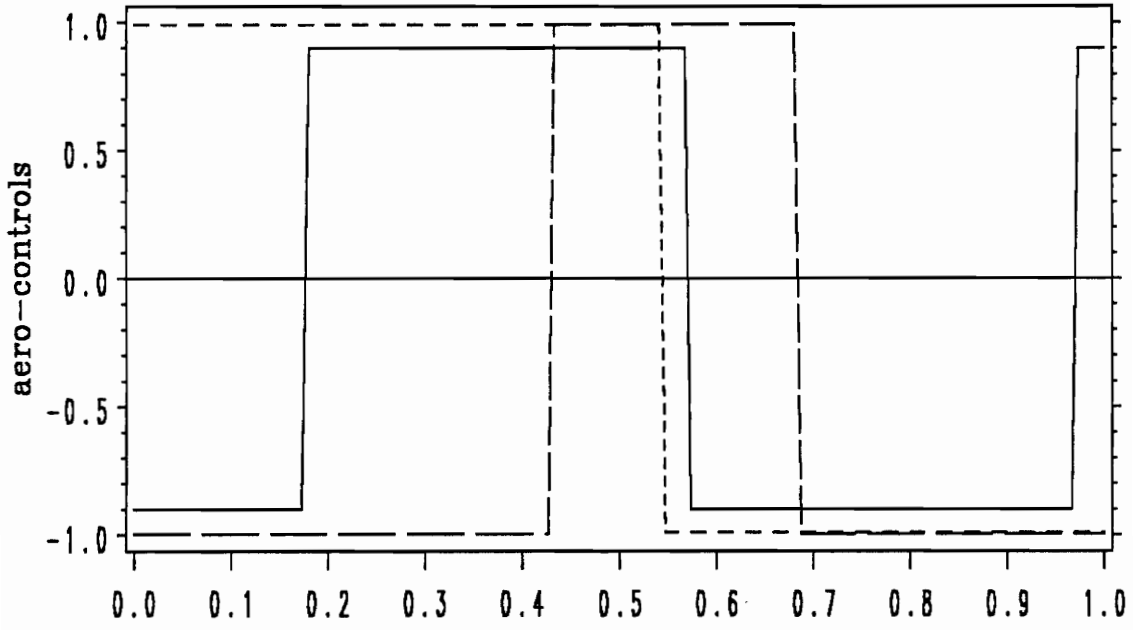


Figure 5a — $\Delta\alpha (0.9)$ — δe — $\delta\tau$

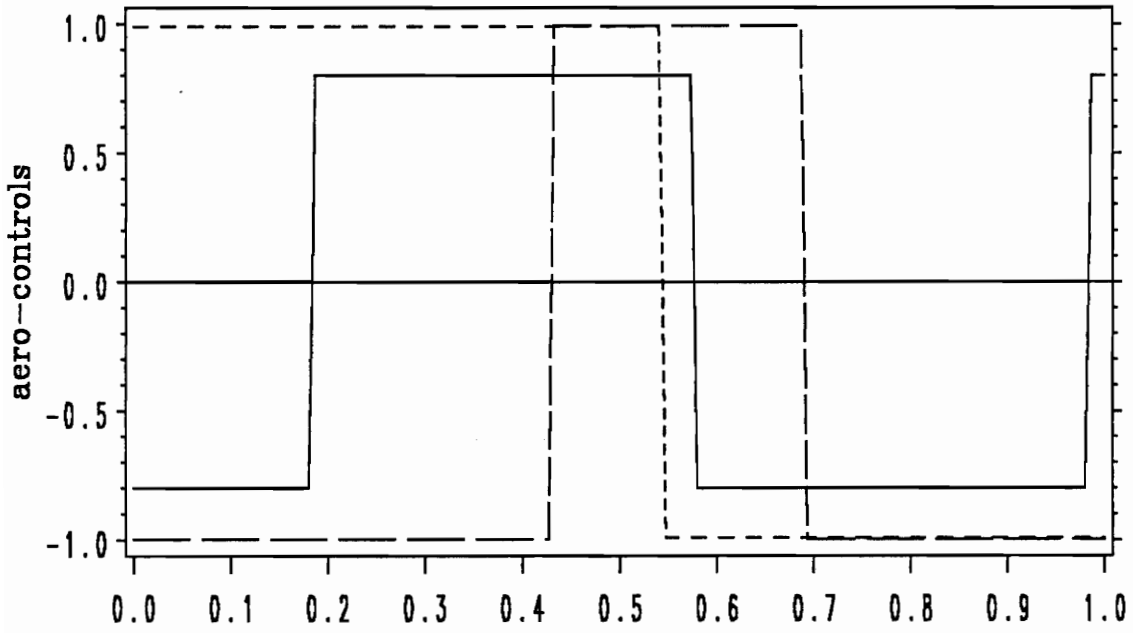


Figure 5b — $\Delta\alpha (0.8)$ — δe — $\delta\tau$

Figure 5. Example of evolution of extremal solutions

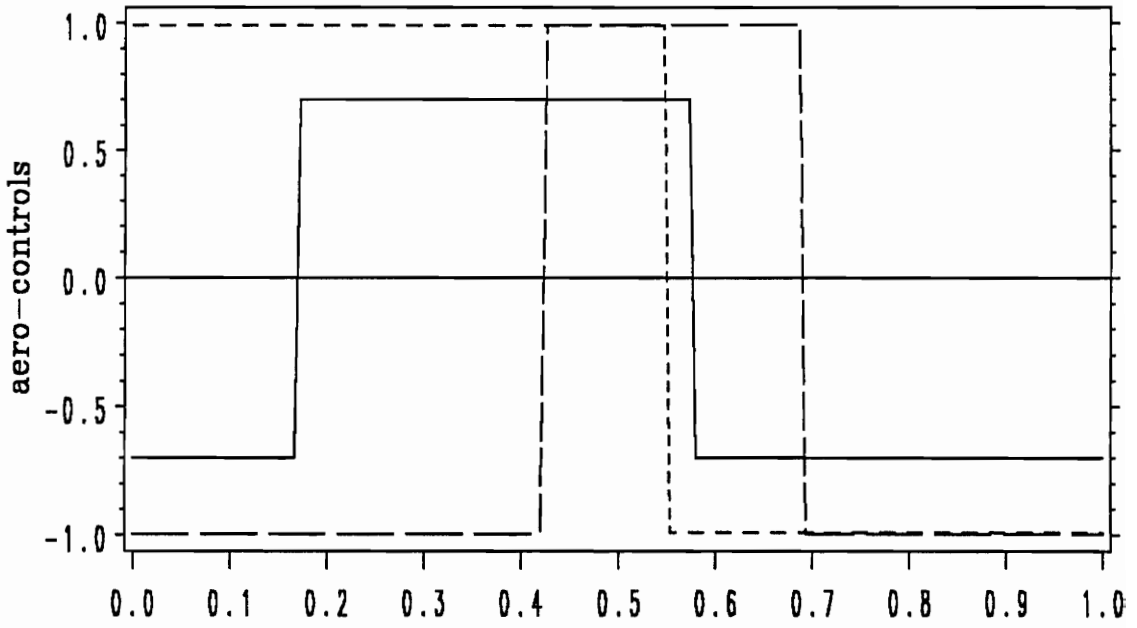


Figure 5c — $\Delta\alpha$ (0.7) — — δe - - - $\delta\tau$

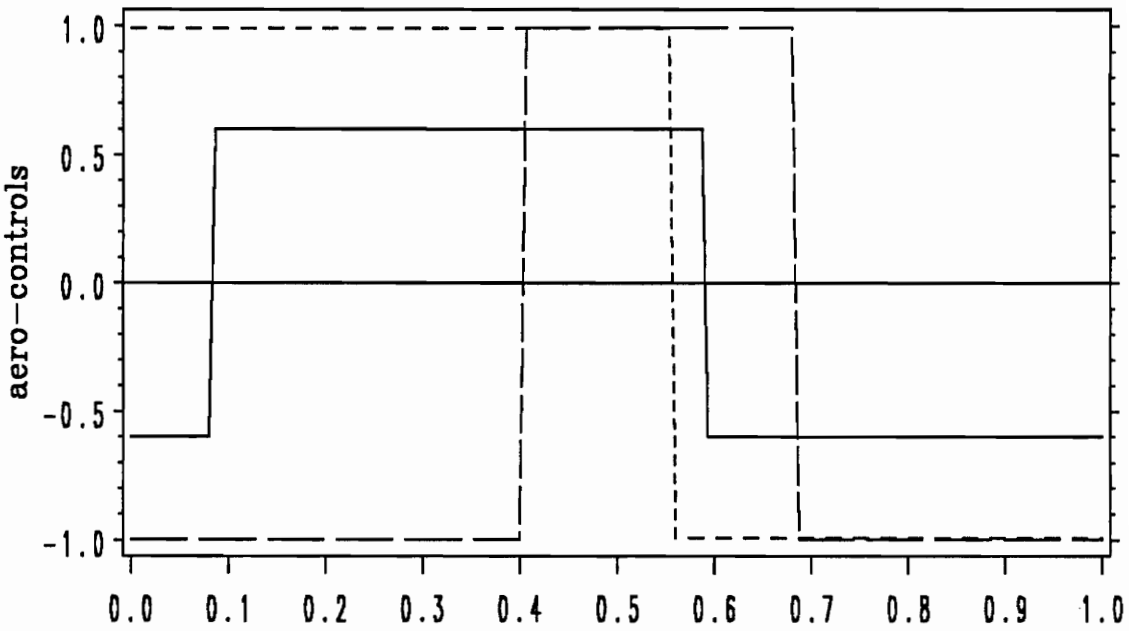


Figure 5d — $\Delta\alpha$ (0.6) — — δe - - - $\delta\tau$

Figure 5. (continued)

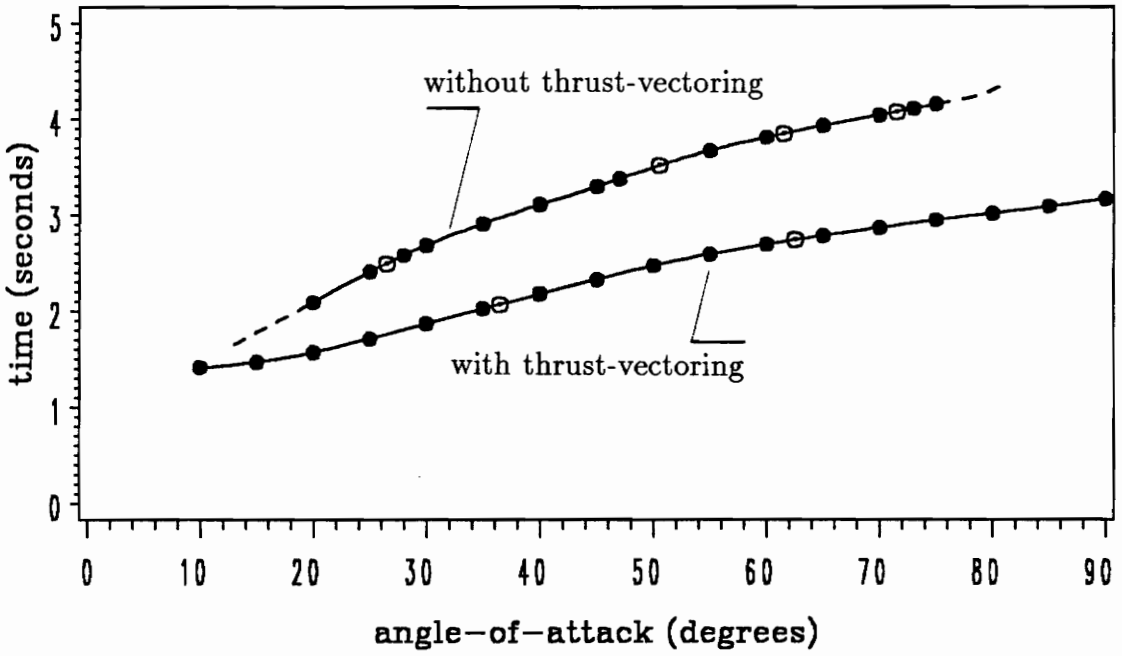


Figure 6a. Maneuver-1: time vs. initial and final angle-of-attack

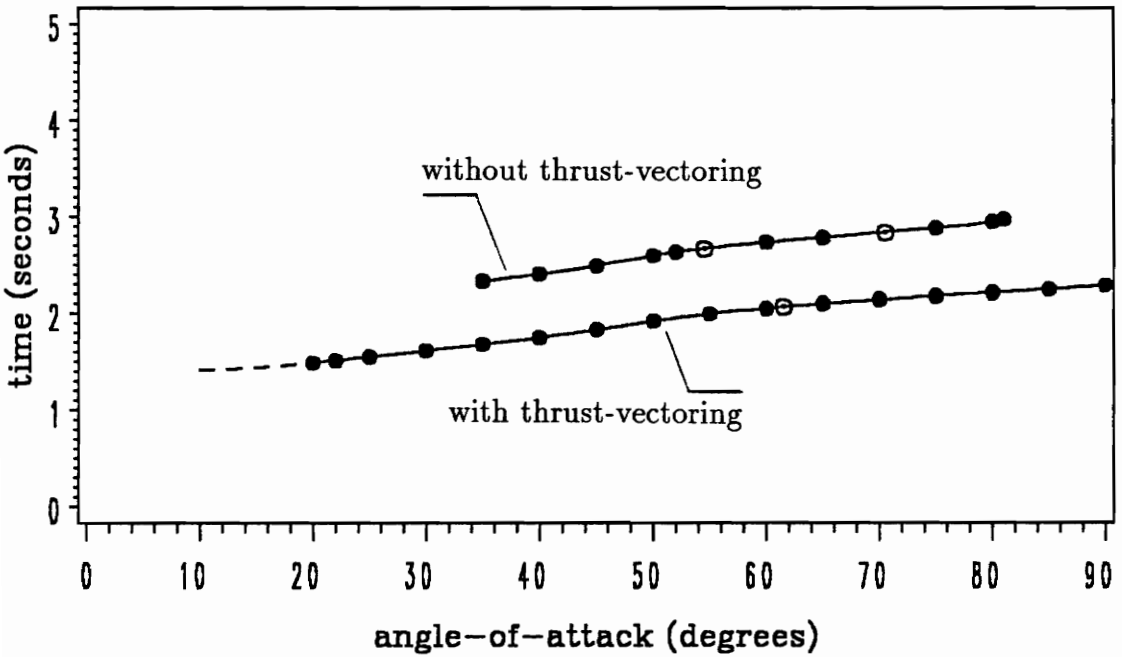


Figure 6b. Maneuver-2: time vs. final angle-of-attack

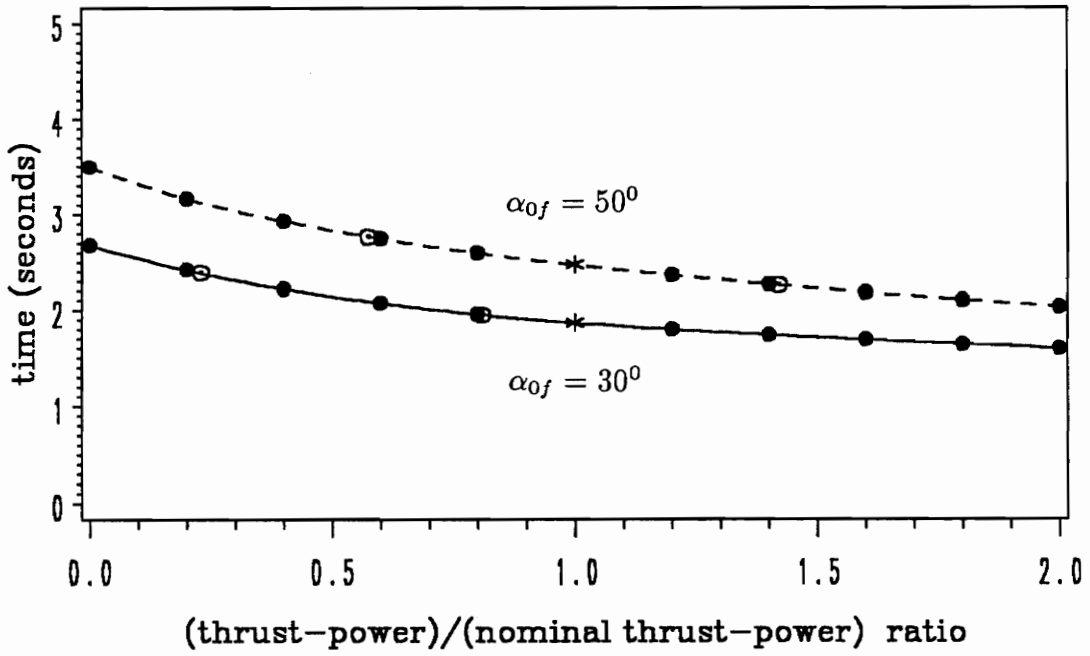


Figure 7a. Maneuver-1: time vs. thrust-vectoring power

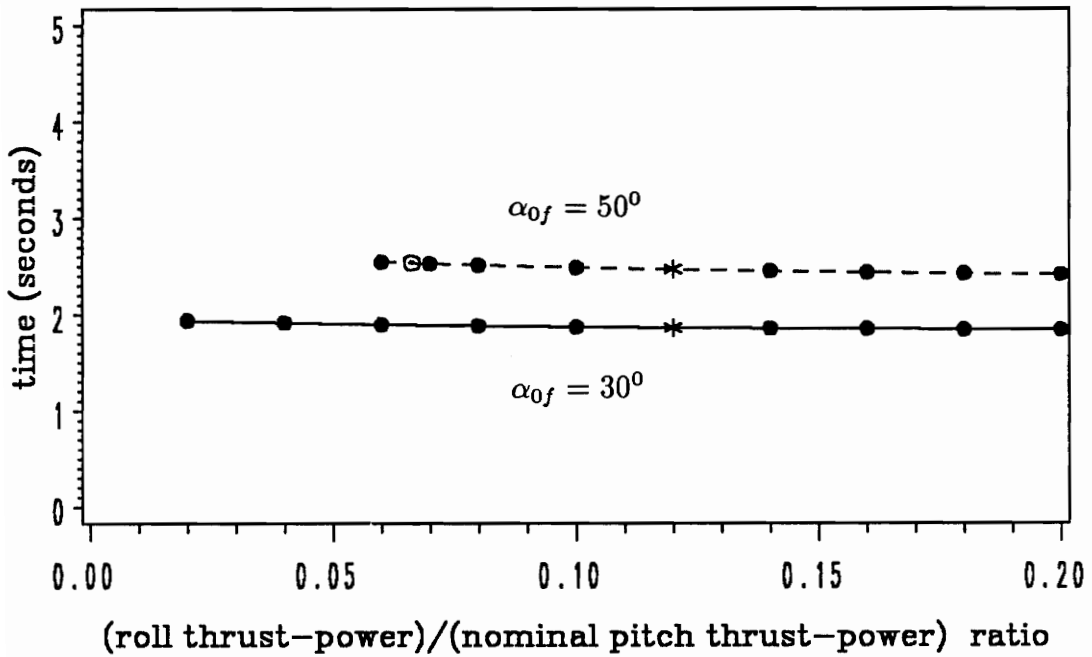


Figure 7b. Maneuver-1: time vs. thrust-vectoring roll-power

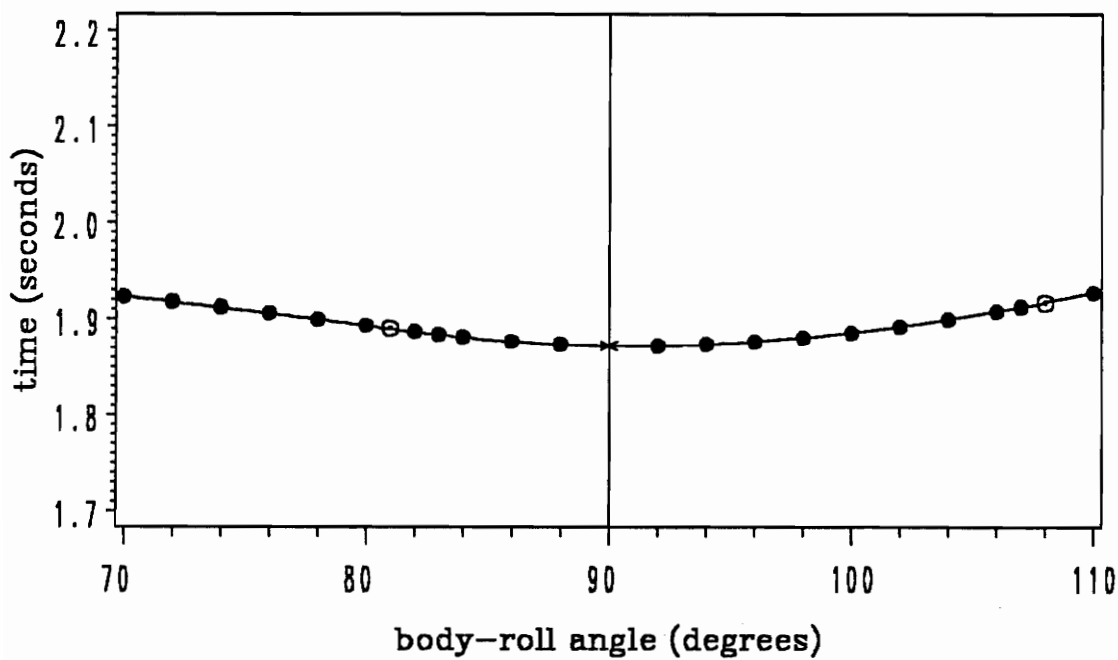


Figure 8a. Maneuver-1: time vs. body-roll angle ϕ_f

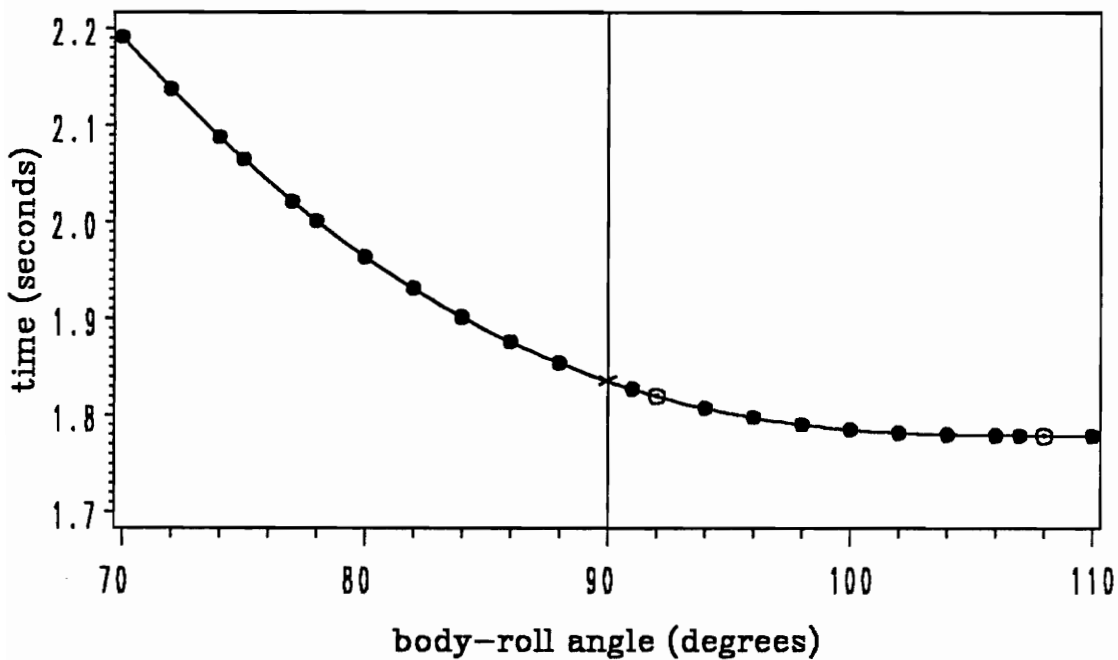


Figure 8b. Maneuver-2: time vs. body-roll angle ϕ_f

APPENDIX A

AERODYNAMIC-MOMENT COEFFICIENTS

The aerodynamic coefficients for the HARV are very complex functions of a number of variables (states and controls). Data from wind-tunnel measurements is available at a certain set of grid-points [15], ranging among all possible combinations of the state and control variables (these vary within certain intervals, for example $\alpha \in [-10^\circ, +90^\circ]$ and $\beta \in [-20^\circ, +20^\circ]$). In addition, a program is available which reads this data and performs linear interpolation in any variable. Thus, for simulation purposes one can have the value of the aerodynamic coefficients for any value of the state and control variables (within their respective domains). However, for the optimization procedures smooth data is needed. In addition, some state-variable derivatives of the aerodynamic-moment coefficients are needed. Thus, it was necessary to develop smooth model functions for the aerodynamic-moment coefficients. These model functions are combinations (sums and products) of some simpler functions (referred to as *shape functions*). The shape functions used and the method used in constructing model functions are discussed in Appendix B. In Appendices A1 to A9 the analytical expressions of the aerodynamic-moment coefficient model functions are given, along with plots of each aerodynamic-moment coefficient data and the corresponding model function (as used in the mathematical model). The data and the model correspond to Mach number 0.30. The model functions depend upon some parameters (constants). The initial estimates of these constants were originally obtained by analyses, then adjusted either by visual comparison with the given data

or by using (parameter-optimization) IMSL least squares fitting software [20]. In the expressions that follow, these parameters are denoted by symbols of the form l_L^n , where the letters take values as follows:

$$l \in \{a, b, c, d, e, w, \alpha\}$$

$$L \in \{L, Q, R, E, T, S, Y, Z\}$$

$$n \in \{1, 2, 3, 4\}$$

Each capital letter corresponds to a certain shape function; each lower case letter corresponds to a certain parameter of a shape function; and the numbers denote the component shape function within a model function. The numerical values of the constants are given in [25].

In the appendices A1 to A9, the notation is tailored so as to show more clearly the structure of the analytical model functions.

Appendix A1. Static roll coefficient

$$C_i^0(\alpha, \beta) = A_{i,0}(\alpha, \beta) \cdot B_{i,0}(\alpha, \beta)$$

where

$$A_{i,0}(\alpha, \beta) = L_{i,0}^1(\alpha) + Q_{i,0}^2(\alpha) + E_{i,0}^3(\alpha) + E_{i,0}^4(\alpha)$$

$$B_{i,0}(\alpha, \beta) = Y_{i,0}^1(\alpha, \beta) + Z_{i,0}^2(\alpha, \beta)$$

and the components have the following form:

$$L_{i,0}^1(\alpha) = a_L^1 \cdot \alpha + b_L^1$$

$$Q_{i,0}^2(\alpha) = \frac{c_Q^2}{1 + \left(\frac{\alpha - \alpha_Q^2}{w_Q^2}\right)^2}$$

$$E_{i,0}^3(\alpha) = c_E^3 \cdot \exp \left[- \left(\frac{\alpha - \alpha_E^3}{w_E^3} \right)^2 \right]$$

$$E_{i,0}^4(\alpha) = c_E^4 \cdot \exp \left[- \left(\frac{\alpha - \alpha_E^4}{w_E^4} \right)^2 \right]$$

$$Y_{i,0}^1(\alpha, \beta) = [a_Y^1 \cdot \arctan(b_Y^1 \cdot \beta)] \cdot \frac{1}{1 + \left(\frac{\alpha - \alpha_Y^1}{w_Y^1}\right)^2}$$

$$Z_{i,0}^2(\alpha, \beta) = [b_Z^2 \cdot \beta] \cdot \frac{\left(\frac{\alpha - \alpha_Z^2}{w_Z^2}\right)^2}{1 + \left(\frac{\alpha - \alpha_Z^2}{w_Z^2}\right)^2}$$

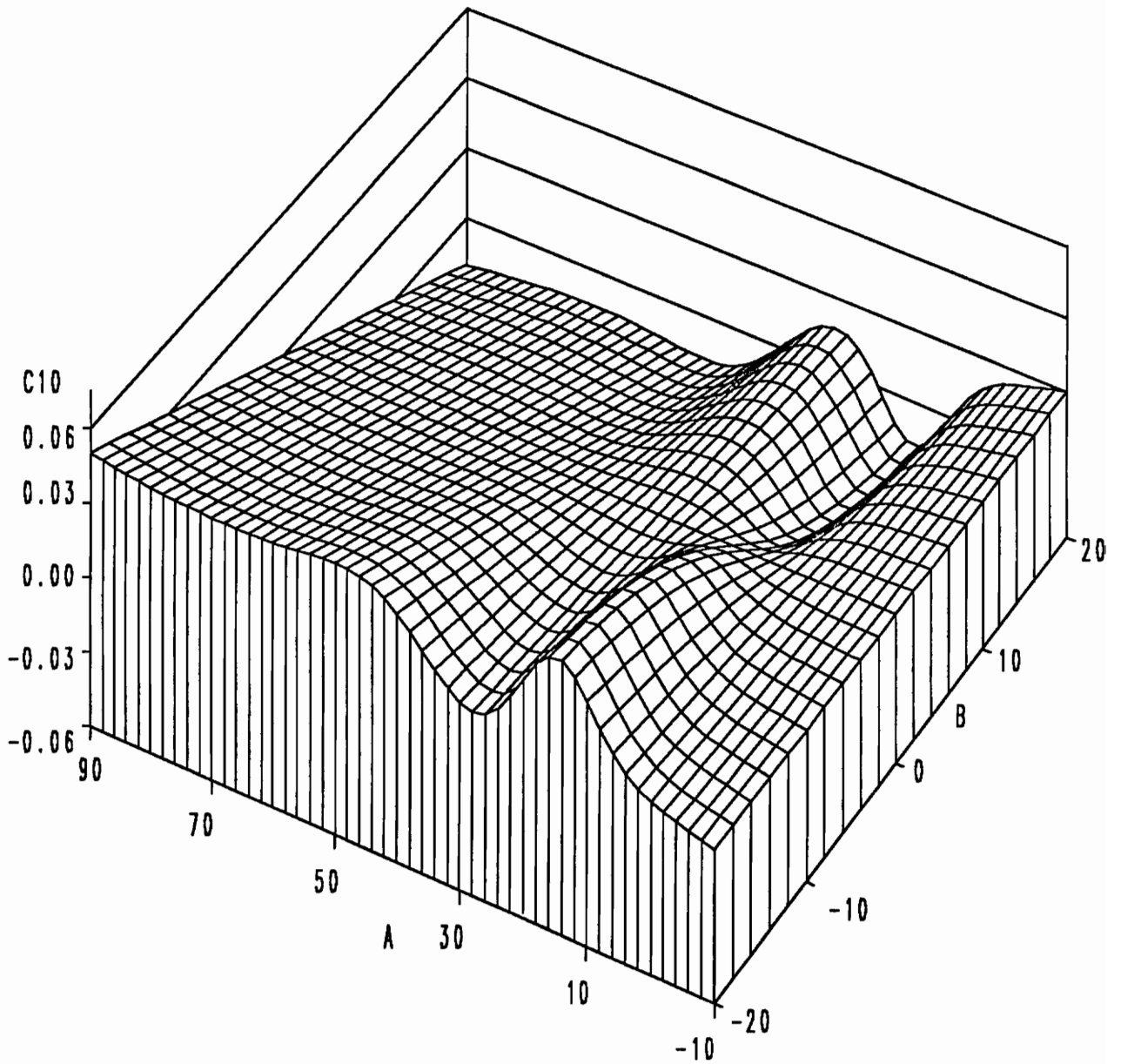


Figure A-1a. Static roll coefficient (analytical model)

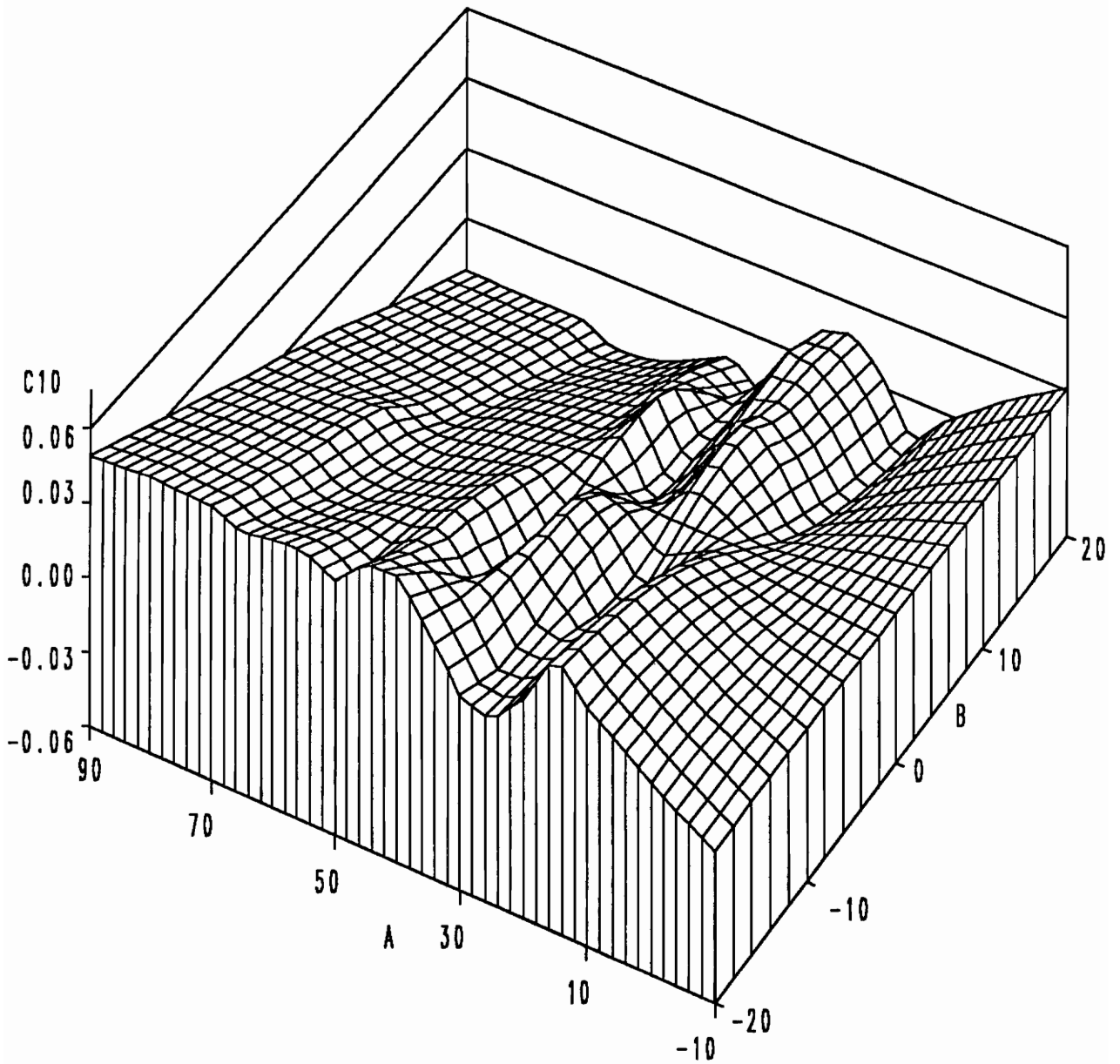


Figure A-1b. Static roll coefficient (HARV data)

Appendix A2. Static pitch coefficient

$$C_m^0(\alpha, \beta) = A_{m,0}(\alpha, \beta) \cdot B_{m,0}(\alpha, \beta)$$

where

$$A_{m,0}(\alpha, \beta) = L_{m,0}^1(\alpha) + Q_{m,0}^2(\alpha)$$

$$B_{m,0}(\alpha, \beta) = 1$$

and the components have the following form:

$$L_{m,0}^1(\alpha) = a_L^1 \cdot \alpha + b_L^1$$

$$Q_{m,0}^2(\alpha) = \frac{c_Q^2}{1 + \left(\frac{\alpha - \alpha_Q^2}{w_Q^2}\right)^2}$$

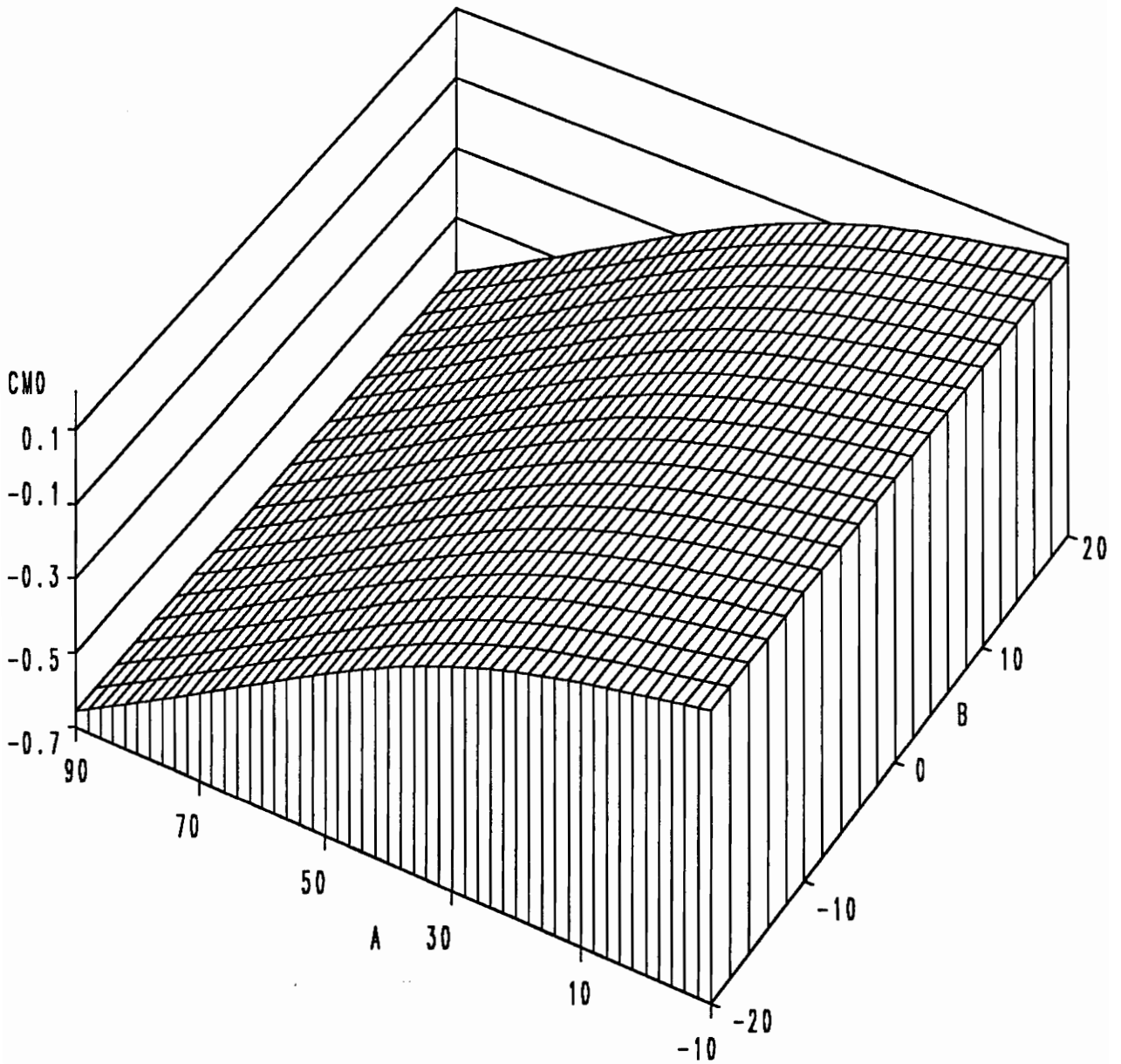


Figure A-2a. Static pitch coefficient (analytical model)

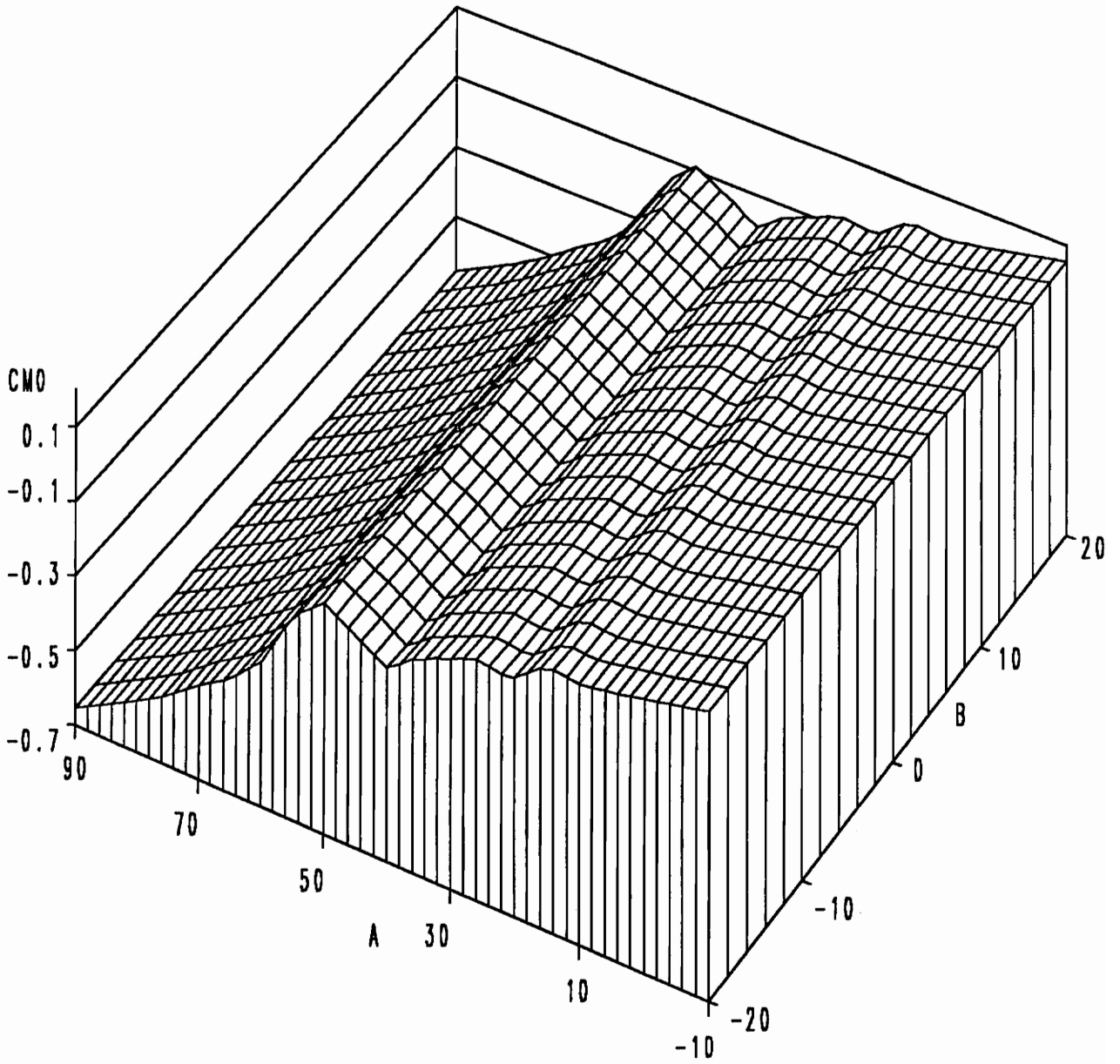


Figure A-2b. Static pitch coefficient (HARV data)

Appendix A3. Static yaw coefficient

$$C_n^0(\alpha, \beta) = A_{n,0}(\alpha, \beta) \cdot B_{n,0}(\alpha, \beta)$$

where

$$A_{n,0}(\alpha, \beta) = L_{n,0}^1(\alpha) + Q_{n,0}^2(\alpha) + E_{n,0}^3(\alpha) + E_{n,0}^4(\alpha)$$

$$B_{n,0}(\alpha, \beta) = Y_{n,0}^1(\alpha, \beta) + Z_{n,0}^2(\alpha, \beta)$$

and the components have the following form:

$$L_{n,0}^1(\alpha) = a_L^1 \cdot \alpha + b_L^1$$

$$Q_{n,0}^2(\alpha) = \frac{c_Q^2}{1 + \left(\frac{\alpha - \alpha_Q^2}{w_Q^2}\right)^2}$$

$$E_{n,0}^3(\alpha) = c_E^3 \cdot \exp \left[- \left(\frac{\alpha - \alpha_E^3}{w_E^3} \right)^2 \right]$$

$$E_{n,0}^4(\alpha) = c_E^4 \cdot \exp \left[- \left(\frac{\alpha - \alpha_E^4}{w_E^4} \right)^2 \right]$$

$$Y_{n,0}^1(\alpha, \beta) = [a_Y^1 \cdot \arctan(b_Y^1 \cdot \beta)] \cdot \frac{1}{1 + \left(\frac{\alpha - \alpha_Y^1}{w_Y^1}\right)^2}$$

$$Z_{n,0}^2(\alpha, \beta) = [b_Z^2 \cdot \beta] \cdot \frac{\left(\frac{\alpha - \alpha_Z^2}{w_Z^2}\right)^2}{1 + \left(\frac{\alpha - \alpha_Z^2}{w_Z^2}\right)^2}$$

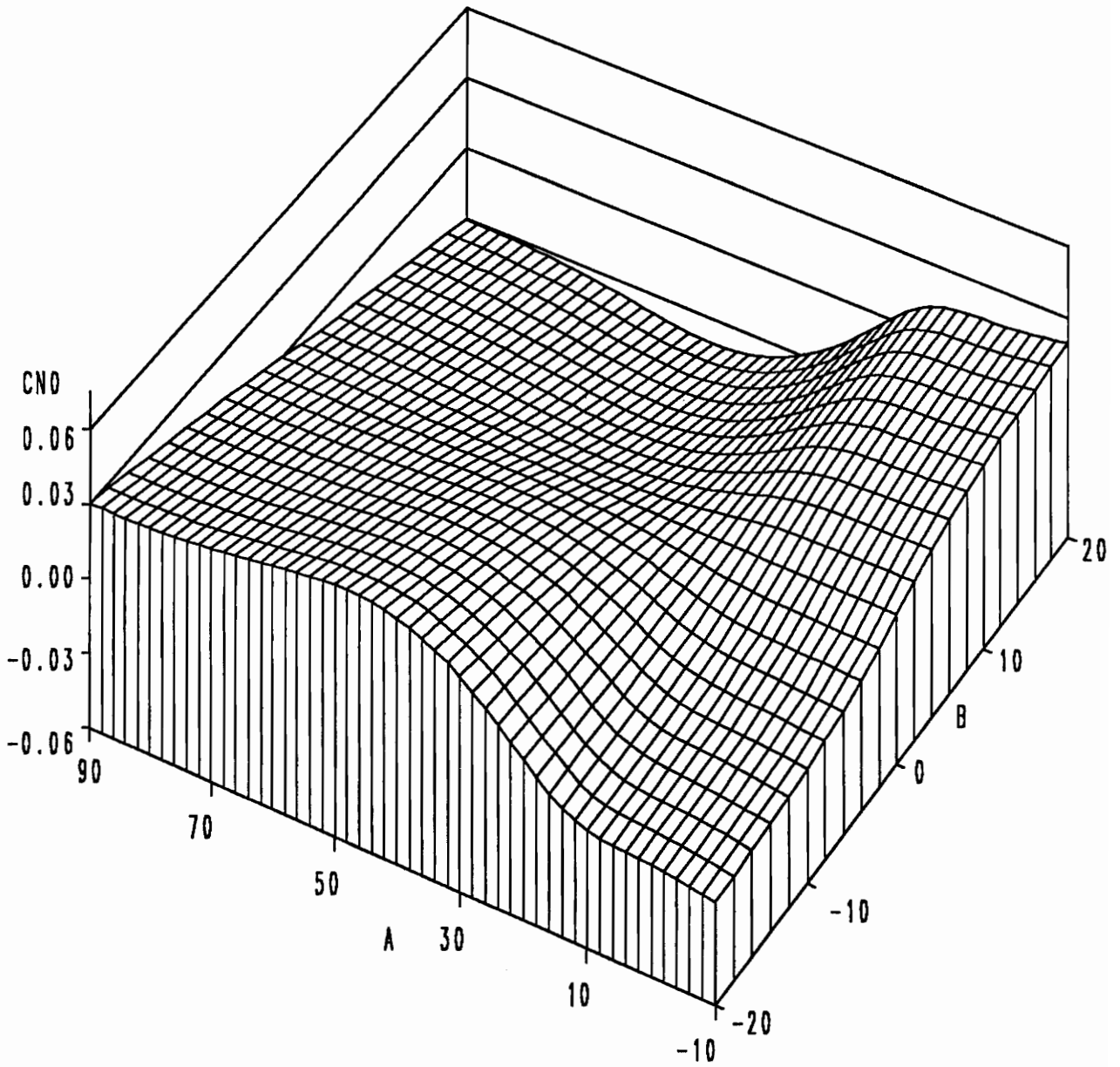


Figure A-3a. Static yaw coefficient (analytical model)

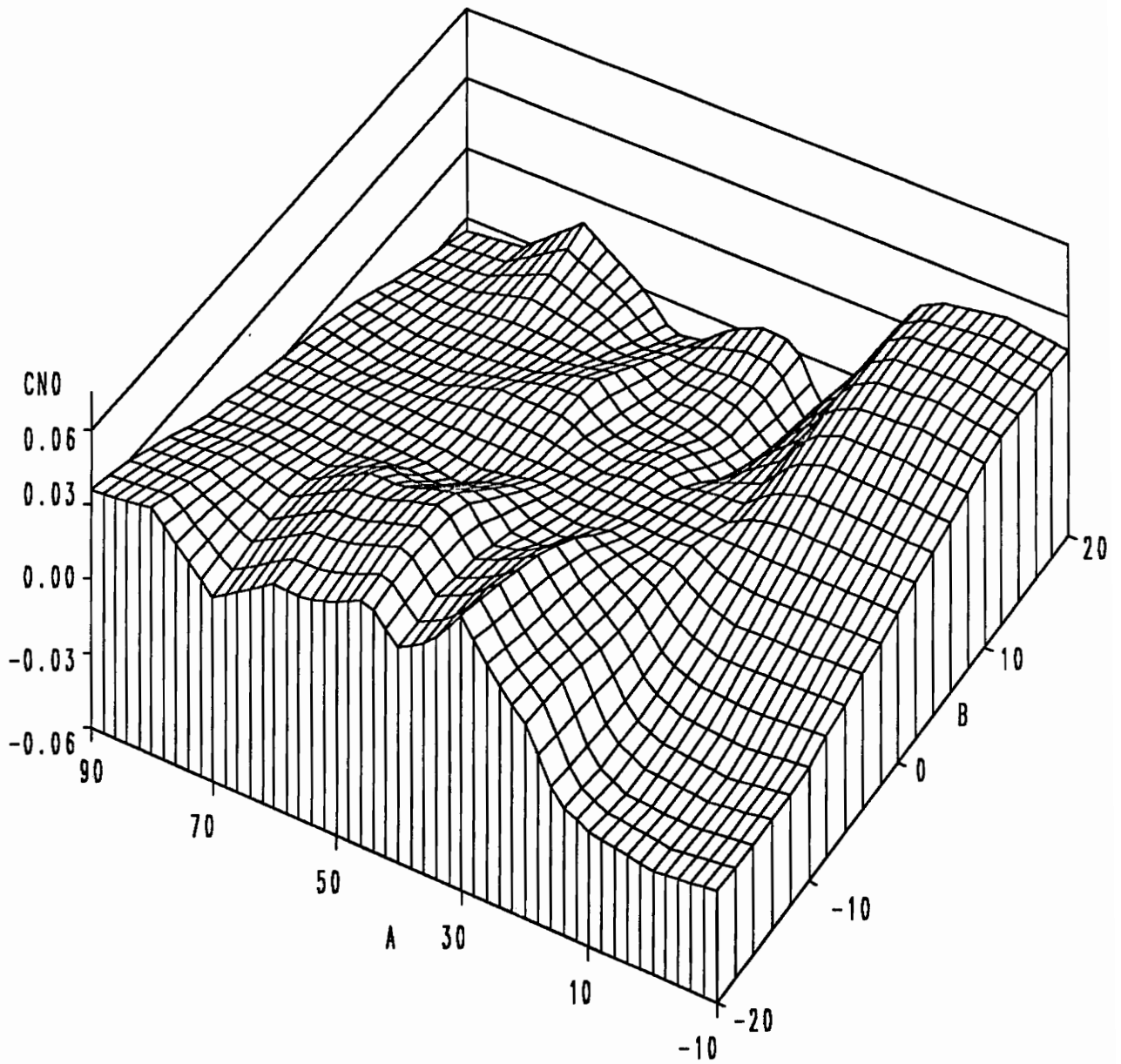


Figure A-3b. Static yaw coefficient (HARV data)

Appendix A4. Roll-damping coefficient

$$C_i^{\zeta}(\alpha, p) = C_i^{\zeta 0}(\alpha) \cdot p$$

where

$$C_i^{\zeta 0}(\alpha) = L_{i,\zeta}^1(\alpha) + Q_{i,\zeta}^2(\alpha) + Q_{i,\zeta}^3(\alpha) + E_{i,\zeta}^4(\alpha)$$

and the components have the following form:

$$L_{i,\zeta}^1(\alpha) = a_L^1 \cdot \alpha + b_L^1$$

$$Q_{i,\zeta}^2(\alpha) = \frac{c_Q^2}{1 + \left(\frac{\alpha - \alpha_Q^2}{w_Q^2}\right)^2}$$

$$Q_{i,\zeta}^3(\alpha) = \frac{c_Q^3}{1 + \left(\frac{\alpha - \alpha_Q^3}{w_Q^3}\right)^6}$$

$$E_{i,\zeta}^4(\alpha) = c_E^4 \cdot \exp \left[- \left(\frac{\alpha - \alpha_E^4}{w_E^4} \right)^2 \right]$$

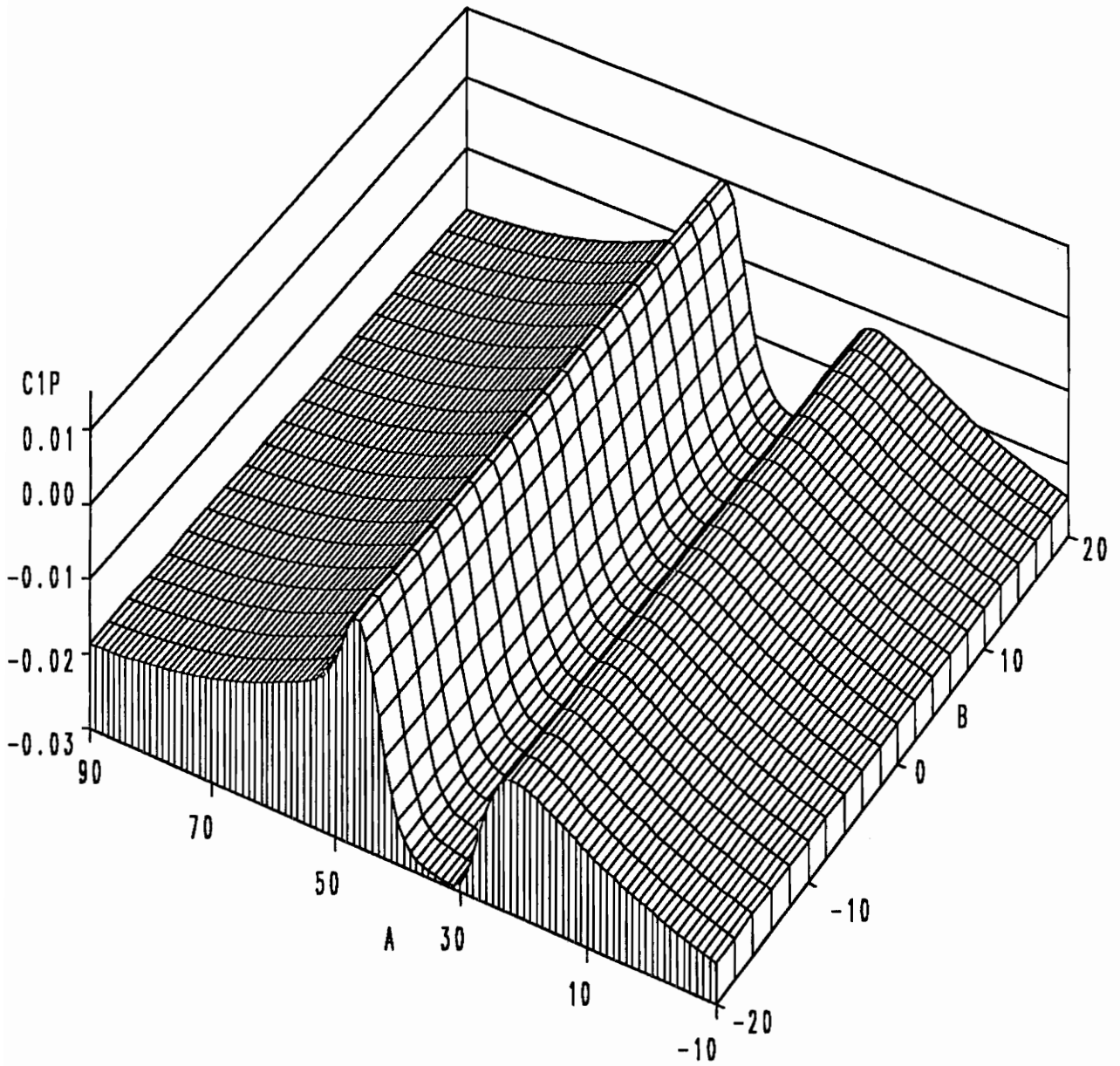


Figure A-4a. Roll-damping coefficient (analytical model)

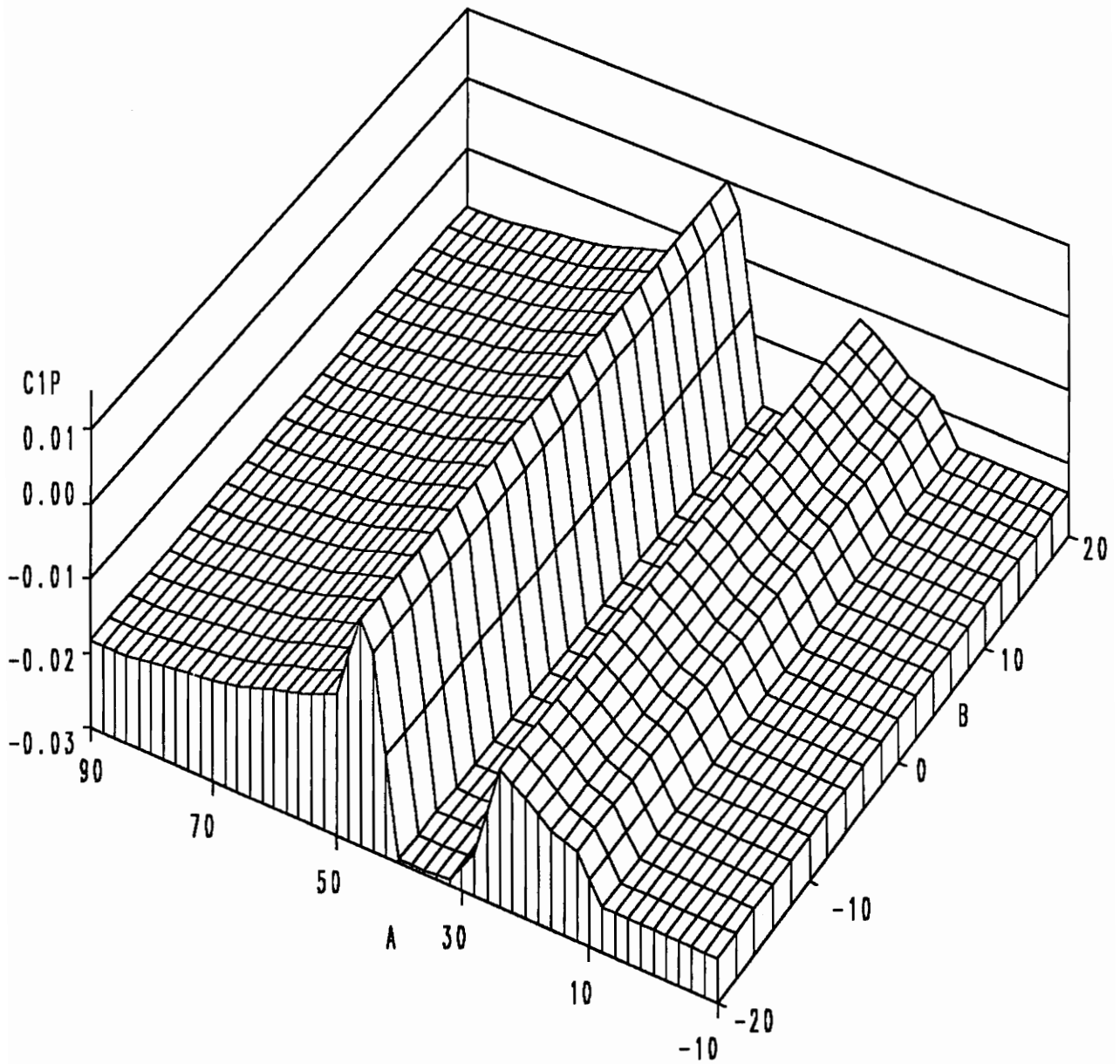


Figure A-4b. Roll-damping coefficient (HARV data)

Appendix A5. Pitch-damping coefficient

$$C_m^\zeta(\alpha, q) = C_m^{\zeta 0}(\alpha) \cdot q$$

where

$$C_m^{\zeta 0}(\alpha) = L_{m,\zeta}^1(\alpha) + Q_{m,\zeta}^2(\alpha) + E_{m,\zeta}^3(\alpha)$$

and the components have the following form:

$$L_{m,\zeta}^1(\alpha) = a_E^1 \cdot \alpha + b_E^1$$

$$Q_{m,\zeta}^2(\alpha) = \frac{c_Q^2}{1 + \left(\frac{\alpha - \alpha_Q^2}{w_Q^2}\right)^2}$$

$$E_{m,\zeta}^3(\alpha) = c_E^3 \cdot \exp \left[- \left(\frac{\alpha - \alpha_E^3}{w_E^3} \right)^2 \right]$$

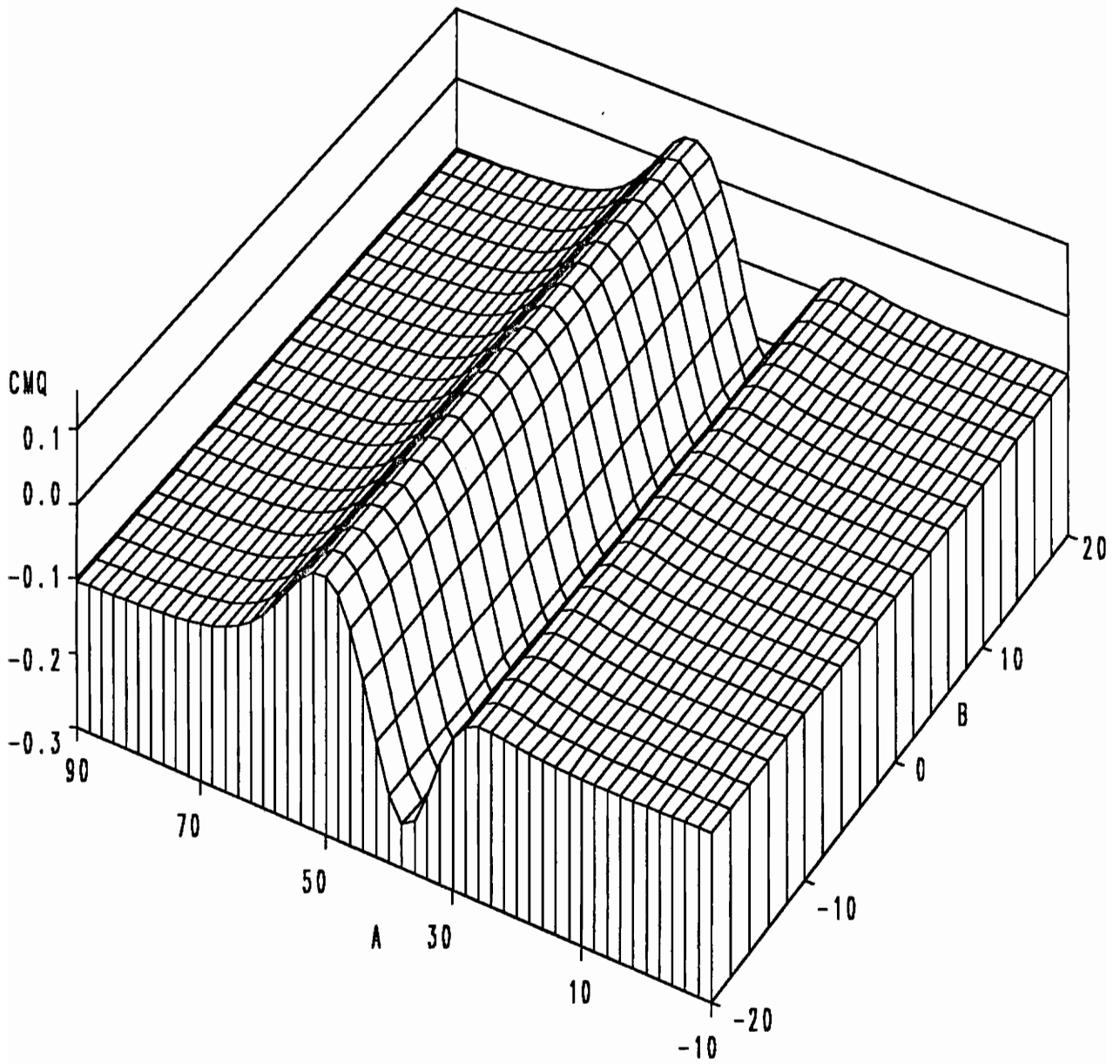


Figure A-5a. Pitch-damping coefficient (analytical model)

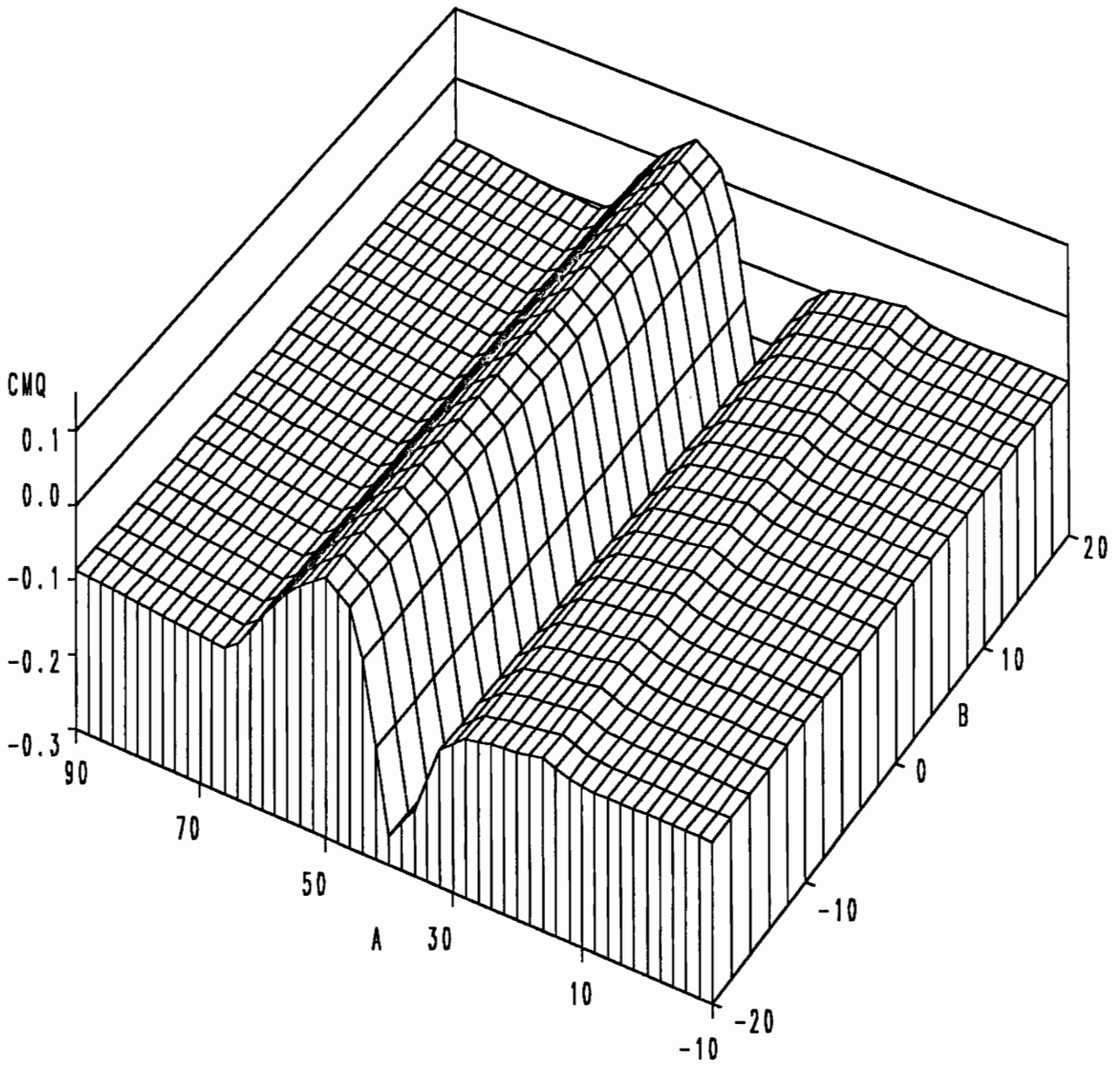


Figure A-5b. Pitch-damping coefficient (HARV data)

Appendix A6. Yaw-damping coefficient

$$C_n^\zeta(\alpha, r) = C_n^{\zeta 0}(\alpha) \cdot r$$

where

$$C_n^{\zeta 0}(\alpha) = L_{n,\zeta}^1(\alpha) + Q_{n,\zeta}^2(\alpha) + Q_{n,\zeta}^3(\alpha) + E_{n,\zeta}^4(\alpha)$$

and the components have the following form:

$$L_{n,\zeta}^1(\alpha) = a_L^1 \cdot \alpha + b_L^1$$

$$Q_{n,\zeta}^2(\alpha) = \frac{c_Q^2}{1 + \left(\frac{\alpha - \alpha_Q^2}{w_Q^2}\right)^2}$$

$$Q_{n,\zeta}^3(\alpha) = \frac{c_Q^3}{1 + \left(\frac{\alpha - \alpha_Q^3}{w_Q^3}\right)^6}$$

$$E_{n,\zeta}^4(\alpha) = c_E^4 \cdot \exp \left[- \left(\frac{\alpha - \alpha_E^4}{w_E^4} \right)^2 \right]$$

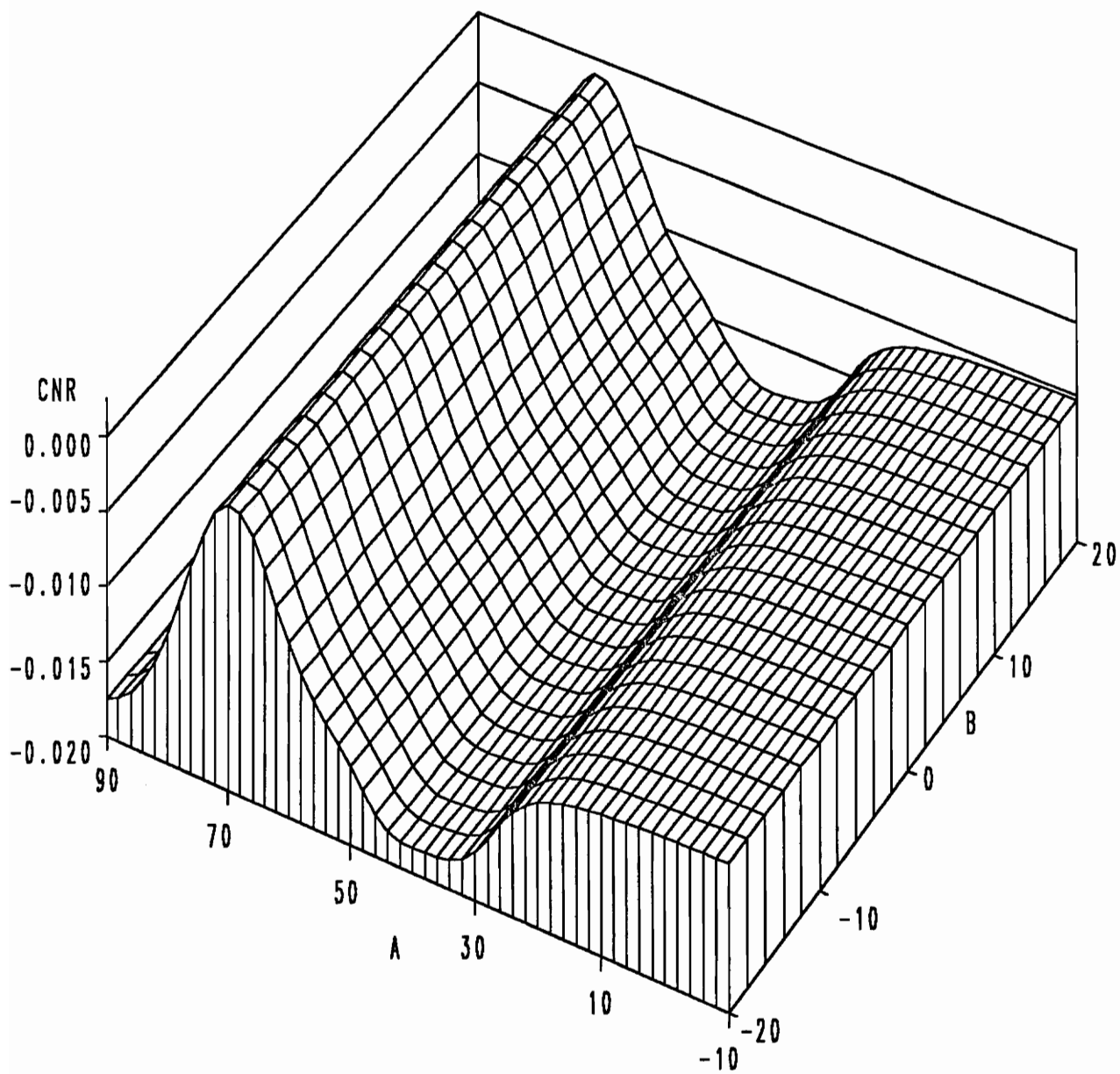


Figure A-6a. Yaw-damping coefficient (analytical model)

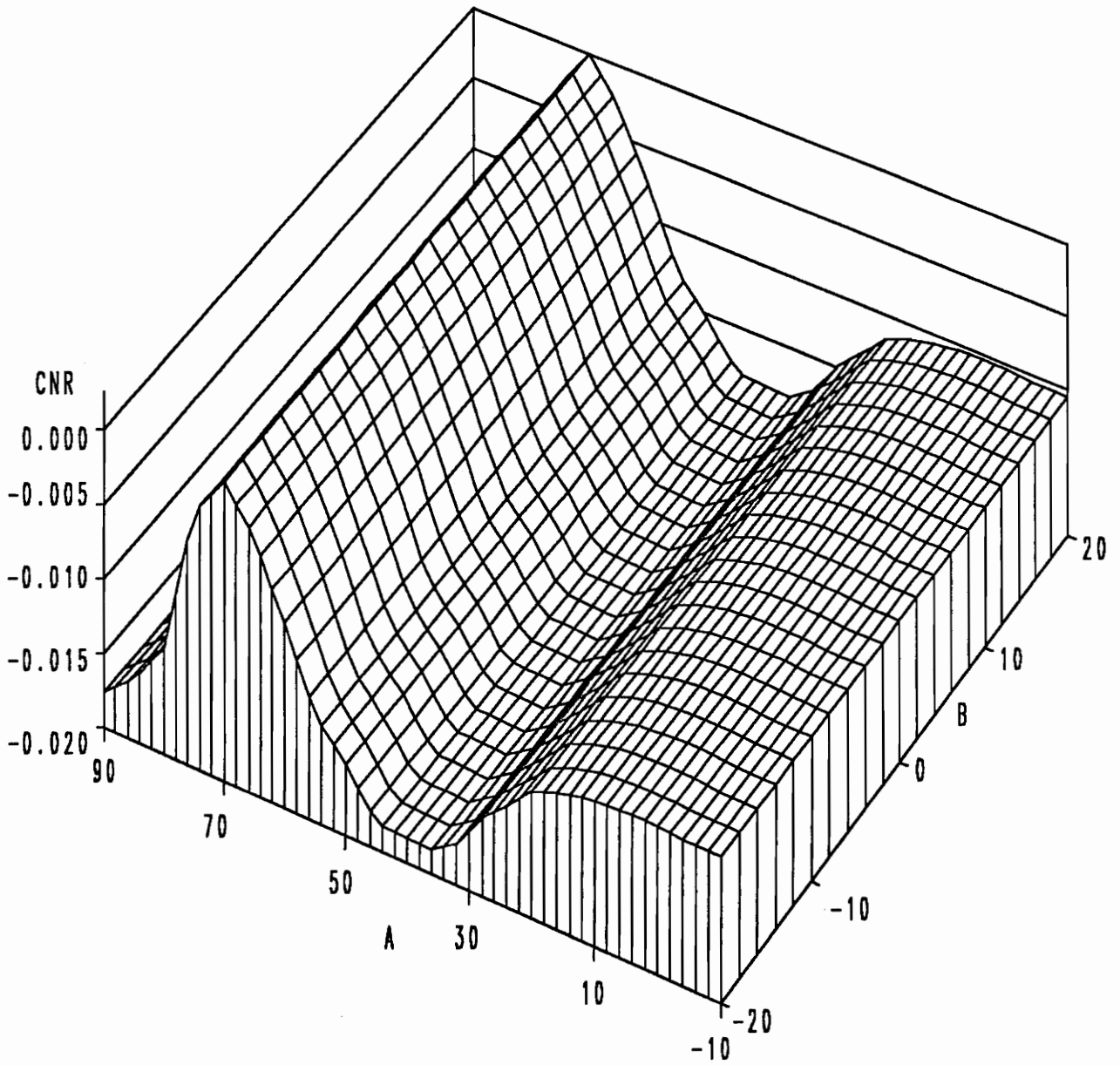


Figure A-6b. Yaw-damping coefficient (HARV data)

Appendix A7. Roll coefficient due to differential aileron

$$C_l^c(\alpha, \Delta_a) = A_{l,c}(\alpha) \cdot D_{l,c}(\alpha, \Delta_a)$$

where

$$A_{l,c}(\alpha) = L_{l,c}^1(\alpha) + T_{l,c}^2(\alpha)$$

$$D_{l,c}(\alpha, \Delta_a) = \Delta_a$$

and the components have the following form:

$$L_{l,c}^1(\alpha) = a_L^1 \cdot \alpha + b_L^1$$

$$T_{l,c}^2(\alpha) = c_T^2 \cdot \arctan [d_T^2 \cdot \exp(a_T^2 \cdot \alpha + b_T^2) + e_T^2]$$

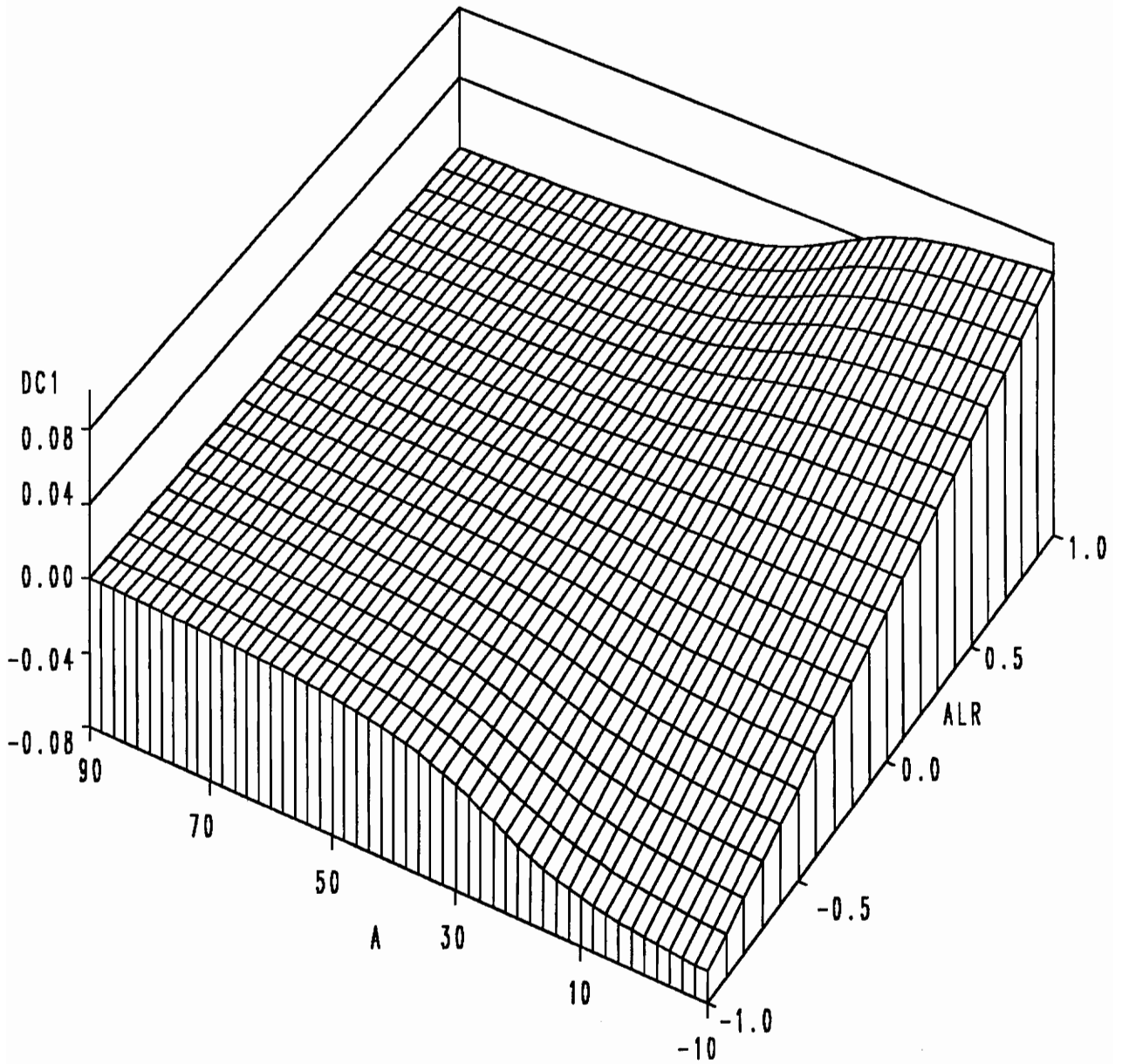


Figure A-7a. Roll coefficient due to differential aileron
(analytical model)

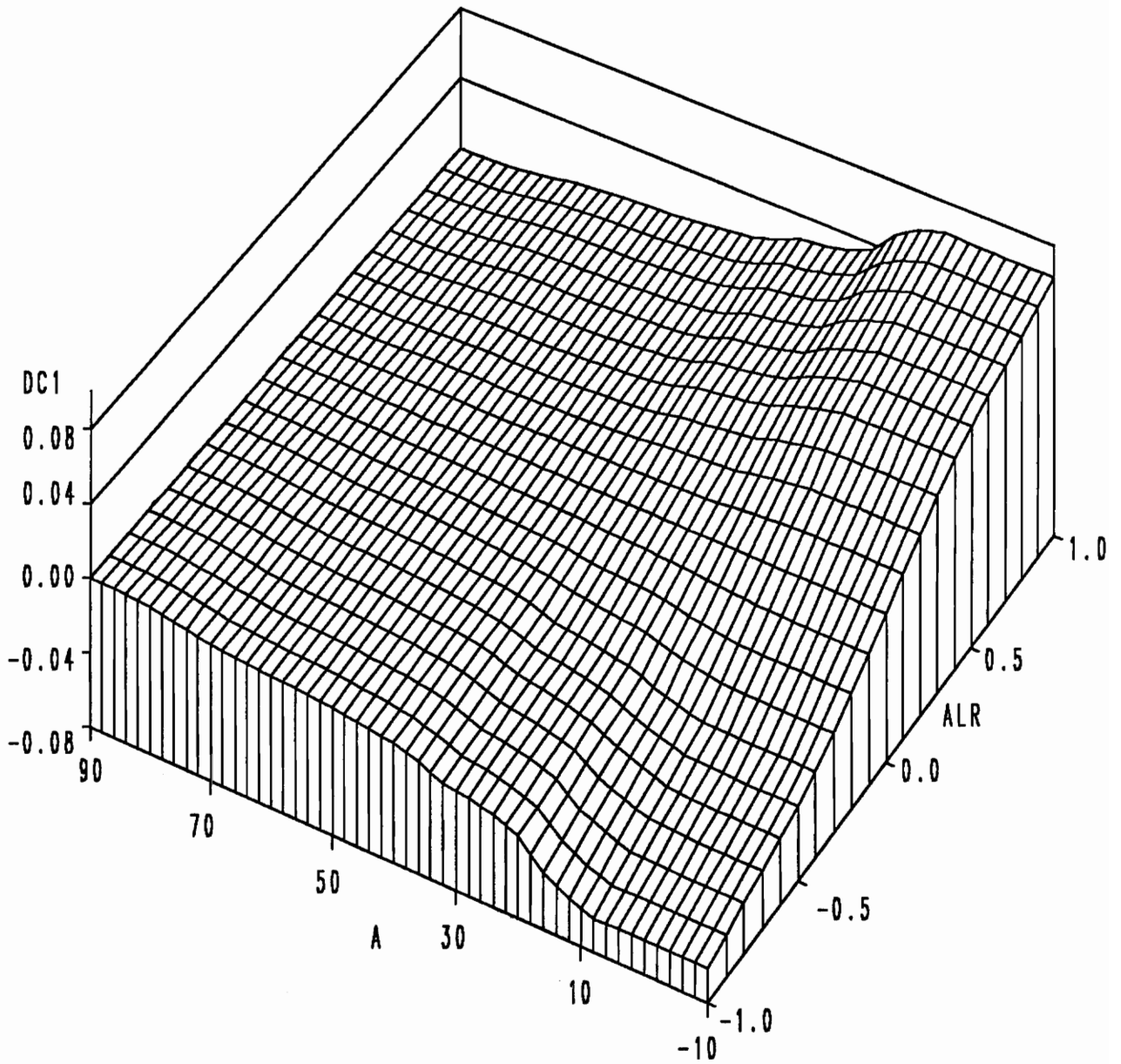


Figure A-7b. Roll coefficient due to differential aileron (HARV data)

Appendix A8. Pitch coefficient due to horizontal tail

$$C_m^c(\alpha, \delta_e) = A_{m,c}(\alpha) + E_{m,c}(\alpha) \cdot \delta_e$$

where

$$A_{m,c}(\alpha) = 0.5 (C_m^{cp}(\alpha) + C_m^{cn}(\alpha))$$

$$E_{m,c}(\alpha) = 0.5 (C_m^{cp}(\alpha) - C_m^{cn}(\alpha))$$

$$C_m^{cp}(\alpha) = L_{m,c}^1(\alpha) + S_{m,c}^2(\alpha)$$

$$C_m^{cn}(\alpha) = L_{m,c}^3(\alpha) + R_{m,c}^4(\alpha)$$

and the components have the following form:

$$L_{m,c}^1(\alpha) = a_L^1 \cdot \alpha + b_L^1$$

$$S_{m,c}^2(\alpha) = c_S^2 \cdot \sin [d_S^2 \cdot \arctan (a_S^2 \cdot \alpha + b_S^2) + e_S^2]$$

$$L_{m,c}^3(\alpha) = a_L^3 \cdot \alpha + b_L^3$$

$$R_{m,c}^4(\alpha) = \frac{c_R^4}{1 + \left| \frac{\alpha - \alpha_R^4}{w_R^4} \right|^{r_R^4}}$$

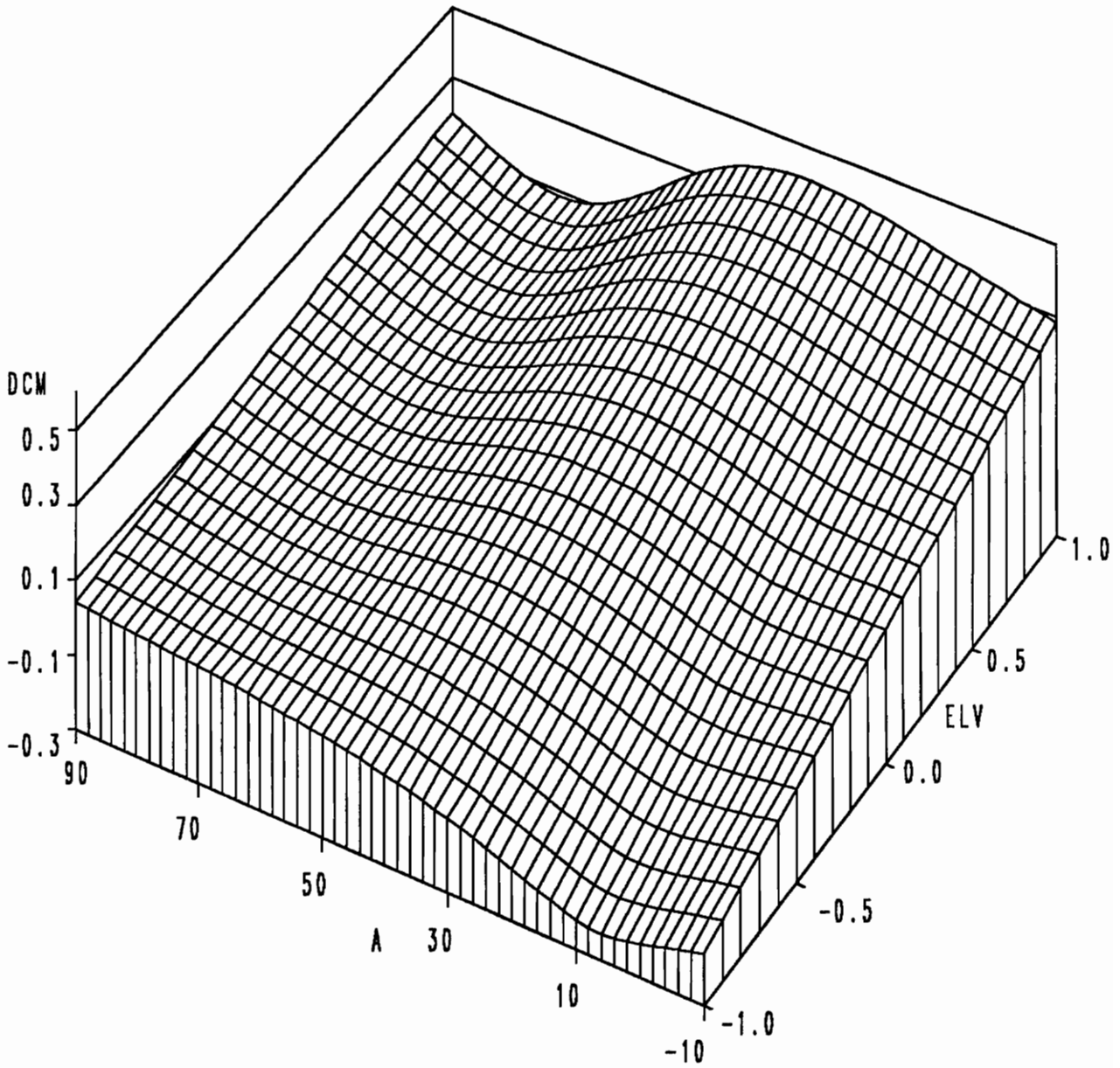


Figure A-8a. Pitch coefficient due to horizontal tail
(analytical model)

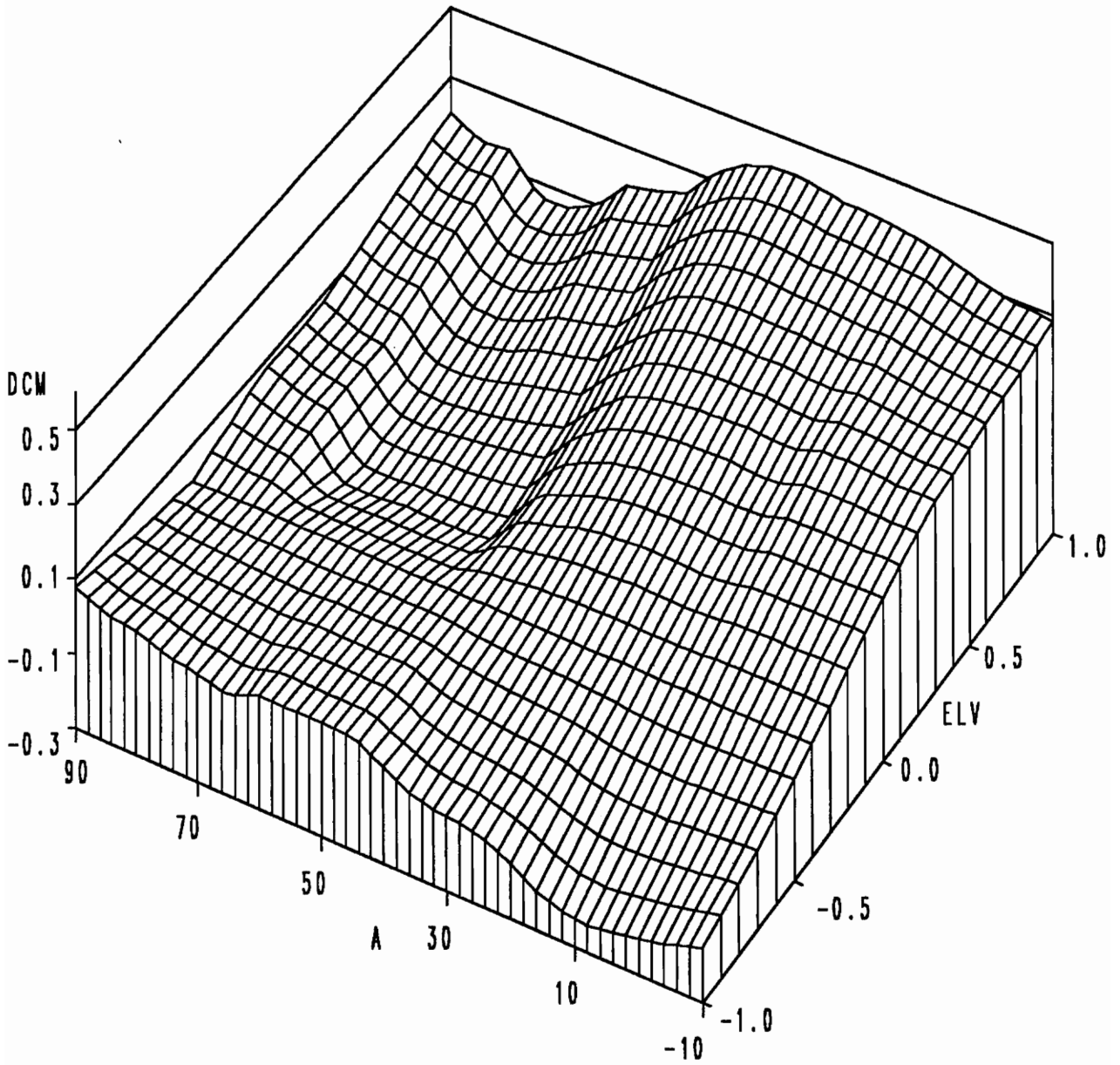


Figure A-8b. Pitch coefficient due to horizontal tail (HARV data)

Appendix A9. Yaw coefficient due to rudder

$$C_n^c(\alpha, \delta_r) = R_{n,c}(\alpha) \cdot D_{n,c}(\alpha, \delta_r)$$

where

$$R_{n,c}(\alpha) = L_{n,c}^1(\alpha) + T_{n,c}^2(\alpha) + R_{n,c}^3(\alpha)$$

$$D_{n,c}(\alpha, \delta_r) = \delta_r$$

and the components have the following form;

$$L_{n,c}^1(\alpha) = a_L^1 \cdot \alpha + b_L^1$$

$$T_{n,c}^2(\alpha) = c_T^2 \cdot \arctan [d_T^2 \cdot \exp(a_T^2 \cdot \alpha + b_T^2) + e_T^2]$$

$$R_{n,c}^3(\alpha) = \frac{c_R^3}{1 + \left| \frac{\alpha - \alpha_R^3}{w_R^3} \right|^{r_R^3}}$$

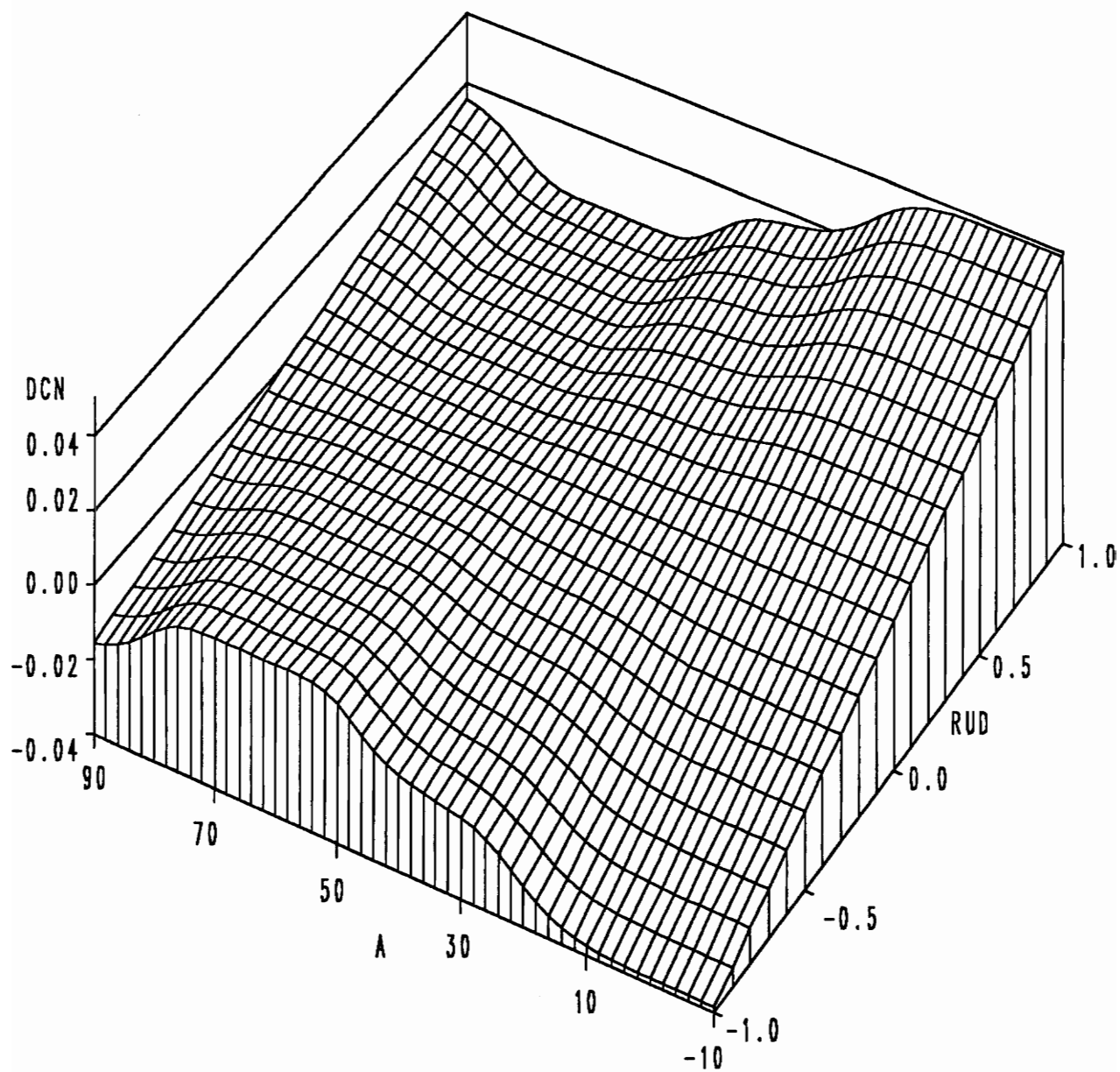


Figure A-9a. Yaw coefficient due to rudder (analytical model)

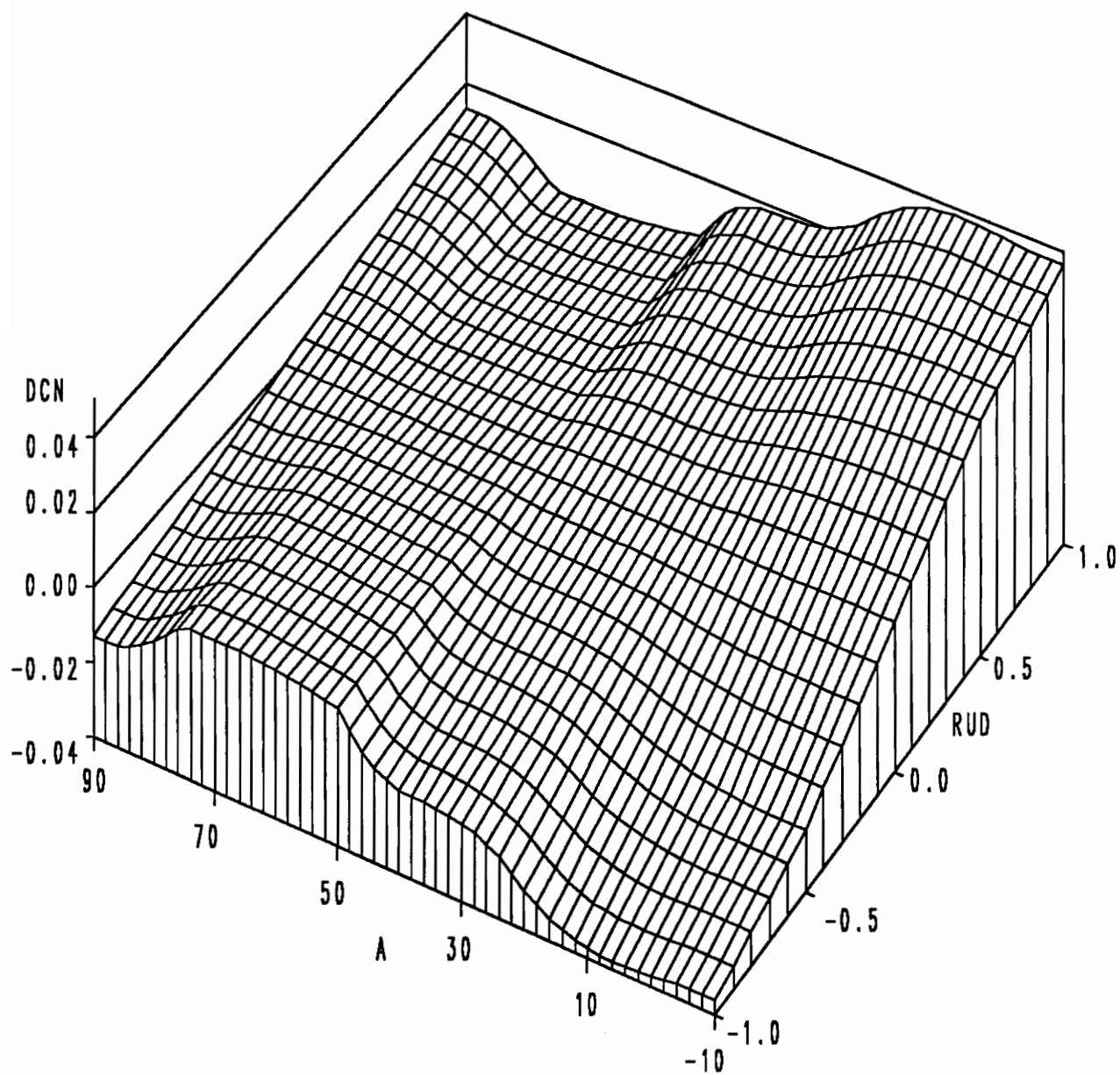


Figure A-9b. Yaw coefficient due to rudder (HARV data)

APPENDIX B

SHAPE FUNCTIONS

A few elementary functions were chosen as a basis in constructing the aerodynamic-moment coefficient model functions. There is no unique way of combining these (or some other) elementary functions to produce the desired model functions. Simply, the chosen ones resemble some shapes and curves in the aerodynamic-moment coefficients data and one can try to combine them in such a way as to achieve a good fit. However, some underlying principles were guiding the choice. Namely, we want to have model functions which reflect the essential characteristics of the aerodynamic-moment coefficients data given. In addition, we want modularity in a sense that we can add some peculiarities of the aerodynamic data (like small humps or valleys in the 2-D surfaces of data) and thus investigate their influence and significance upon the extremal trajectories. Moreover, we want flexibility in a sense that we can easily find a new set of parameters (constants) which will fit well aerodynamic-moment coefficients data at another Mach number. Finally, we want to produce model functions which are smooth (have continuous partial derivatives). If second-order variational tests are to be performed with the mathematical model, then these functions need to be twice continuously differentiable.

Thus, though it might seem that some of the model functions shown in Appendix A could have been satisfactorily generated with polynomials, the above discussion justifies the choice of shape functions.

The following functions are chosen as a basis of shape functions:

$$L(x; a, b) = a \cdot x + b$$

$$Q(x; c, \alpha, w) = \frac{c}{1 + \left(\frac{x-\alpha}{w}\right)^2}$$

$$C(x; c, \alpha, w) = c - Q(x; c, \alpha, w) = \frac{c \cdot \left(\frac{x-\alpha}{w}\right)^2}{1 + \left(\frac{x-\alpha}{w}\right)^2}$$

$$R(x; c, \alpha, w, r) = \frac{c}{1 + \left(\frac{x-\alpha}{w}\right)^r}$$

$$E(x; c, \alpha, w) = c \cdot \exp \left[- \left(\frac{x - \alpha}{w} \right)^2 \right]$$

$$S(x; a, b, c, d, e) = c \cdot \sin [d \cdot \arctan (a \cdot x + b) + e]$$

$$T(x; a, b, c, d, e) = c \cdot \arctan [d \cdot \exp (a \cdot x + b) + e]$$

$$Y(x, y; c, b, \alpha, w) = [c \cdot \arctan(b \cdot y)] \frac{1}{1 + \left(\frac{x-\alpha}{w}\right)^2}$$

$$Z(x, y; b, \alpha, w) = (b \cdot y) \frac{\left(\frac{x-\alpha}{w}\right)^2}{1 + \left(\frac{x-\alpha}{w}\right)^2}$$

In the further discussion the dependence of the shape functions upon the constant parameters will not be explicitly shown.

The linear function $L(x)$ is the most common building-block in the model functions. Indeed, as mentioned in Section 4.1, some homotopy schemes employed linear model functions for the static aerodynamic coefficients, of the form $C(\alpha, \beta) = L^1(\alpha) \cdot L^2(\beta)$. Furthermore, the majority of model functions shown in Appendix A are built primarily by adding humps and valleys to a basic linear function; some model functions make use of the linear function for corrective purposes.

The inverse quadratic function $Q(x)$, the exponential $E(x)$ and the function $R(x)$

have the property that they decrease to zero as the distance from the point where they achieve their maximal value increases. These functions are used to produce humps and valleys in the model functions, by adding them to a basic linear shape. An example is the model function $C_l^0(\alpha, \beta)$. The curve $C_l^0(\alpha, \beta = -20^\circ)$ is obtained by a linear function $L_{l,0}^1(\alpha)$ to which three other functions are superimposed (Appendix A1). The first is $Q_{l,0}^2(\alpha)$, whose effect can not be easily seen. Its center is at $\alpha \approx 40^\circ$ and has a small peak value. The purpose is to neutralize the distant effect of the other two superimposed functions and produce a light non-convexity above $\alpha \approx 50^\circ$. The second superimposed function is $E_{l,0}^3(\alpha)$ and it produces the hump in the region from $\alpha \approx 5^\circ$ to $\alpha \approx 25^\circ$. The third superimposed function is $E_{l,0}^4(\alpha)$ and it produces the valley in the region $\alpha \approx 25^\circ$ to $\alpha \approx 40^\circ$.

The exponential function $E(x)$ decreases fairly rapidly and away from its peak it does not affect the value of the composite function (the sum). Though the width of the humps produced by both $E(x)$ and $Q(x)$ can be controlled by the parameter w , the function $E(x)$ is used in lieu of $Q(x)$ because of the different aspect-ratio in the width of the hump it can produce. For example, one can see the sharp kink in the $C_l^c(\alpha, \beta)$ model function at $\alpha \approx 45^\circ$. It is produced by $E_{l,c}^4(\alpha)$. A similar argument justifies the occasional use of $R(x)$. The parameter r in the exponent controls the aspect ratio of the shape it produces. It is used in the $C_l^c(\alpha, \beta)$ shape to produce the deep valley in the region from $\alpha \approx 30^\circ$ to $\alpha \approx 40^\circ$; in the model function $C_n^c(\alpha, \beta)$ to produce the shallow valley in the region from $\alpha \approx 30^\circ$ to $\alpha \approx 50^\circ$; also in $C_n^c(\alpha, \beta)$.

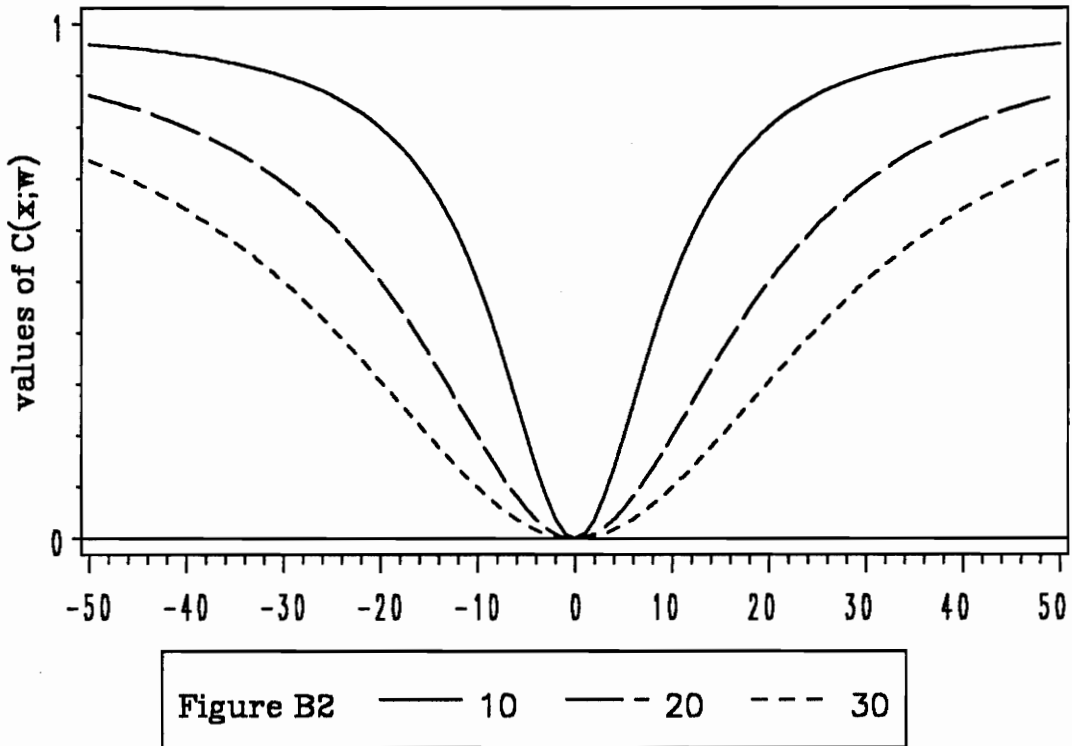
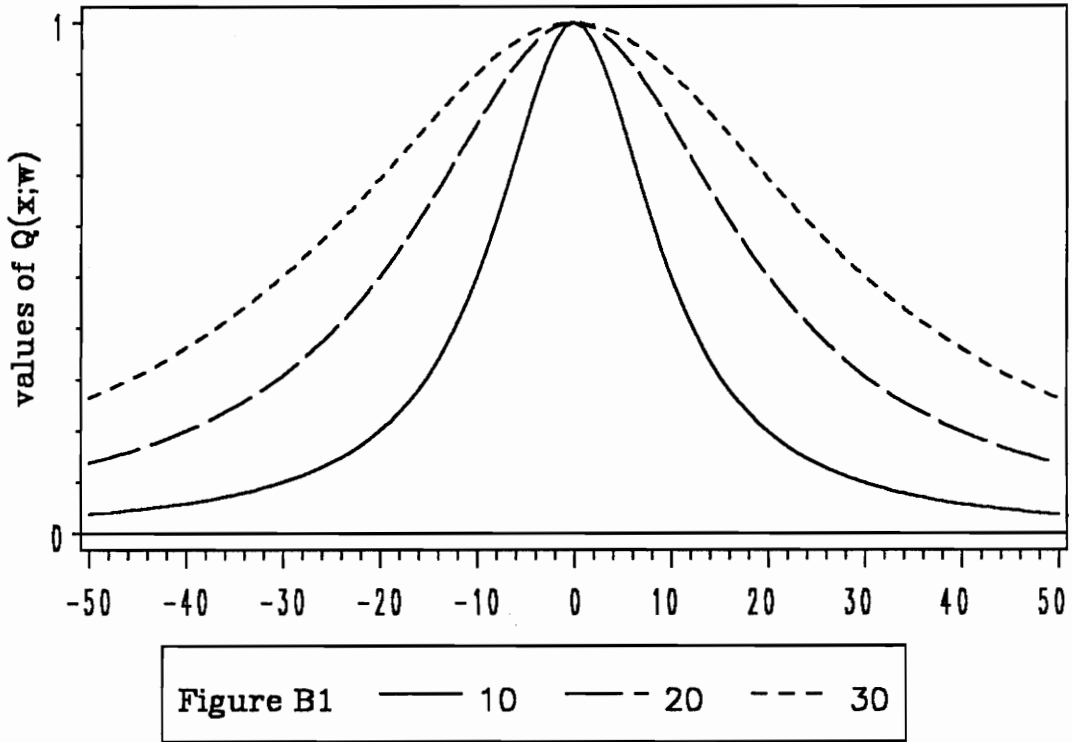
The function $T(x)$ is chosen to produce the model function $C_l^c(\alpha, \Delta_a)$. In the data one can see that $C_l^c(\alpha, \Delta_a = -1)$ tends to converge towards constant values as α approaches -10° and $+90^\circ$. This suggests that an $\arctan(\cdot)$ can be used. However, the data shows that for $\alpha > 30^\circ$ the function $C_l^c(\alpha, \Delta_a = -1)$ decreases much slower than it increases for $\alpha < 30^\circ$. This can be managed by distorting the the α -axis and

that is done by picking a proper function of α , in particular the $\exp(\cdot)$ function. The some can be done with a polynomial function. However, the parameter-optimization least-square fitting software may experience difficulties in the numerical search since a polynomial function is not in general monotone.

Similar argument justifies the use of the function $S(x)$. It is used in the $C_m^c(\alpha, \delta_e)$ model function, to produce $C_m^c(\alpha, \delta_e = -1)$. An idea behind this model function is worth mentioning. The $C_m^c(\alpha, \delta_e)$ data clearly shows that the functions $C_m^c(\alpha = \text{const}, \delta_e)$ are not monotone in the region above $\alpha \approx 40^\circ$. Thus, when the Minimum Principle is applied, one does not always get a full elevator for control. This problem is solved by a simple trick which effectively transforms the physical elevator control variable into a new one. Namely, what matters for the Minimum Principle, according to the expression for the Hamiltonian of our problem, is that at a given α_* we pick the control δ_e such that the lowest or the highest value of $C_m^c(\alpha_*, \delta_e)$ is achieved (depending upon whether λ_Q is positive or negative, respectively). If so, we can find functions $C_m^{cp}(\alpha_*) = \max_{\delta_e} [C_m^c(\alpha_*, \delta_e) \text{ data}]$ and $C_m^{cn}(\alpha_*) = \min_{\delta_e} [C_m^c(\alpha_*, \delta_e) \text{ data}]$ and assign these to be values of a model function $C_m^c(\alpha, \delta_e)$ for $\delta_e = +1$ and $\delta_e = -1$, respectively. Then we can linearly interpolate between these values for $\delta_e \in (-1, +1)$. The Minimum Principle will yield $\delta_e = -1$ or $\delta_e = +1$. In the process of homotopy, where the aerodynamic controls are assumed not to be independent, the results are not correct (the model function is correct for $\delta_e = -1$ and $\delta_e = +1$ only). But this is not a problem, since ultimately we are interested in results with independent aerodynamic controls (bang-bang). In a similar manner this model is not good if singular trajectories are to be studied with the model. Once we have an extremal trajectory, we can transform δ_e back to the actual physical value. Note that linearization in the control variable is also done in the model functions $C_l^c(\alpha, \Delta_a)$ and $C_n^c(\alpha, \delta_r)$.

The functions $Y(x, y)$ and $Z(x, y)$ are used to control the β -dependence of the model functions $C_l^0(\alpha, \beta)$ and $C_n^0(\alpha, \beta)$. Both of these functions are odd in β . Thus, $C_l^0(\alpha, -\beta) = -C_l^0(\alpha, \beta)$ and $C_l^0(\alpha, 0) = 0$. One can notice that the $C_l^0(\alpha = \text{const}, \beta)$ data has $\arctan(\beta)$ shape in the region of $\alpha \approx 5^\circ$ to $\alpha \approx 35^\circ$ and linear behavior outside that region. Thus, one needs to multiply the curve $C_l^0(\alpha, \beta = -20^\circ)$ by such a function of β , which is antisymmetric, has zero value for $\beta = 0^\circ$, $\arctan(\beta)$ shape for α in the region from 5° to 35° , linear shape outside this region and unit value for $\beta = -20^\circ$. This can be accomplished by a sum of functions $Y(\alpha, \beta)$ and $Z(\alpha, \beta)$. $Y(\alpha, \beta)$ shows the desired $\arctan(\beta)$ shape in the β direction. It contains a $Q(\alpha)$ multiplier to bring its value to zero outside the desired region (Figure B7). Similarly, $Z(\alpha, \beta)$ has linear behavior, with the desired slope, almost everywhere except in the region where we want it not to have a lot of effect. This is accomplished by multiplying a linear function of β by $C(\alpha)$, a function which is in a sense a complement of $Q(\alpha)$.

Those are some of the basic principles that guided the development of the model functions for the aerodynamic-moment coefficients.



Figures B1 & B2. Shape functions Q and C for $w=10, 20, 30$

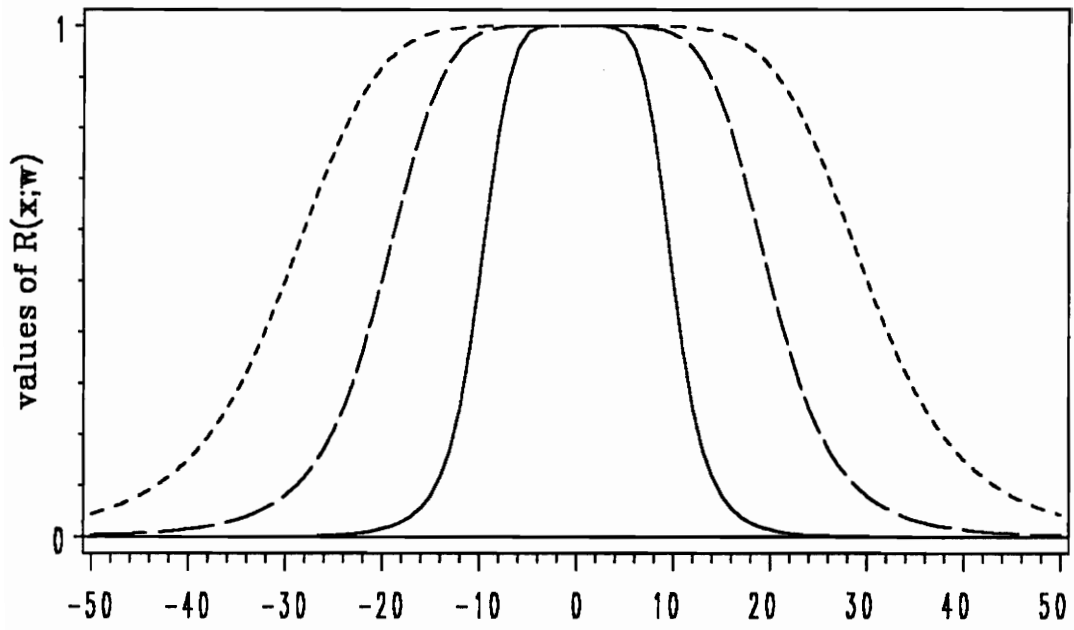


Figure B3 — 10 — - 20 - - - 30

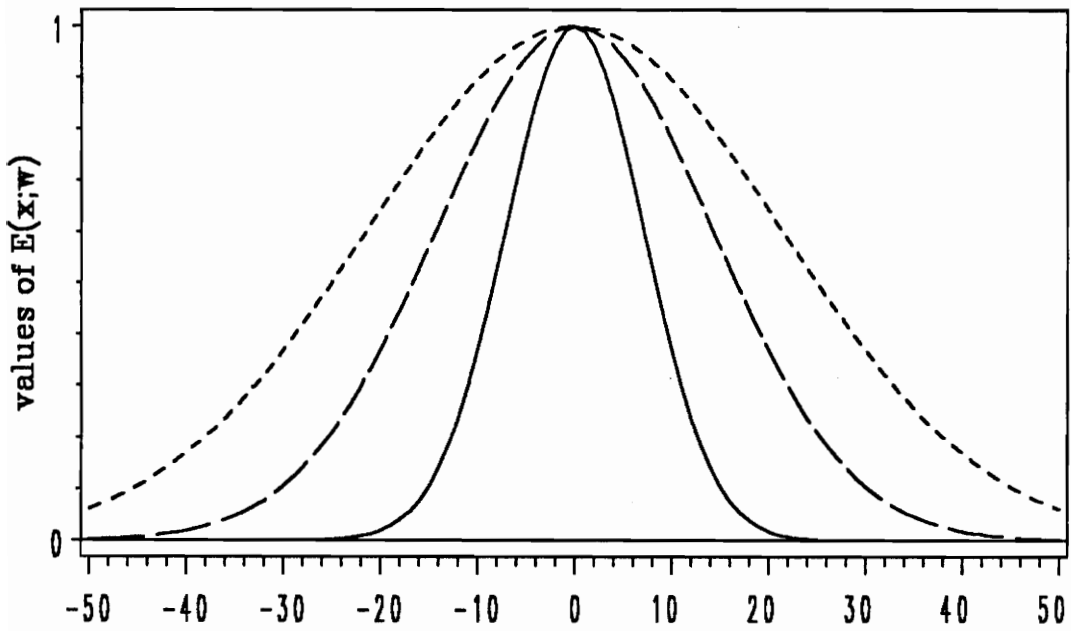
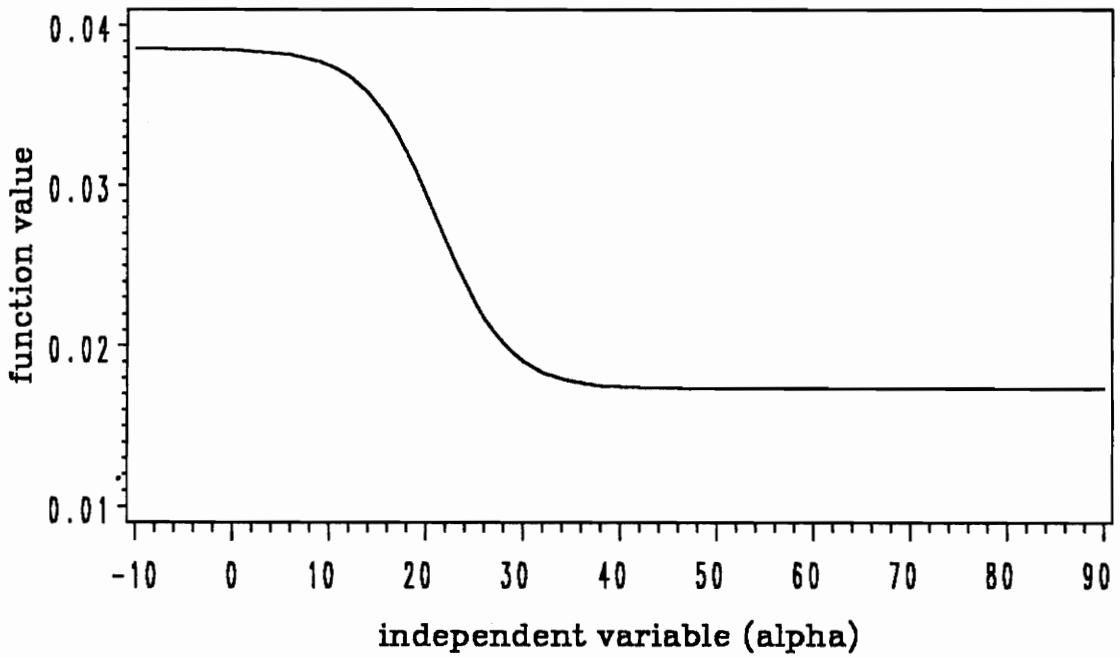
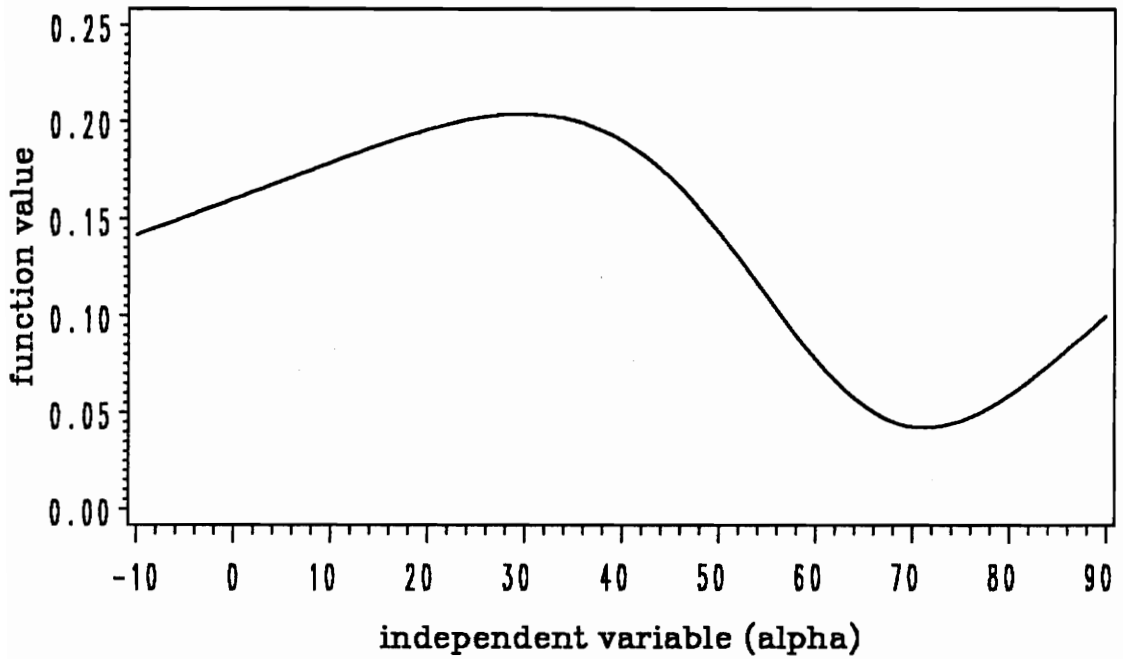


Figure B4 — 10 — - 20 - - - 30

Figures B3 & B4. Shape functions R and E for $w = 10, 20, 30$

Figure B5. Shape function $T(\alpha)$ Figure B6. Shape function $S(\alpha)$

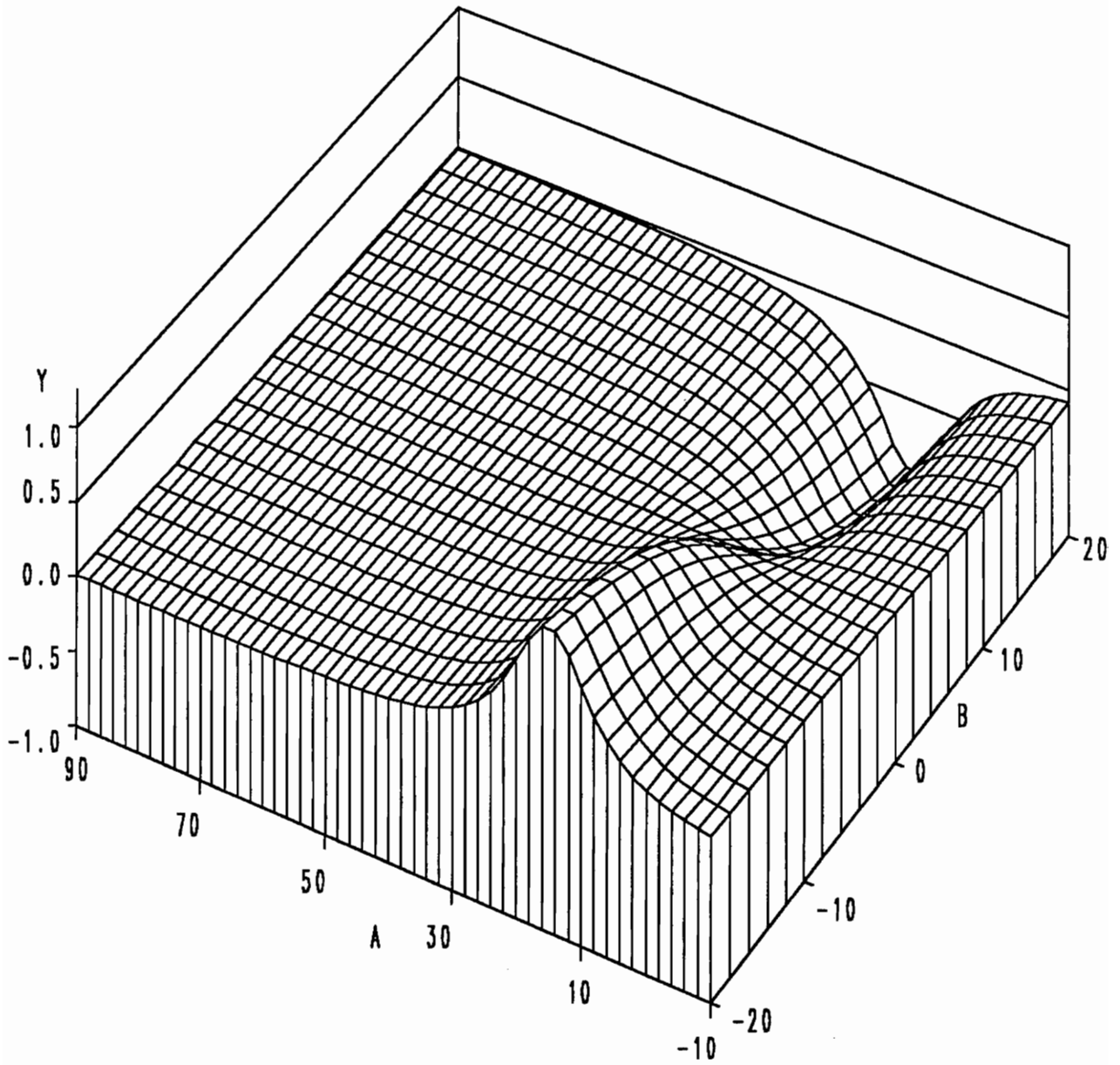


Figure B7. Shape function $Y(\alpha, \beta)$

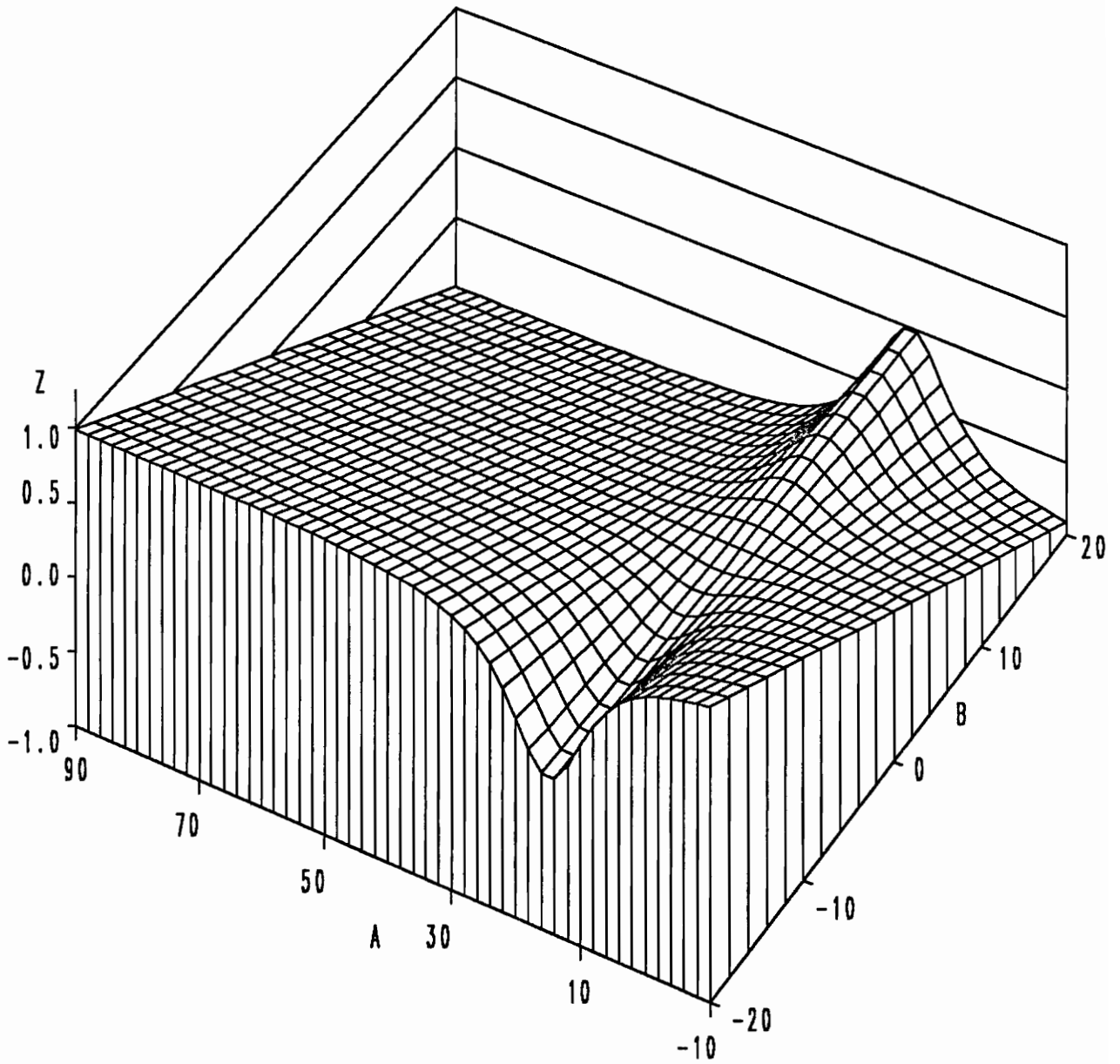
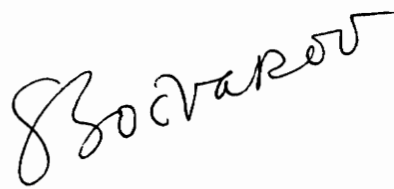


Figure B8. Shape function $Z(\alpha, \beta)$

V I T A

The author was born on August 15, 1962 in Štip, Yugoslavia. He received his Bachelor of Electrical Engineering from University of Belgrade, Yugoslavia, in September 1985. Following that, he worked in Research Institute Mihailo Pupin, Belgrade, as a research engineer in the Department for Digital Electronics and Control. In February 1988 he received a Masters of Science degree in Real-Time Control Systems from University of Belgrade. In August 1988 he enrolled in a Doctor of Philosophy program at the Aerospace and Ocean Engineering Department at Virginia Polytechnic Institute and State University.

The author is member of Tau Beta Pi National Honorary Society.

A handwritten signature in black ink, appearing to read "J. Zocvarov". The signature is written in a cursive style and is slanted upwards from left to right.